NATURAL ORGANIC MATTER IN DRINKING WATER SOURCES: ITS CHARACTERISATION AND TREATABILITY

Report to the
Water Research Commission

by

J Haarhoff, B Mamba, R Krause, S van Staden,
T Nkambule, S Dlamini, and KP Lobanga
Department of Applied Chemistry
Department of Civil Engineering Science
University of Johannesburg

WRC Report No. 1883/1/12
ISBN 978-1-4312-0354-3

January 2013

Obtainable from

Water Research Commission
Private Bag X03
Gezina, 0031

orders@wrc.org.za or download from www.wrc.org.za

EXECUTIVE SUMMARY

Background and motivation

The design of potable water treatment plants is conventionally based on physical and microbial properties of the raw water, such as colour, turbidity, odour, pathogenic bacteria and others. A relatively recent addition to this list is natural organic matter (NOM), normally crudely quantified as total organic carbon (TOC). Natural organic matter, however, is not a stand-alone problem, but affects water quality in many ways. It could be responsible for the colour, undesirable taste and odour of natural waters, it is a source of nutrients for heterotrophic bacteria, it inhibits precipitation processes which form the backbone of drinking water treatment, it is a major membrane foulant, it promotes bacterial re-growth in the distribution system which compromises water quality, it accelerates corrosion of the distribution network, it increases turbidity at the point of consumption, it causes high disinfectant demand, and it may interact with the disinfectant to form carcinogenic and mutagenic disinfection by-products (DBPs). There is no question that NOM, as a precursor to or direct cause of such problems, should be one of the critical design and operational parameters for drinking water treatment at locations where raw water is NOM-rich. The practical consequences of more efficient NOM removal could be far-reaching, including improved water quality leading to better customer satisfaction, better and therefore cheaper designs, lower operational costs, improved water stability during distribution, and lower corrosion of networks leading to a longer lifetime of expensive assets.

As a consequence, three new unit processes have been applied at existing South African water treatment plants during the past decade. The processes, widely touted in the international literature as effective methods to reduce NOM to acceptable levels, are enhanced coagulation (EC), activated carbon (AC) and ozone. Also, there is an interest in some European countries in using ion exchange (IEX), a process mostly limited to industrial water treatment applications, for large-scale municipal drinking water treatment. These newer applications yielded mixed and often disappointing results in South Africa, with their efficiencies strongly influenced by location and season, despite them being compliant to the best international practices. Upon critical analysis of many different SA surface water sources, it became apparent that the specific ultraviolet absorbance (SUVA) values for South African water were uncharacteristically low compared to most of the waters on which the international studies had been based. Low SUVA values imply that the NOM is dominated by non-humic substances, which is in line with the observation that much of the NOM in South African waters is contributed by treated sewage return flows. These observations form the basis of the hypothesis that there are fundamental differences in the nature and occurrence of NOM in South African raw water sources in both space and time, when compared to international literature. Without a deeper understanding of NOM in South African raw water supplies, and its treatability by different treatment technologies, water treatment plant design and operation will not be able to deal with increasing NOM levels in a predictable and satisfactory way.

Natural organic matter in water is mostly characterised by a single TOC value, derived from the amount of carbon dioxide formed upon NOM incineration. The latest South African National Standard for drinking water (SANS 241), for example, places a NOM limit in drinking water in terms of TOC. While this provides a first important indicator, it is inadequate. Natural organic matter is a heterogeneous mixture of structurally complex organic compounds derived from plants, animals and micro-organisms and their waste and metabolic products. Total organic carbon is found in all natural water as either particulate organic carbon (POC) or dissolved organic carbon (DOC).

Natural organic matter can further be split into six major groups, namely humic substances, hydrophilic acids, carboxylic acids, carbohydrates, amino acids, and hydrocarbons. Their relative abundance depends both on the water source and the chemical and biological degradation of the NOM. A deeper understanding of NOM in natural water requires the development and use of newer, advanced analytical methods for its measurement.

Research objectives

The project was guided by the following research objectives:

- Investigate the nature of NOM appearing in source water in representative parts of South Africa.
- Investigate and assess the NOM removal efficiency of selected drinking water treatment plants. The plants should reflect typical unit processes used throughout the country. Samples should be taken at various points in time throughout the year.
- Identify the NOM categories which are not removed efficiently by extant drinking water treatment systems. Work on actual plants should be supplemented by suitable bench-scale process simulation investigations.
- Apply advanced analysis techniques to provide relevant insight in the NOM composition, and how it affects in water treatment and water quality in the distribution network.
- Develop models to predict the NOM reduction by different treatment processes.
- Investigate the use of suitable existing and novel processes which could be employed to remove the problematic NOM fractions. The focus will be on five technologies, namely EC, activated carbon, ozonation, IEX and nanoporous polymers.
- Compile a guideline on the efficient removal of NOM from South African source waters. The guideline should include techniques suitable to both large and small water treatment systems, optimised operational procedures, and suitable methods of analysis for the relevant NOM fractions.
- Compile an awareness-creating pamphlet (and/or similar information transfer means) on this guide. Arrange at least six information transfer workshops throughout the country, where the guideline will be presented to the consulting fraternity and Water Services Authority representatives.

Major results and conclusions

The sampling programme provided useful profiles of the raw waters investigated, to contextualise the treatment studies that follow. The conventional water quality parameters confirmed the anticipated profiles:

- The waters that were influenced by the return flows from sewage treatment plants had higher alkalinity, pH and hardness, as well as higher levels of nutrients (Midvaal, Rietvlei and Olifantsvlei). The return effluents tend to stabilise these sources and there is relatively less variation in water quality.
- The water from the coastal impoundments are softer, low in alkalinity (Umzonyana, Wiggins) and, along the southern coast, progressively higher in colour (Loerie, Plettenberg Bay).

The organic parameters provided a less clear-cut classification of the different raw waters:

- Both the UV_{254} absorbance and the DOC ranges were remarkably similar for most of the waters, with two exceptions. The Plettenberg Bay samples were clearly higher, and the Wiggins

samples clearly lower than the remaining six samples, which cover about the same range. The SUVA values, which represent the ratio between UV absorbance (UVA) at 254 nm wavelength (UVA_{254}) and DOC, were also quite similar. The Plettenberg Bay samples had higher SUVA values than the rest (suggesting better removal by EC) and the Wiggins samples very low SUVA values (suggesting poor removal by EC).

- The BDOC/DOC ratios of the samples covered a broad range, 20% to 65%. Two sites had practically constant ratios (covering a range of 6% or less), while others covered ranges as high as 39%. No explanations for these large, and possibly important differences, can be offered yet. The sources with less eutrophic sources (Vereeniging and Loerie) had a high BDOC/DOC ratio, but so did the treated sewage effluent (Olifantsvlei). The Wiggins samples (lowest organic content of all the sources) had the lowest ratio, but the Plettenberg Bay samples (highest organic content of all the sources) also had some of the lowest ratios on some occasions.
- The Fluorescence Emission Excitation Method (FEEM) results showed that the Plettenberg Bay samples had very broad peaks for hydrophobic acids across all rounds of sampling. The results also indicated that the Plettenberg Bay samples had high amounts of hydrophobic NOM. The other samples had low aromatic content, as shown by the narrow peaks, or no peaks where peaks for humic substances would be expected.
- The fractionation of NOM by Polarity Rapid Assessment Method (PRAM) varied substantially depending on the type and source of water. The Plettenberg Bay samples had a greater percentage of the hydrophobic fraction and a lesser but equal distribution of the hydrophilic and transphilic fraction. The Rietvlei samples had an almost equal distribution of the hydrophobic, transphilic and hydrophilic fraction while the other samples had low percentages of hydrophobic fraction and slightly higher percentages of transphilic and hydrophilic NOM fractions.

The treatment plants were monitored during each sampling round. Although these plants were not operated with NOM removal as a primary objective, the results helped to establish a benchmark for typical UVA removal. In summary, the average removal of UVA_{254} was:

- 36% by ozonation
- 88% by coagulation and settling (highly coloured water)
- Inconsistent removal by coagulation, flocculation, settling/dissolved air flotation and filtration (non-ozonated water) from 20% to 74% of the raw water UVA, with the differences mainly due to the choice of coagulants
- An increase of 27% to 100% by coagulation, flocculation, settling and filtration (ozonated waters)
- 5% removal of raw water UVA by sand filtration
- 19% removal of raw water UVA by GAC filtration

A detailed procedure for the evaluation of enhanced coagulation (EC) was developed, and applied to all the raw water samples. The general findings were:

- Enhanced coagulation did not compromise the removal of turbidity – the dosages required for EC were slightly higher than for turbidity removal only.
- The raw water SUVA and coagulation pH were the key factors determining the efficiency of EC, a finding in line with previous international studies.
- A titration curve was used with success to target specific pH values for jar testing purposes. Optimum dosage for EC, for all samples irrespective of water source and season, corresponded

to pH values between about 4.5 and 7.0. Waters of low alkalinity required the addition of lime to maintain the pH in this range.
- The data allowed a good estimate of the UVA removal that can be achieved by EC if the SUVA value is above 2, with the associated ferric chloride dosage.

The adsorptive capacity of crushed activated carbon was determined by equilibrium testing, in the laboratory. The main findings were:

- The results could be adequately modelled with the Freundlich isotherm.
- The isotherm allowed the calculation of the activated carbon dosage to remove 50% of the raw water UVA_{254} absorbance. These values did not suggest a practical treatment technology, but illustrated that raw waters with similar UVA values would respond quite differently to activated carbon treatment.
- Although the emphasis of this project is on UVA_{254} as NOM parameter, control tests using DOC as response parameter showed similar removal of UVA_{254} and DOC for the same order of activated carbon dosage. UVA_{254} can therefore be used for preliminary adsorption testing, but should be confirmed with more detailed test work with parallel DOC measurement.
- Different samples required different dosages of activated carbon, demonstrating the different nature of NOM at different locations.

Similar adsorptive capacity tests were carried out with strong and weak IEX resins, and demonstrated that:

- A contact time of three days was adequate to reach equilibrium.
- Over the wide range of dosages used (up to 1280 mg/ℓ), the Freundlich isotherm did not provide a good fit and a polynomial had to be used to get a satisfactory fit.
- The calculated dosage to remove 50% of the UVA_{254} differed amongst the different raw waters, and was very high in comparison to typical usage rates in practice.
- In terms of UVA only, the weak IEX resin did not perform as well as the strong IEX resin – on average, about 2.4 times more weak resin had to be used to obtain the same UVA removal.

The project allowed for some fundamental work using nanomaterials. Visible-light active N, Pd co-doped TiO_2 was successfully synthesised by a modified sol-gel method. Co-doping reduced the band gap of TiO_2 and shifted the absorption edge to the visible-light region. This resulted in successful application of visible light for activating the co-doped TiO_2 for NOM photodegradation. The nanocatalyst was found to be efficient in NOM degradation compared to conventional NOM treatment methods. Improved photoactivity was attributed to the synergistic effects of N and Pd co-doping of TiO_2. The hydrophobic fraction showed the highest degradation efficiency of 96% because of the increased interaction with the nanoparticles. Results from this study showed that N, Pd co-doped TiO_2 is a promising photocatalytic material for NOM removal in water-treatment systems and can be considered a good candidate for future photocatalytic applications.

The measurement of UVA_{254} was an immediate, more robust parameter that is accessible to water treatment plant personnel, both in terms of cost and operational skills. It was adopted as the principal indicator of NOM in this project, with good results. It provided a useful profile of the different raw water sources (in close agreement with DOC), and served well to measure the removal of NOM through the typical treatment plant processes. In the laboratory, it provided a smooth response to increasing coagulant dosages (much less erratic than DOC) which enabled the accurate pinpointing of the coagulant dosages required for EC. For adsorption studies, it provided isotherms

of good fit for activated carbon and IEX resins. In the case of activated carbon, the isotherms were also determined in terms of DOC removal and, once again, there were reasonable parallels between UVA_{254} and DOC. For those researchers and water providers interested to further investigate NOM during water treatment, this project suggests that the measurement of UV_{254}, or full-spectrum UV scans should be seriously considered, and always included as a routine parameter for quality control.

The units of UVA that could be loaded onto unit masses of $FeCl_3$, AC and IEX resin, were calculated as a means to compare the removal capacity of EC, AC and IEX. In general, the removal capacity of $FeCl_3$ was significantly higher than the others. These results show a way forward in terms of practical process design. In most cases, EC allowed the highest solids loading and can be implemented at no great cost, other than slightly higher coagulant demand. Enhanced coagulation can therefore be considered as the first barrier for NOM reduction, and the more expensive adsorption options should be reserved to add an extra step of NOM removal.

Project evaluation

The project met almost all of the stated research objectives. Notable exceptions were the exclusion of small treatment plants from the sampling programme, and exclusion of treated water samples taken from water distribution systems. Also, the advanced methods took much longer to develop than anticipated and only came on line during the final year of the investigation. Although useful information was obtained from the advanced methods, the database was not broad enough to allow for a general synthesis of the results obtained. On the other hand, some new, important elements were introduced which were not covered in the proposal. This includes much more extensive investigation of the IEX resins, and the introduction of the FEEM for NOM characterisation. Of the six knowledge transfer workshops planned, only three were held, but the third workshop at the 2012 WISA Conference in Cape Town (arranged through facilitation of the Water Research Commission) reached a broad, national audience which had large impact.

The project explored some new ground not published before:

- The sampling programme was unique in its coverage, both spatially and temporally – eight treatment plants visited five times each over two years, covering all the main seasons.
- The collective battery of advanced analytical methods of FEEM, BDOC and PRAM analyses had never been applied in South Africa before.
- A detailed, systematic procedure for the evaluation of EC was developed with suggested endpoints to bring uniformity to EC feasibility testing.

The project endeavoured to raise the awareness of the importance of NOM removal during drinking water treatment. With better awareness, water providers will measure their own performance more carefully and include NOM removal as one of their treatment objectives. As raw water sources are more intensively used and their quality compromised as a result, engineers need to consider NOM removal more carefully during process design. This project paves the way by suggesting methods for analytical measurement and process evaluation.

Capacity development and research outputs

In terms of capacity building, four doctoral candidates and one master's degree candidate were involved in the project. All five students were of African descent – one female and four males.

As part of the project, two internal seminars (project team only) were held in 2010 and 2011. One seminar was held with the reference group in 2010, and a further three seminars were held with international associates (TUDelft, University of Massachusetts, and TUDelft) during November 2010, February 2011 and May 2011 respectively. All of these seminars proved invaluable in terms of research input and international perspectives on the research covered by the project.

Two formal technology transfer meetings were held in 2011 with the permission of the WRC, coinciding with the visit of Professor Rietveld from TUDelft in May/June 2011. During these meetings the completed parts of the study were presented and generally stimulated lively interest and good discussions. The meetings were attended by a total of 40 participants.

As part of the research outputs emanating from the project, 13 peer-reviewed papers were published, eight oral and three poster presentations were made at local conferences, and six oral and three poster presentations were made at international conferences.

Recommendations for further research

This project suggests some important and interesting avenues for future research:

- The results of the advanced NOM characterisation methods must be matched better with the performance of different treatment technologies. Once this is achieved, the advanced methods could inform more rational and optimal process design for new and existing water treatment plants.
- The activated carbon and IEX test procedures must be focused more narrowly on secondary NOM removal after EC, covering smaller dosage ranges to obtain better isotherm descriptions. These processes are costly to implement and operate, therefore requiring careful testing and design. The equilibrium testing done for this study needs to be expanded to column studies to capture their kinetic behaviour.
- The treatment performance studies must be broadened to include TOC and some of the advanced NOM characterisation techniques. Whereas this study uses UVA_{254} as the primary NOM indicator, the treatment performance also needs to be expressed in terms of TOC to allow alignment with the legal requirements of SANS 241.
- Membrane filtration should be included as a treatment process for NOM removal, as it is likely to find wider application in the years to come.

ACKNOWLEDGEMENTS

The success of the project hinged upon frequent and close interaction with the eight treatment plants which provided the samples on no less than five occasions. Throughout, the project team received the full, unconditional support from the managers and operators at the treatment plants. They were:

- Bitou Municipality (Pikkie Lombard)
- Buffalo City Metropolitan Municipality (Willie Kieck)
- Johannesburg Water (Rob Boyd)
- Midvaal Water (Marina Kruger)
- Nelson Mandela Metropolitan Municipality (John de Kock)
- Rand Water (John Geldenhuys and James Parsons)
- Tshwane Metropolitan Municipality (Leanne Coetzee)
- Umgeni Water (Rachi Rajagopaul)

Generous support was provided by Chris Swartz and Rachi Rajagopaul who arranged the venues and invitations for the workshops presented in Knysna and Durban. Dr Burgess of the WRC provided letters of introduction to some of the treatment plants where required. Prof Luuk Rietveld (Delft Technical University) with doctoral students Anke Grefte and Petra Ross participated during two visits to South Africa in November 2010 and June 2011 and provided useful interaction with the project team during site visits and research seminars. The team also had project discussions and seminars with visiting professors at UJ: Prof Dave Reckhow (University of Massachusetts) during February to March 2011; Prof Arne Verliefde (Ghent University) during July 2011; and Professor Simon Judd (Cranfield University) during June 2011.

REFERENCE GROUP

Dr JE Burgess	Water Research Commission (Chairperson)
Dr AD Ceronio	CSV Water
Ms L Coetzee	Tshwane Metropolitan Municipality
Prof J Maree	Tshwane University of Technology
Mr J Menge	City of Windhoek
Mr J Parsons	Rand Water
Mr R Rajagopaul	Umgeni Water
Dr M van der Walt	Bigen Africa
Mrs M Kruger	Midvaal Water

TABLE OF CONTENTS

LIST OF FIGURES

LIST OF TABLES

LIST OF ABBREVIATIONS

AC	Activated carbon
$AlCl_3$	Aluminium chloride
Alk	Alkalinity
APHA	American Public Health Association
APK	Auckland Park Kingsway campus of the University of Johannesburg
AU	Arbitrary units
AWWA	American Water Works Association
BDOC	Biodegradable dissolved organic carbon
C18	Cartridge that generates HPO fraction
C_3H_8O	2-propanol
$Ca(OH)_2$	Calcium hydroxide
$CaCO_3$	Calcium carbonate
C-C	Double carbon bond
CCD	Cooled charged coupled device
CN	Cartridge that elutes HPI fraction
DAF	Dissolved air flotation
DFC	Doornfontein campus of the University of Johannesburg
DOC	Dissolved organic carbon
DOM	Dissolved organic matter
EC	Enhanced coagulation
EC	Enhanced coagulation
e^-CB	Empty conduction band
EDTA	Ethylene diamine tetra-acetic acid
EDX	Energy dispersive X-ray spectrometer (y)
EEM	Emission excitation matrix (ces)
$FeCl_3$	Ferric chloride
FEEM	Fluorescence emission excitation matrix (ces)
FT-IR	Fourier Transform Infrared
FWHM	Full width at half maximum
G	George
GAC	Granular activated carbon
gGAC	Ground granular activated carbon
h^+VB	Holes in the valence band
HCl	Hydrochloric acid
HPI	Hydrophilic fraction
HPO	Hydrophobic fraction
IEX	Ion exchange
IWA	International Water Association
K and n	Freundlich constants
L	Loerie
M	Midvaal
MP	Macroporous
Na_2CO_3	Sodium carbonate
NaOH	Sodium hydroxide
NH_2	Cartridge that generates TPI fraction
NH_3	Ammonia

nm	Nanometres
NOM	Natural organic matter
NTU	Turbidity in nephelometric turbidity units
Olifantsvlei	Olifantsvlei
P	Plettenberg Bay
PAC	Powdered activated carbon
$Pd(NH_3)_2Cl_2$	Palladium diamine dichloride
PODR	Point of diminishing return (s)
PRAM	Polarity rapid assessment method
R	Rietvlei
rpm	Revolutions per minute
RW	Raw water
SA	South Africa (n)
SEM	Scanning electron microscope (y)
SPE	Solid Phase Extraction
SUVA	Specific ultraviolet absorbance
TDS	Total dissolved solids
TEM	Transmission electron microscope (y)
TGA	Thermogravimetric analysis
THM	Trihalomethane
$Ti(OC_3H_7)_4$	Titanium isopropoxide
TiO_2	Titanium oxide
TKN	Total Kjeldahl nitrogen
TOC	Total organic carbon
TPI	Transphilic fraction
U	Umzonyana
UJ	University of Johannesburg
USEPA	United States Environmental Protection Agency
UVA	Ultraviolet absorbance e.g. UVA_{254} : ultraviolet absorbance at wavelength 254 nm; or UVA_i : initial ultraviolet absorbance
V	Vereeniging
W	Wiggins
WISA	Water Institute of Southern Africa
WPCF	Water Pollution Control Federation
WRC	Water Research Commission
XRD	X-ray diffraction

CHAPTER 1. PROJECT AIMS

This report summarises the findings of a research project conducted over a three-year period, starting in 2009. The project included the following aims:

1. Investigate the nature of natural organic matter (NOM) appearing in source water in representative samples taken throughout South Africa.

   This is covered in Chapter 2 of this report.

2. Investigate and assess the efficiency of selected drinking water treatment plants. The plants should reflect typical unit processes and raw water types used throughout the country. Samples should be taken at various points in time throughout the year.

   This is covered in Chapter 3 of this report.

3. Classify the NOM categories according to their removal efficiency. Work on actual plants should be supplemented by suitable bench-scale process simulation investigations.

   This aim is covered in the chapters relevant to each process. The treatment performance of full-scale treatment plants provided limited detail, which necessitated extensive bench-scale work to allow better classification.

4. Apply advanced analysis techniques to provide relevant insight in the NOM composition related to their effects in water treatment.

   Three advanced methods were sufficiently developed to apply in the project, namely BDOC, FEEM and modified Polarity rapid assessment method. These methods took significant effort and cost to develop and they could only be applied to the samples towards the end of the project.

5. Investigate the use of suitable existing and novel techniques and processes which could be employed to remove the problematic NOM fractions.

   Enhanced coagulation (Chapter 4), carbon adsorption (Chapter 5) and ion exchange, both weak and strong resin, (Chapter 6) were extensively investigated. Exploratory work on nanomaterials was done towards the end of the project (Chapter 7).

6. Compile methodological guidelines to investigate the efficient removal of NOM from raw water.

   This material is presented as Appendix A.

The report is concluded with some general conclusions, with pointers towards critical future research areas.

These are presented in Chapter 8.

CHAPTER 2. RAW WATER CHARACTERISATION

2.1 Sampling Sites

Eight sampling sites were used throughout this project, located in Figure 2.1 and named in Table 2.1.

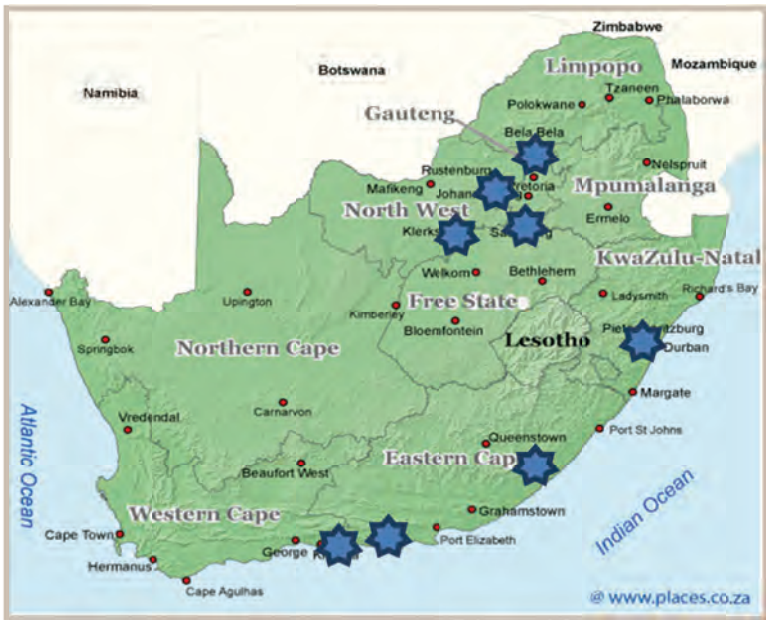

Figure 2.1 Map showing project sampling sites

Table 2.1 Raw water sampling sites

Water treatment plant name	Code*
Loerie	L
Midvaal	M
Olifantsvlei	O
Plettenberg Bay	P
Rietvlei	R
Umzonyana	U
Vereeniging	V
Wiggins	W

* Codes used in the rest of the report

The raw water sources for these water treatment plants are:

- The Loerie water is from a small impoundment, supplied from the Kouga Dam.
- The Midvaal water is pumped from the Vaal River.
- The Olifantsvlei water is purified effluent from the Olifantsvlei wastewater treatment plant, taken before and after the maturation ponds.
- The Plettenberg Bay water is pumped from the Keurbooms River.
- The Rietvlei water is supplied from Rietvlei Dam.
- The Umzonyana water is pumped from the Buffalo River a few kilometres downstream of the Bridle Drift Dam, into a raw water storage dam (about 14 days) adjacent to the treatment plant.
- The Vereeniging water is supplied directly from Vaal Dam.
- The Wiggins water is supplied directly from Inanda Dam.

The purified effluent from Olifantsvlei was included despite it not being a source of drinking water. Many of the problems with NOM in South Africa emanate from eutrophic or hyper-eutrophic rivers and impoundments, where the eutrophication is caused by large return flows from wastewater treatment plants which constitute large fractions of the natural river flows. Although there would be some NOM transformation in the natural systems between discharge and subsequent abstraction for drinking water treatment, it was thought that it would be a useful complementary contribution to measure the profile of the NOM of the treated wastewater as primary driver of eutrophication.

The sampling sites were each visited five times during the project, and each visit was labelled Round 1 to Round 5. After Round 1, the George water treatment plant was replaced with the

Plettenberg Bay water treatment plant to simplify the logistics – their raw water qualities are very similar. The plants were sampled on the dates in Table 2.2.

Table 2.2 Sampling dates

	Round 1 *(Summer- Autumn)*	**Round 2** *(Winter)*	**Round 3** *(Spring)*	**Round 4** *(Summer)*	**Round 5** *(Autumn)*
Loerie	8 Apr 2010	27 Jul 2010	25 Nov 2010	14 Feb 2011	31 May 2011
Midvaal	23 Mar 2010	14 Jul 2010	19 Nov 2010	10 Feb 2011[1]	30 Jun 2011
Olifantsvlei	16 Feb 2010	15 Jul 2010	16 Nov 2010	8 Feb 2011	24 May 2011
P. Bay[2]	(George) 8 Apr 2010	27 Jul 2010	25 Nov 2010	14 Feb 2011	30 May 2011
Rietvlei	9 Mar 2010	15 Jul 2010	16 Nov 2010	8 Feb 2011	24 May 2011
Umzonyana	9 Apr 2010	28 Jul 2010	23 Nov 2010	15 Feb 2011	1 Jun 2011
Vereeniging	9 Feb 2010	14 Jul 2010	19 Nov 2010	10 Feb 2011	30 Jun 2011
Wiggins	10 Apr 2010	29 Jul 2010	22 Nov 2010	17 Feb 2011	3 Jun 2011

[1]Taken during a time of high river flow. [2]Plettenberg Bay

During each sampling event, the temperature, turbidity and conductivity of the water were measured on site. Two small samples were taken (one with acid preservation and the other without), kept cool during travelling and refrigerated in the laboratory, and sent to an external, certified laboratory (WaterLab Research in Pretoria) for analysis. Another 40 ℓ of raw water were taken for the treatability studies required of this project. From the collected data base of analyses, the raw water quality profile for each sampling site could be assembled. The profiles thus represent five independent samples from each site, with the exceptions of Plettenberg Bay (not visited during Round 1) and Loerie (Round 3 sample inadvertently taken when recovered backwash water was blended with the raw water), as shown in Tables 2.3 and 2.4 . A few additional data problems were encountered, described in section 2.2.

The water quality parameters in Tables 2.3 and 2.4 are difficult to interpret. Figures 2.2(a) to 2.2(p) on pages 6 to 11 provide a condensed version in graphical form, indicating the minimum, maximum and median values for all the measured raw water parameters. They are followed by a brief discussion.

Table 2.3 Characteristics of raw waters examined

Sample ID Site & round no.	pH	Temp. (°C)	Turbidity (NTU)	Cond. (mS/cm)	Alkalinity as $CaCO_3$	Calcium hardness as Ca	UV_{254} (m^{-1})	DOC (mg/ℓ)	SUVA ($\ell \cdot m^{-1} \cdot mg^{-1}$)
George 1	6.1	21	14.6	0.19	3	13.2	84.3	13.43	6.28
P. Bay 2*	6.7	13.7	1.9	0.12	3.3	5.1	24.5	7.3	3.36
P. Bay 3	7.7	21.3	1.3	0.07	12	5.6	35.5	9.2	3.86
P. Bay 4	-	26	3.4	0.1	3	4.8	69.5	12.0	5.79
P. Bay 5	-	14.2	8.8	0.12	3	4.0	46.5	15.3	3.04
Loerie 1	7.97	22.6	12.2	0.2	13.6	14.4	23.3	7.45	3.13
Loerie 2	6.9	13.5	7.5	0.27	16	14	14.5	7.1	2.04
Loerie 3	-	-	-	-	-	-	-	-	-
Loerie 4	-	26.2	-	0.28	19	11	11.5	6.9	1.67
Loerie 5	-	15.6	29.7	0.34	18	13	15.5	8.4	1.85
Vereeniging 1	7.15	23.1	48.4	0.19	65	-	23.4	9.64	2.43
Vereeniging 2	-	-	-	-	59	22	17.5	8.3	2.11
Vereeniging 3	7.7	21.1	90.8	-	58	17	15.5	8.0	1.94
Vereeniging 4	8.9	23.8	99.8	0.18	53	15	27.5	9.6	2.86
Vereeniging 5	8.3	10.9	84.3	0.18	47	16	32.5	9.3	3.49
Wiggins 1	7.9	24.9	1.01	0.09	52	20.8	6.2	3.19	1.94
Wiggins 2	8	17.1	3.2	0.23	54	26	4.8	4.6	1.04
Wiggins 3	8.5	23.4	1.5	0.22	58	16	3.5	3.2	1.09
Wiggins 4	-	26.1	1	0.29	58	17	3.6	3.2	1.13
Wiggins 5	-	19.3	1.1	0.29	57	18	4.8	4.3	1.12
Olifantsvlei 1	7.7	22	1.63	-	83	-	9.8	8.99	1.09
Olifantsvlei 2	7.5	15.9	1.9	0.46	93	50	12.5	5.8	2.16
Olifantsvlei 3	8.8	22.9	3.6	0.42	99	43	13.5	7.0	1.93
Olifantsvlei 4	9.6	26	3.6	0.51	88	39	12.5	6.7	1.87
Olifantsvlei 5	7.6	19.4	3.3	0.52	92	43	14.5	9.2	1.58
Rietvlei 1	7.91	22.9	1.99	0.38	111	-	18.8	8.24	2.28
Rietvlei 2	8.07	12.4	1.8	0.42	121	41	13.5	5.9	2.29
Rietvlei 3	9.5	21.3	6.4	0.43	136	44	16.5	9.6	1.72
Rietvlei 4	7.8	21.2	3.6	0.39	97	38	21.5	8.1	2.65
Rietvlei 5	8.9	15.6	4.9	0.38	98	35	16.5	9.7	1.70
Umzonyana 1	8.53	22.9	20.3	0.68	138	46.8	14.2	5.94	2.39
Umzonyana 2	8.2	16.2	35.7	0.68	131	28	12.5	6.2	2.02
Umzonyana 3	8.2	19.6	52.1	0.56	129	29	14.5	7.2	2.01
Umzonyana 4	-	27.1	-	0.55	107	34	16.5	8.0	2.06
Umzonyana 5	-	16.9	88.7	0.41	64	17	22.5	6.7	3.36
Midvaal 1	7.78	22.1	24.8	0.49	103	-	16.3	8.45	1.93
Midvaal 2	-	-	-	-	152	74	13.5	6.1	2.21
Midvaal 3	8.6	23.7	18.1	0.62	136	75	15.5	7.5	2.07
Midvaal 4	8.1	25.7	114	0.27	67	31	33.5	10.0	3.35
Midvaal 5	9.7	10.8	18.9	0.72	153	61	14.5	8.4	1.73

* P. Bay = Plettenberg Bay

Table 2.4 WaterLab Research results

Sample ID*	Colour (PtCo)	Total hardness as $CaCO_3$ (mg/ℓ)	Cl (mg/ℓ)	SO_4 (mg/ℓ)	Nitrate as N (mg/ℓ)	Nitrite as N (mg/ℓ)	Ortho-phosphate as P (mg/ℓ)	Kjeldahl Nitrogen (mg/ℓ)	Free & saline ammonia as N (mg/ℓ)	Na (mg/ℓ)	K (mg/ℓ)	Mg (mg/ℓ)	Al (mg/ℓ)	Fe (mg/ℓ)	Mn (mg/ℓ)
George 1	365	33	58	7	0.2	<0.1	<0.2	0.8	<0.2	23	<1.0	4	0.566	3.58	0.206
P. Bay 2*	92	17	39	8	<0.2	<0.1	<0.2	0.8	<0.2	18	<1.0	3	0.243	0.228	<0.025
P. Bay 3	151	11	25	<5	<0.2	<0.1	<0.2	0.3	0.3	9	<1.0	2	0.232	0.446	0.036
P. Bay 4	262	12	22	<5	<0.2	<0.1	<0.2	0.3	<0.2	11	<1.0	2	0.337	0.74	<0.025
P. Bay 5	126	13	43	13	1.3	<0.1	<0.2	1.7	<0.2	24	<1.0	3	0.991	1.14	<0.025
Loerie 1	91	36	49	7	0.3	<0.1	<0.2	0.8	<0.2	24	1.8	5	0.501	1.64	0.071
Loerie 2	62	37	67	13	0.5	<0.1	<0.2	0.3	<0.2	35	1.8	6	0.212	0.632	0.099
Loerie 3	10	460	70	11	0.3	<0.1	<0.2	0.3	0.2	35	2.2	3	0.949	0.16	<0.025
Loerie 4	31	94	81	17	1.1	<0.1	<0.2	0.8	<0.2	64	4.5	12	0.206	0.276	0.062
Loerie 5	44	55	79	13	0.3	<0.1	<0.2	2	<0.2	43	2.1	7	0.456	<0.025	0.218
Vereeniging 2	-	65	9	24	0.4	<0.1	<0.2	1.1	<0.2	9	3.4	8	1.5	1.74	0.04
Vereeniging 3	-	69	11	21	0.4	<0.1	<0.2	0.3	0.3	7	3.9	8	1.8	3.28	0.064
Vereeniging 4	-	61	11	23	0.5	<0.1	<0.2	0.6	<0.2	9	3.6	7	1.23	1.65	0.07
Vereeniging 5	-	67	11	26	0.4	<0.1	<0.2	1.4	<0.2	11	4.2	8	0.784	0.067	0.052
Wiggins 1	12	52	27	11	0.8	<0.1	<0.2	<0.2	<0.2	19	2.3	6	<0.100	0.047	<0.025
Wiggins 2	9	55	29	16	0.8	<0.1	<0.2	0.8	<0.2	24	2.6	6	<0.100	0.054	0.041
Wiggins 3	12	75	33	16	1	<0.1	<0.2	0.6	0.3	23	3.5	8	<0.100	0.054	0.029
Wiggins 4	7	60	34	17	0.5	<0.1	<0.2	0.3	<0.2	27	2.6	6	<0.100	0.033	0.032
Wiggins 5	9	65	33	17	0.2	<0.1	<0.2	0.3	<0.2	29	3.2	7	<0.100	5.92	0..172
Olifantsvlei 2	31	105	51	41	4.3	<0.1	0.3	1.1	<0.2	46	9.1	10	<0.100	0.058	0.044
Olifantsvlei 3	28	141	51	44	2.8	<0.1	0.2	1.1	0.2	39	13.3	10	<0.100	0.057	0.070
Olifantsvlei 4	-	89	16	35	0.6	<0.1	<0.2	0.3	<0.2	14	4.2	10	1.24	1.78	0.169
Olifantsvlei 5	34	141	46	61	4	<0.1	0.2	1.4	<0.2	48	9.9	12	<0.100	0.437	0.046
Rietvlei 2	28	132	35	33	1.6	<0.1	0.2	3.4	<0.2	32	6.7	15	<0.100	0.137	0.06
Rietvlei 3	35	189	47	47	1	<0.1	0.2	0.3	<0.2	43	12.7	20	<0.100	0.111	0.062
Rietvlei 4	44	109	25	33	0.9	<0.1	0.3	1.1	<0.2	23	5.8	12	<0.100	0.195	0.279
Rietvlei 5	32	131	30	37	0.5	<0.1	<0.2	0.8	0.6	29	6.6	15	<0.100	0.805	0.041
Umzonyana 1	28	117	121	18	0.5	<0.1	<0.2	<0.2	<0.2	88	4.9	15	0.318	0.293	0.081
Umzonyana 2	51	112	119	25	0.6	<0.1	<0.2	0.6	<0.2	84	4.6	15	0.246	0.369	0.058
Umzonyana 3	28	153	96	20	0.7	<0.1	<0.2	0.3	0.3	7	6.6	20	<0.100	<0.025	<0.025
Umzonyana 4	24	123	45	49	4.4	<0.1	<0.2	0.6	<0.2	41	9.6	10	<0.100	0.034	0.037
Umzonyana 5	79	76	63	19	0.8	<0.1	<0.2	0.8	<0.2	48	9.9	12	<0.100	0.043	0.113
Midvaal 2	33	235	58	112	1.3	<0.1	0.5	2.2	<0.2	49	8.1	25	0.146	0.172	0.124
Midvaal 3	37	215	61	57	0.5	<0.1	5	0.3	0.3	44	11.6	21	0.23	0.391	0.276
Midvaal 4	18	36	61	8	0.3	<0.1	<0.2	<0.2	<0.2	31	1.6	5	<0.100	0.611	0.159
Midvaal 5	49	249	55	106	1.4	<0.1	<0.2	1.7	<0.2	51	9.1	27	0.658	0.458	0.115

*Plettenberg Bay. Samples Vereeniging 1, Olifantsvlei 1, Rietvlei 1 and Midvaal 1 were not tested by WaterLab.

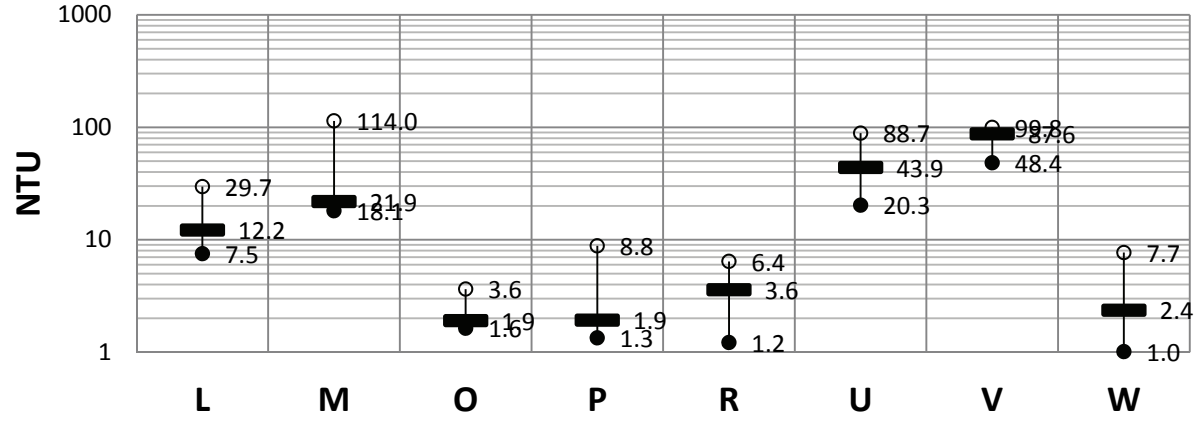

L = Loerie, M = Midvaal, O = Olifantsvlei, P = Plettenberg Bay, R = Rietvlei, U = Umzonyana, W = Wiggins.

Figure 2.2 (a) Summary of raw water turbidity.

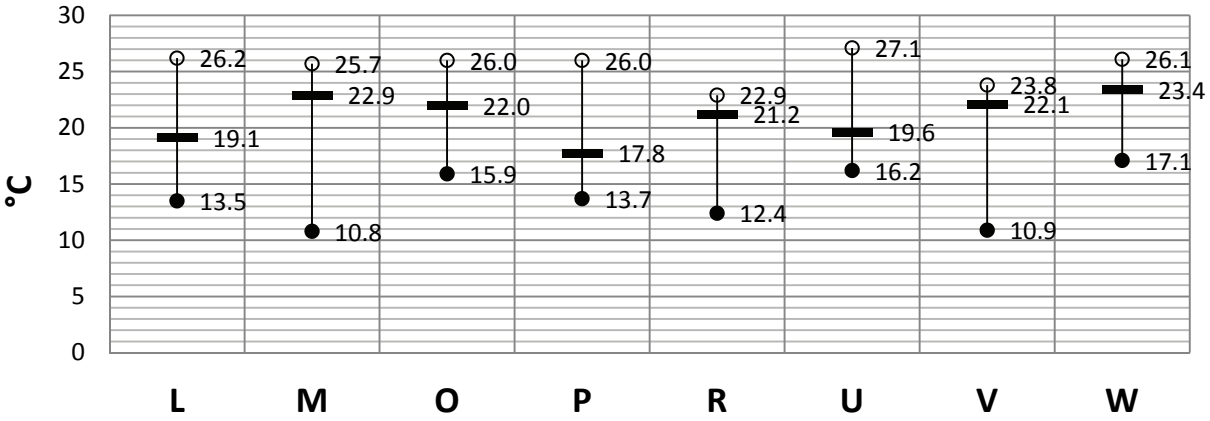

L = Loerie, M = Midvaal, O = Olifantsvlei, P = Plettenberg Bay, R = Rietvlei, U = Umzonyana, W = Wiggins.

Figure 2.2 (b) Summary of raw water temperature

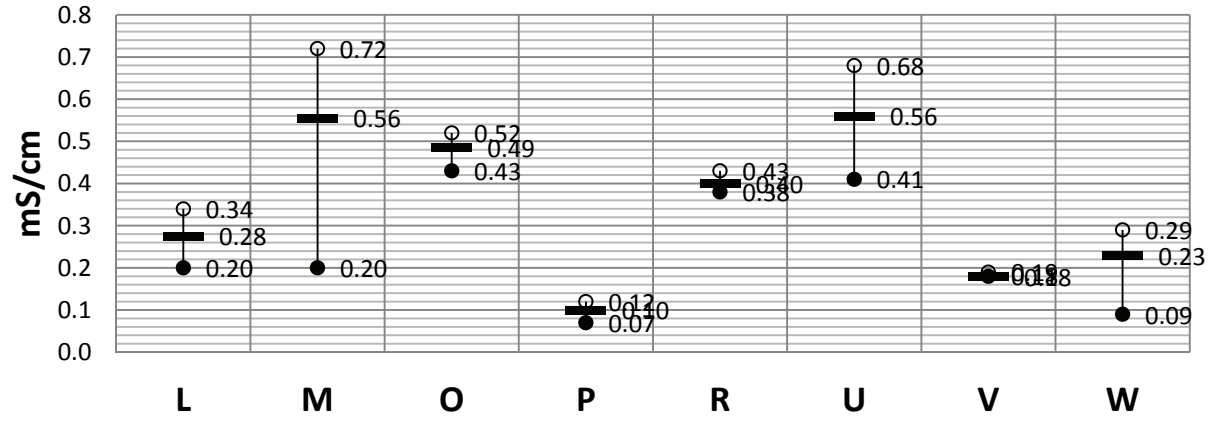

L = Loerie, M = Midvaal, O = Olifantsvlei, P = Plettenberg Bay, R = Rietvlei, U = Umzonyana, W = Wiggins.

Figure 2.2 (c) Summary of raw water conductivity

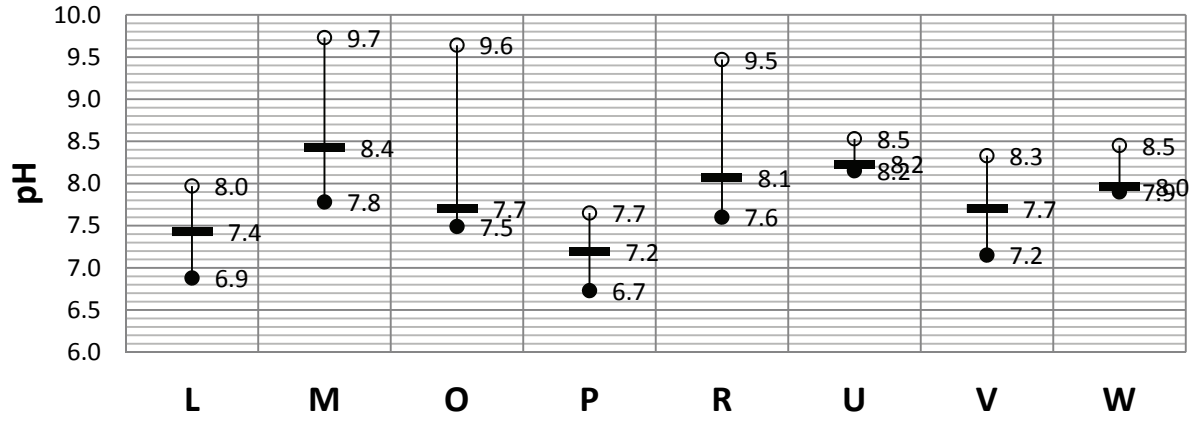

L = Loerie, M = Midvaal, O = Olifantsvlei, P = Plettenberg Bay, R = Rietvlei, U = Umzonyana, W = Wiggins.

Figure 2.2 (d) Summary of raw water pH

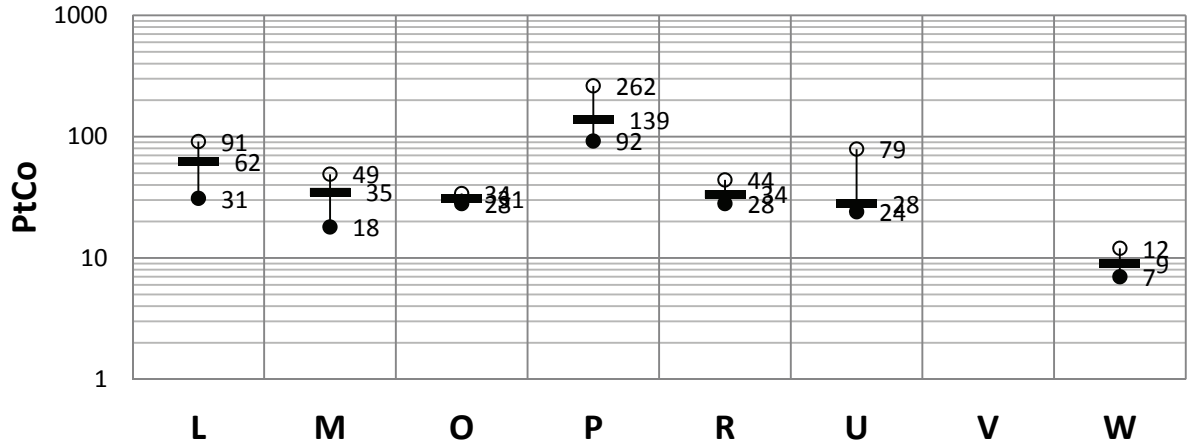

L = Loerie, M = Midvaal, O = Olifantsvlei, P = Plettenberg Bay, R = Rietvlei, U = Umzonyana, W = Wiggins.

Figure 2.2 (e) Summary of raw water colour

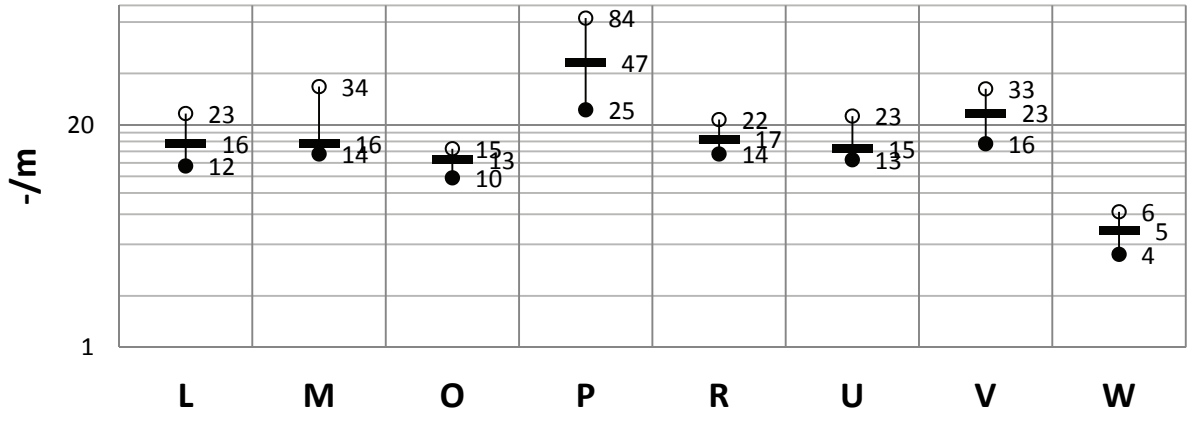

L = Loerie, M = Midvaal, O = Olifantsvlei, P = Plettenberg Bay, R = Rietvlei, U = Umzonyana, W = Wiggins.

Figure 2.2 (f) Summary of raw water UV_{254}

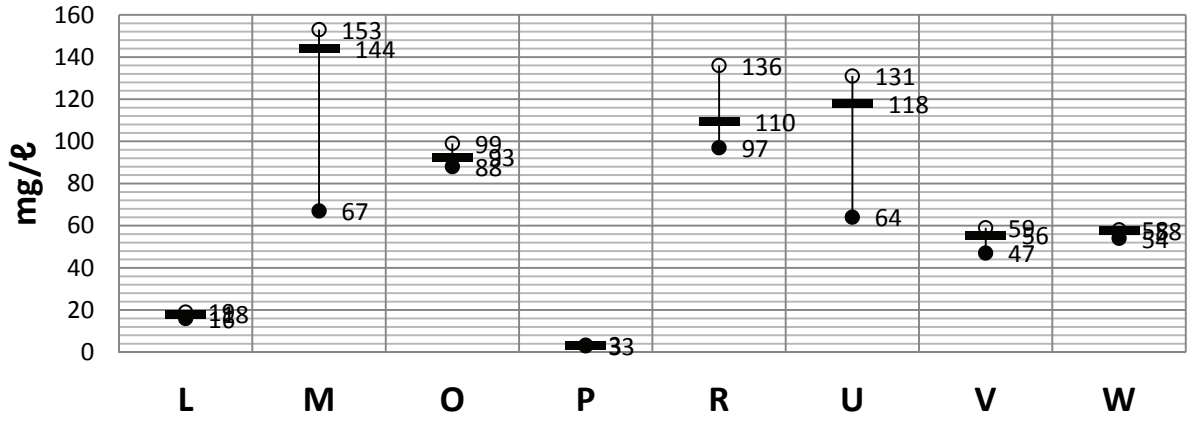

L = Loerie, M = Midvaal, O = Olifantsvlei, P = Plettenberg Bay, R = Rietvlei, U = Umzonyana, W = Wiggins.

Figure 2.2 (g) Summary of raw water alkalinity

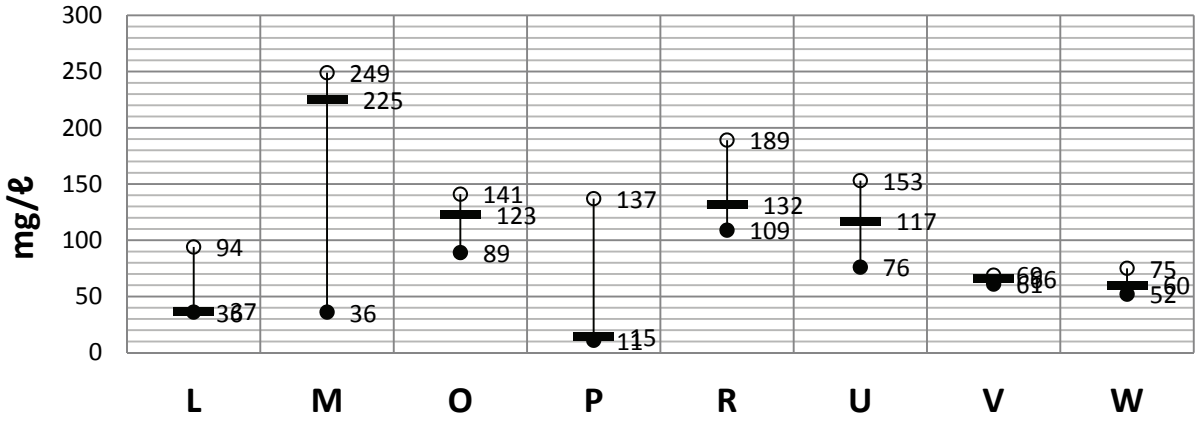

L = Loerie, M = Midvaal, O = Olifantsvlei, P = Plettenberg Bay, R = Rietvlei, U = Umzonyana, W = Wiggins.

Figure 2.2 (h) Summary of raw water hardness

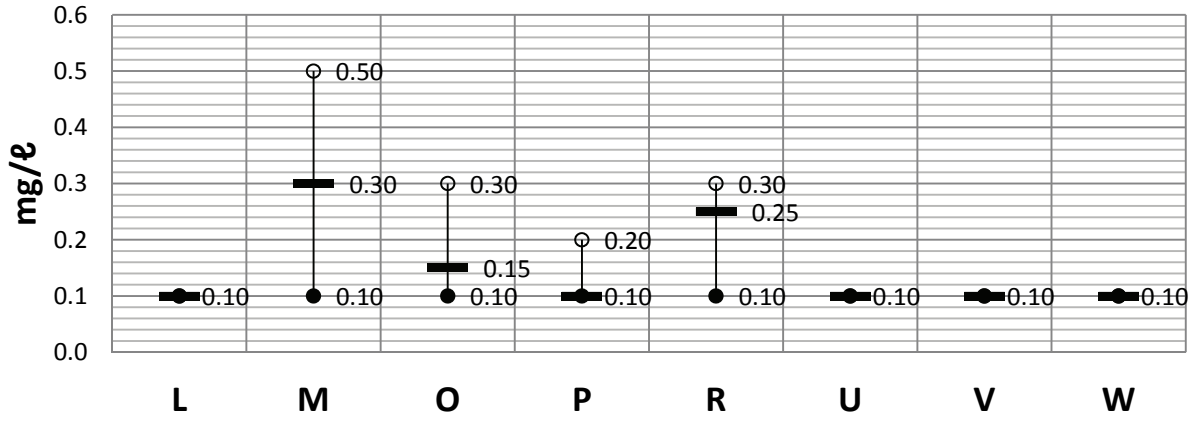

L = Loerie, M = Midvaal, O = Olifantsvlei, P = Plettenberg Bay, R = Rietvlei, U = Umzonyana, W = Wiggins.

Figure 2.2 (i) Summary of raw water orthophosphate

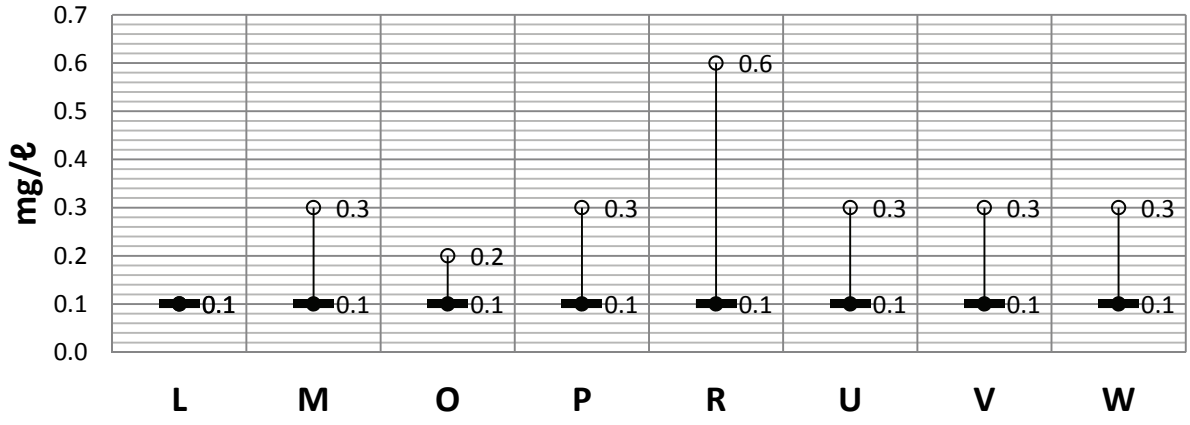

L = Loerie, M = Midvaal, O = Olifantsvlei, P = Plettenberg Bay, R = Rietvlei, U = Umzonyana, W = Wiggins.

Figure 2.2 (j) Summary of raw water ammonia (NH_3)

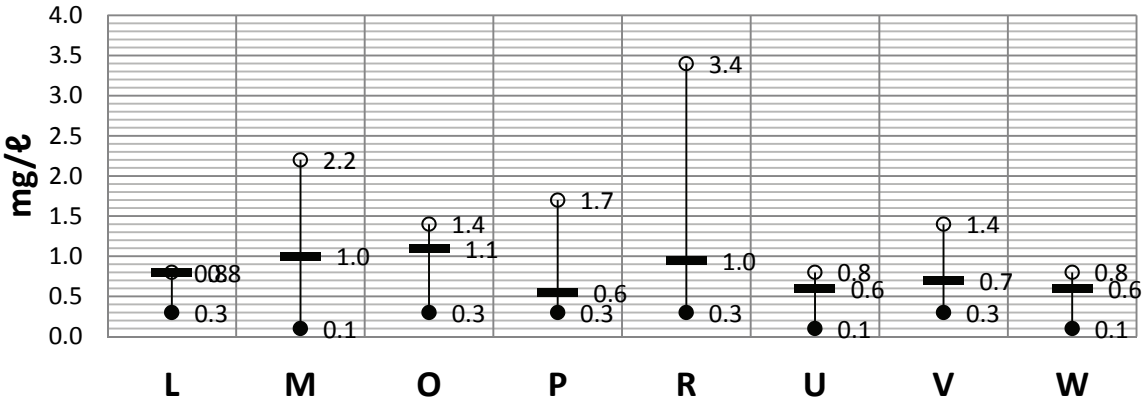

L = Loerie, M = Midvaal, O = Olifantsvlei, P = Plettenberg Bay, R = Rietvlei, U = Umzonyana, W = Wiggins.

Figure 2.2 (k) Summary of raw water nitrate and nitrite (N)

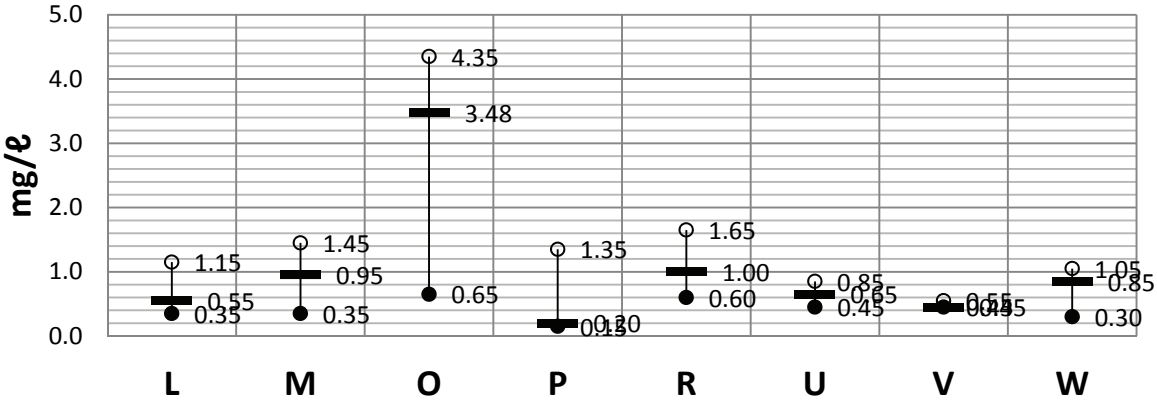

L = Loerie, M = Midvaal, O = Olifantsvlei, P = Plettenberg Bay, R = Rietvlei, U = Umzonyana, W = Wiggins.

Figure 2.2 (l) Summary of raw water total Kjeldahl nitrogen (TKN) as N

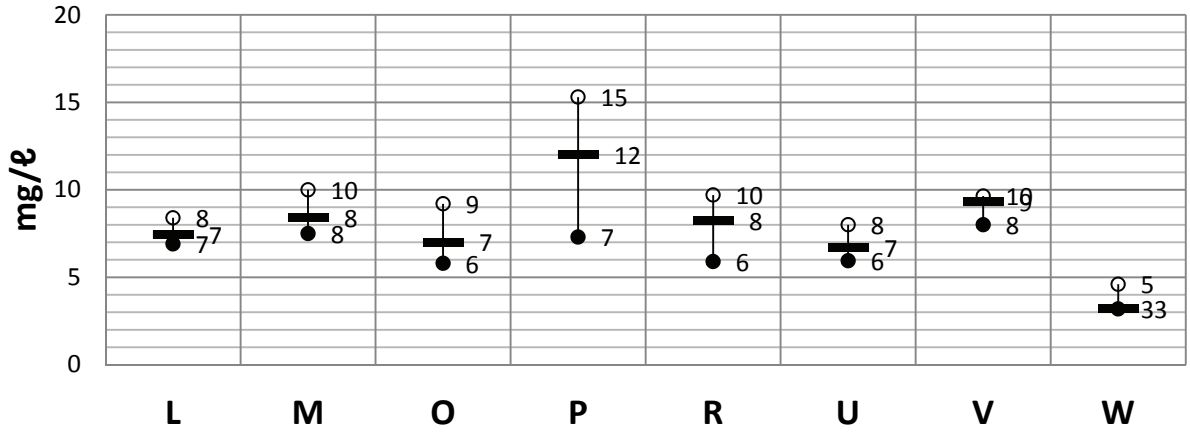

L = Loerie, M = Midvaal, O = Olifantsvlei, P = Plettenberg Bay, R = Rietvlei, U = Umzonyana, W = Wiggins.

Figure 2.2 (m) Summary of raw water DOC

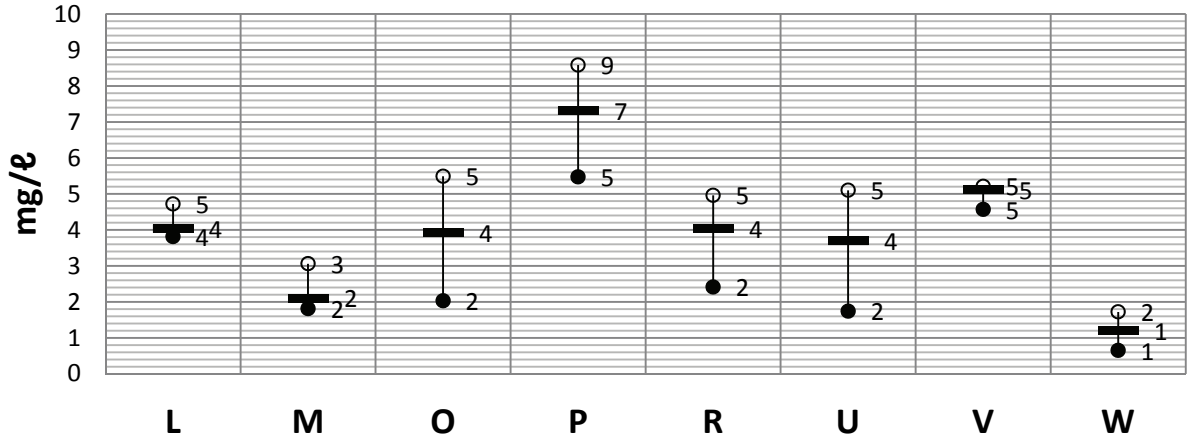

L = Loerie, M = Midvaal, O = Olifantsvlei, P = Plettenberg Bay, R = Rietvlei, U = Umzonyana, W = Wiggins.

Figure 2.2 (n) Summary of raw water biodegradable DOCs (BDOC)

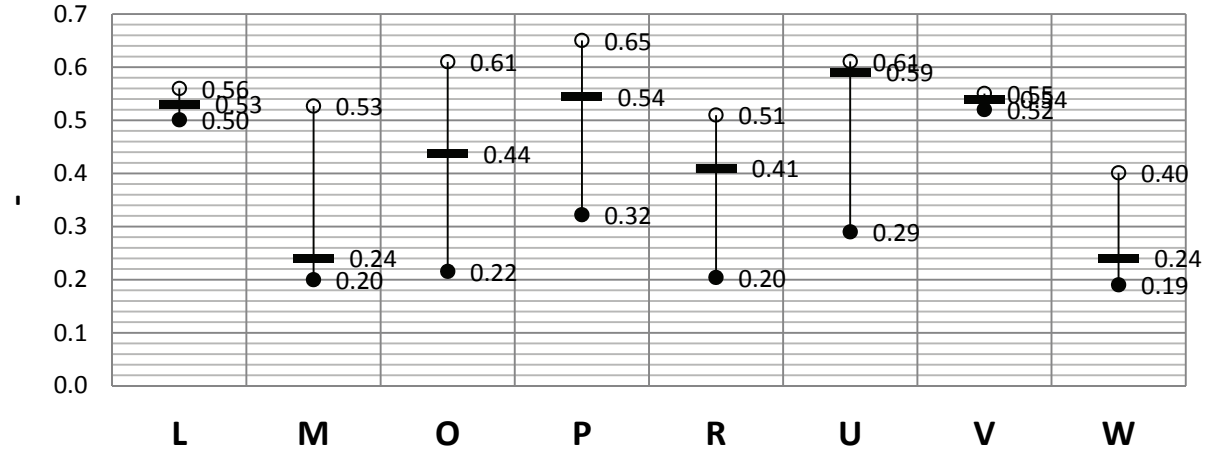

L = Loerie, M = Midvaal, O = Olifantsvlei, P = Plettenberg Bay, R = Rietvlei, U = Umzonyana, W = Wiggins.

Figure 2.2 (o) Summary of raw water biodegradable fractions (BDOC/DOC)

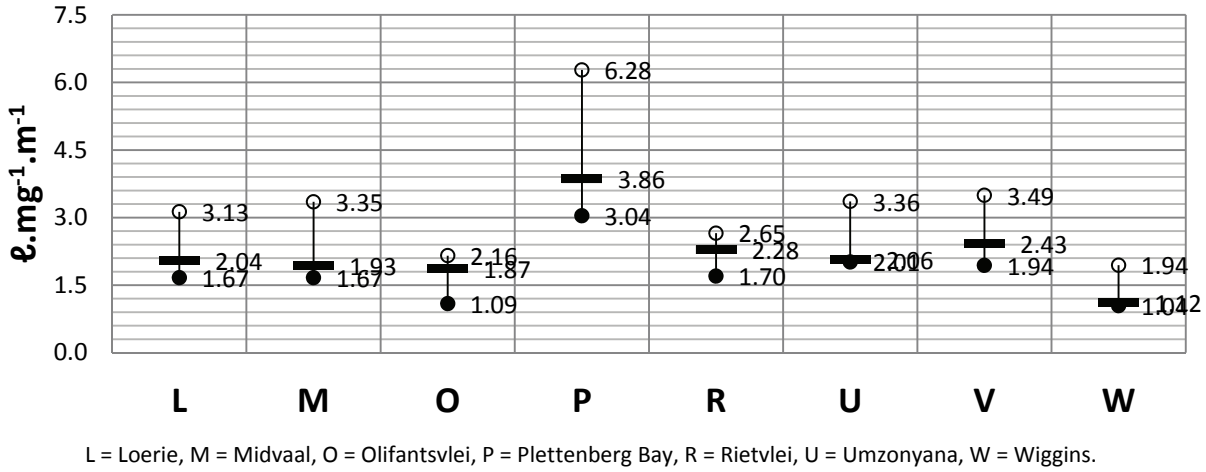

L = Loerie, M = Midvaal, O = Olifantsvlei, P = Plettenberg Bay, R = Rietvlei, U = Umzonyana, W = Wiggins.

Figure 2.2 (p) Summary of raw water specific UV absorbance (SUVA)

2.2 Physical Parameters

2.2.1 Temperature

The temperature values are quite close together, with the median temperatures slightly lower for the three mountain catchments (Loerie; Plettenberg Bay; Umzonyana). The waters on the Highveld were the coldest (Midvaal; Rietvlei; Vereeniging) and the water from the large coastal impoundment the warmest (Wiggins).

2.2.2 Turbidity

The removal of turbidity by any treatment process is important for subsequent treatment processes. The site turbidimeter malfunctioned during Rounds 2 (Midvaal and Vereeniging) and 4 (Plettenberg Bay, Loerie, Umzonyana and Wiggins) and those data points were eliminated. The turbidity graph suggests three turbidity categories, namely high (Umzonyana; Vereeniging), medium (Loerie; Midvaal) and low (Olifantsvlei; Plettenberg Bay; Rietvlei; Wiggins)

2.2.3 pH

Many researchers have found pH to be the parameter having the greater effect on achieving maximal NOM removal by coagulation (Bell-Ajy *et al*., 2000; Sharp *et al*., 2006; Yu *et al*., 2007). The dependence of coagulant performance on pH can be linked to the varying distribution of the metal coagulants' species, and their hydrolyzing behaviour in raw water with low temperature (Yu *et al*., 2007). This can be explained in terms of the different mechanisms in which coagulation occurs (i.e. charge neutralisation, adsorption and sweep coagulation). The monomeric positively-charged ion species of the metallic salts, particularly $AlCl_3$ and $FeCl_3$, dominate under acidic pH conditions. These ions are capable of combining with the acidic functional groups of NOM via charge neutralisation to form soluble organic complexes (Cheng, 2002).

The off-site pH values should be interpreted with caution, as they were taken after some time in storage. As they are, they show higher pH for eutrophic sources (Midvaal; Olifantsvlei; Rietvlei) and lowest for the coastal mountain catchments (Plettenberg Bay; Loerie).

2.2.4 Conductivity

The conductivity graph shows large variations for the waters taken directly from the rivers (Midvaal; Umzonyana). The water from the large impoundments and wastewater treatment plant varied least.

2.2.5 Colour

The colour from the coastal river in the Southern Cape is extremely high (Plettenberg Bay), while the water from a larger impoundment some distance inland shows medium colour (Loerie). The others have typical colour values, with the water from the Drakensberg escarpment having very low colour (Wiggins).

2.2.6 Alkalinity

The alkalinity of water is a measure of its capacity to neutralise acids. The alkalinity of natural water is primarily due to the salts of weak acids, although weak or strong bases may also contribute. It is a significant parameter in the treatment of natural and wastewaters. Since alkalinity is generally a function of carbonate, bicarbonate, and hydroxide content, it is therefore taken as an indication of the concentration of these constituents (Sawyer and McCarty, 1967; APHA *et al*., 1985).

The alkalinity values suggest three categories – low alkalinity (Loerie; Plettenberg Bay), medium alkalinity (Vereeniging; Wiggins) and high alkalinity (Midvaal; Olifantsvlei; Rietvlei; Umzonyana).

2.2.7 Hardness

The hardness values suggest three categories – low hardness (Loerie; Plettenberg Bay; Vereeniging; Wiggins), medium hardness (Olifantsvlei; Rietvlei; Umzonyana) and high hardness (Midvaal).

2.2.8 Orthophosphate

The detection limit of orthophosphate hinders the interpretation of the orthophosphate data somewhat, but the values are generally low, except for the two eutrophic sources (Midvaal; Rietvlei) as anticipated.

2.2.9 The nitrogen species

The nitrogen cycle in natural waters is complex. Three parameters were included to obtain a better understanding, namely ammonia/ammonium (usually indicating some evidence of raw sewage or anaerobic conditions in the hypolimnion), nitrite and nitrates (some evidence of ammonia oxidation or nitrification) and total Kjeldahl nitrogen (TKN – organic nitrogen plus ammonia/ammonium). The graphs of these three parameters show that one water source had alarmingly high ammonia levels (Rietvlei) while the treated wastewater showed evidence of nitrification (Olifantsvlei). The two eutrophic water sources (Midvaal; Rietvlei) had the highest levels of TKN.

2.3 Natural Organic Matter Parameters

2.3.1 Ultraviolet absorbance

The UVA_{254} values are remarkably similar, with the exceptions of one high value (Plettenberg Bay) and one low value (Wiggins). All samples were filtered with small-diameter membrane filters

before UVA analysis. When the raw water turbidity was high, these filters did not work well. In an attempt to improve matters, a different type of filter paper was used for Round 4 samples, which did not work at all. The results for Round 4 (suspect filter paper) and all the results for plant Vereeniging (high turbidity) therefore had to be discarded.

Ultraviolet absorbance is an important NOM indicator recommended as the simplest and most practical routine parameter for use at treatment plants, especially small ones. Some aspects of UVA measurement are discussed next. Initially, the absorbance measurements were made at four different wavelengths. The wavelengths were 214 nm (indicative of nitrite and nitrate), 254 nm (the usual indicator for double bonds), 272 nm (reported in the literature be the [marginally] best predictor for THM formation) and 300 nm (used as a secondary indicator for colour, amongst others by Rand Water). The readings at 214 nm were erratic and ignored. Which of the remaining wavelengths would be the best to use? Table 2.5 shows the readings at 272 and 300 nm, expressed as a fraction of the absorbance at 254 nm. All the fractions available for each sampling site were averaged over Rounds 1 to 5. The ratios in the table show little variation and are probably not statistically significant. It therefore does not seem to matter which wavelength is used – the relative removal would be about the same, regardless of which wavelength is used. As UVA_{254} is the most commonly reported wavelength in the international literature, it was selected for all the UVA values reported for this project.

Table 2.5 Ratios between UVA readings

	UVA_{272}/UVA_{254}	**UVA_{300}/UVA_{254}**
Loerie	84%	56%
Midvaal	85%	56%
Olifantsvlei	82%	53%
Plettenberg Bay	86%	62%
Rietvlei	82%	53%
Umzonyana	82%	51%
Vereeniging	84%	55%
Wiggins	82%	53%
Mean	83%	55%

It was unavoidable to store some samples for longer periods while awaiting the different treatability and characterisation tests by different members of the project team. How were the UVA values affected by prolonged cold storage at 4°C? An extensive database was built up with UVA measurements taken from the same samples at different times. Three representative samples are shown in Figures 2.3 (a) to (c), with the respective UVA measurements shown over time. The readings at the other wavelengths were similarly stable for all the samples. The longer periods of refrigeration, which are unavoidable for this project, do not seem to invalidate any of the readings taken at wavelengths 254, 272 and 300 nm.

2.3.2 Dissolved organic carbon (DOC)

The concentration of NOM in all water samples was determined by measuring DOC levels with a total organic carbon (TOC) analyzer. Similar to the UVA_{254} values, the values were similar, except for Plettenberg Bay (high) and Wiggins (very low).

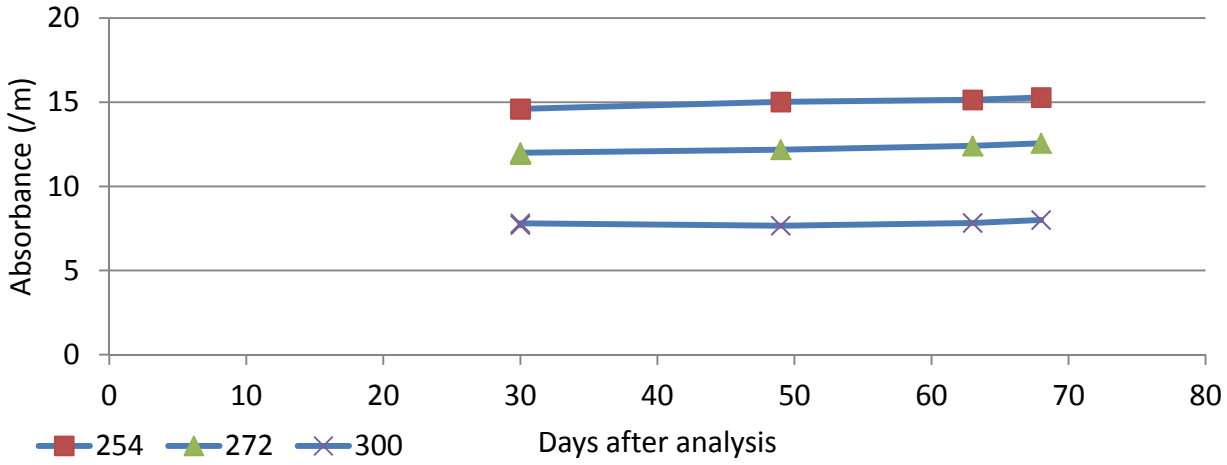

Figure 2.3 (a) Variation in UVA at three different wavelengths (254, 272 and 300 nm) with time in cold storage (raw water sample from Loerie taken during round 4)

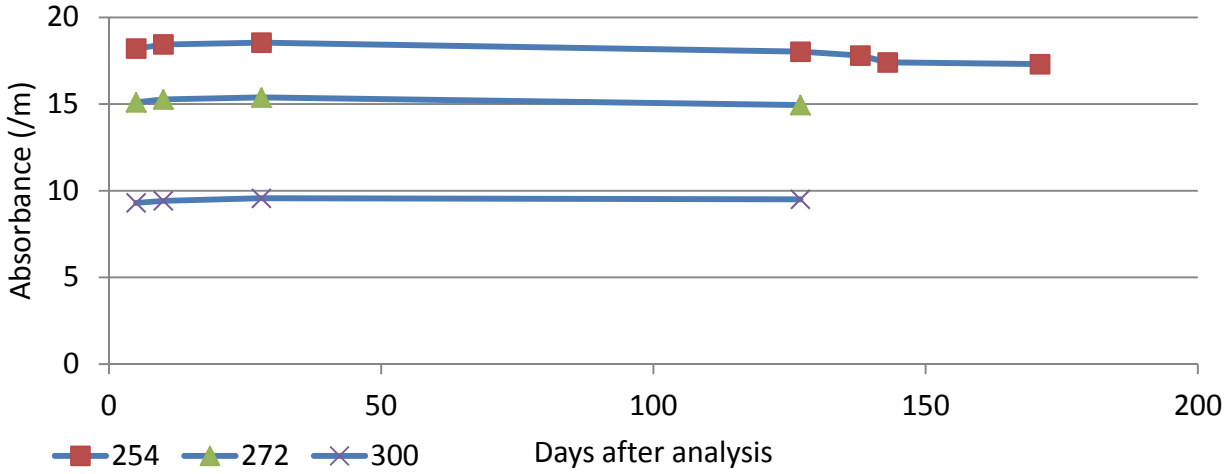

Figure 2.3 (b) Variation in UVA at three different wavelengths (254, 272 and 300 nm) with time in cold storage (raw water sample from Midvaal taken during round 4)

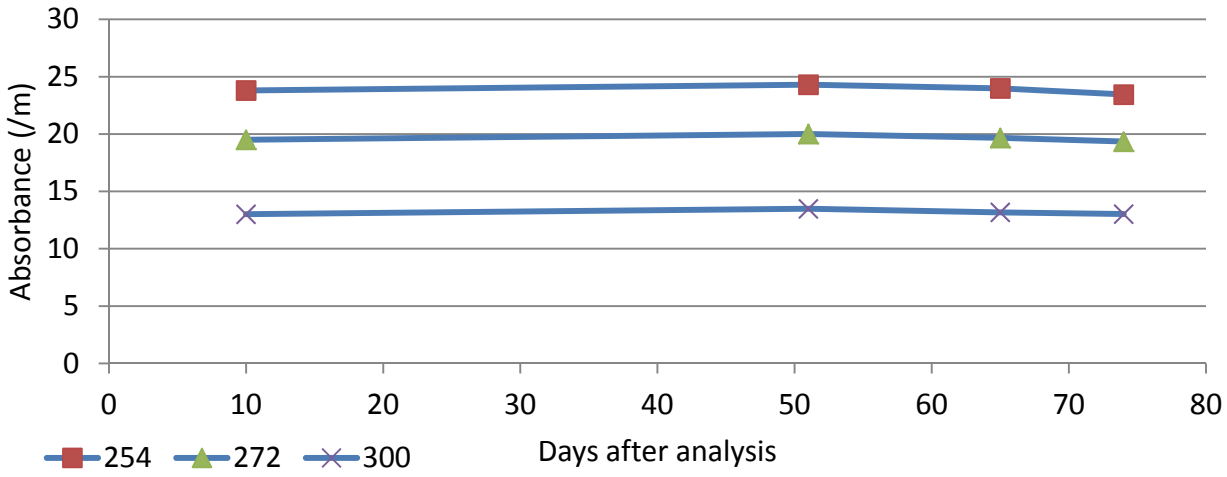

Figure 2.3 (c) Variation in UVA at three different wavelengths (254, 272 and 300 nm) with time in cold storage (raw water sample from Rietvlei taken during round 4)

2.3.3 Specific UV absorbance (SUVA)

The ratio of UVA_{254} to DOC (SUVA), illustrated in equation 2.1, gives an indication of the aromaticity or the hydrophobicity of NOM as well as the concentration of humic substances relative to non-humic substances of the water samples (Edzwald and Haarhoff, 2012).

$$SUVA\ \left(\frac{l}{m \cdot mg}\right) = \frac{UV_{254}(m^{-1})}{DOC(\frac{mg}{l})} \tag{2.1}$$

Various studies showed that coagulation preferentially removes the high molecular weight, hydrophobic humic acid fractions of NOM. Specific ultraviolet absorbance may therefore provide insight on the treatability of water by coagulation (Weishaar *et al.*, 2003). The composition of NOM for source waters is presented in Table 2.6, with respect to three different SUVA ranges.

Table 2.6 Characterisation of NOM and TOC removals for SUVA values for raw water supplies (Edzwald and Tobiason, 2011)

SUVA/m	Composition	Effects	TOC removal by coagulation
>4	High fraction of aquatic humic matter High aromatic and hydrophobic character High molecular weight (MW)	High UVA	60- 80% Higher end for waters with high TOC
2-4	Mixture of aquatic humic and non-humic matter Mixture of aliphatic and aromatic character Mixture of low to high MW	Medium UVA	40-60% Higher end for waters with high TOC
<2	High fraction of non-humic matter High aliphatic and low hydrophobic character Low MW	Low UVA	20-40% Higher end for waters with high TOC

Only one of the samples (Plettenberg Bay) was in the high SUVA range, where good removal with enhanced coagulation (EC) can be expected. Two samples (Olifantsvlei and Wiggins) were in the low range where EC was not expected to do well at all, with the remaining five in the intermediate range.

2.3.4 Biodegradable organic carbon (BDOC)

The BDOC values, viewed in isolation, do not provide much insight on their own. The BDOC/DOC ratio is more meaningful. Figure 2.2(o) provides new and interesting insights not seen before. It is striking that three sites (Loerie, Umzonyana and Vereeniging) showed very little variation throughout the sampling period, with values constantly between 50% and 60%. These waters came from large impoundments with minimal return flows to their catchments. The other samples showed much higher variability – it is noted that the samples were taken from rivers, impoundments with high return flows, or from a wastewater treatment plant. The surprising observation is that the upper end of each range was roughly in the region 50% to 60% (Wiggins is lower), but that large variances were found towards the lower end of the range, where the biodegradable fraction was lower. No clear explanation is offered at this point.

2.3.5 Resin fractionation (polarity rapid assessment method)

The Modified polarity rapid assessment method (PRAM), instead of producing all six NOM fractions of the original PRAM method, only provides three fractions, but is a more rapid method of NOM characterisation. This method quantifies the hydrophobic (HPO), the hydrophilic (HPI) and the transphilic (TPI) NOM fractions. This detailed fractionation of NOM should provide information to water treatment practitioners about the dominant fraction in the NOM and, thus, employ appropriate treatment methods. If, for example, a particular NOM fraction accounts for a high THM formation potential, such a fraction should be removed before disinfecting the water with chlorine.

The hydrophilic fraction has more affinity for water and is composed mainly of low molecular weight carbohydrates, proteins and amino acids. The hydrophobic fraction has less affinity for water (making it more soluble in organic solvents) and consists mainly of humic and fulvic acids. Not all the samples were fractionated using the Modified PRAM as this method first had to be modified and optimized to be able to give reliable fractionation, which took a long time to achieve. Figure 2.4 and Figure 2.5 show the distribution of the NOM fractions of the Plettenberg Bay 1 and Rietvlei 1 samples over the three rounds of sampling. As previously discussed in earlier sections, the Plettenberg Bay samples had mostly hydrophobic NOM and it thus can be concluded from Figure 2.4 that a large fraction of the NOM sample was the HPO. This finding is in agreement with earlier analysis where the NOM sample from the Plettenberg Bay samples was found to contain hydrophobic NOM, which were mainly humic substances.

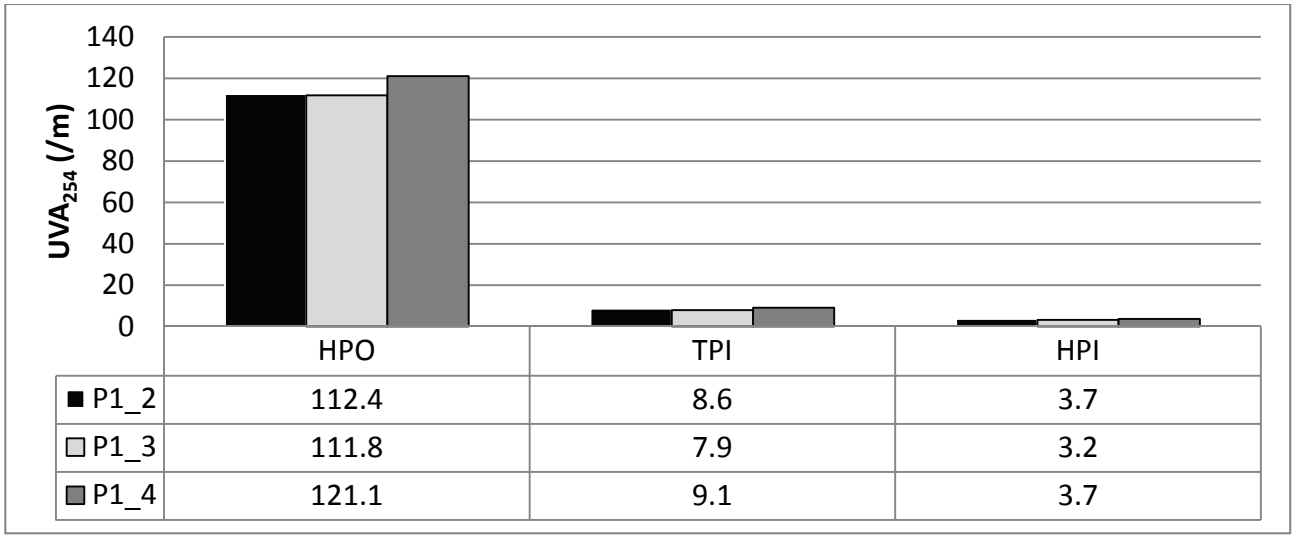

	HPO	TPI	HPI
P1_2	112.4	8.6	3.7
P1_3	111.8	7.9	3.2
P1_4	121.1	9.1	3.7

Figure 2.4 Distribution of NOM fractions of the Plettenberg Bay 1 raw water samples (rounds 2, 3 and 4), obtained after PRAM fractionation

The Rietvlei samples, on the other hand, had almost equal distribution of the different NOM fractions, as can be seen in Figure 2.5. There is almost a 50%-50% spread between the TPI and the HPI fraction, with slightly higher amounts of the HPO fraction.

The DOC-fraction distribution varied substantially depending on the type of source water and type of treatment processes employed. At the Plettenberg Bay water treatment plant, it was found that the HPO fraction in the NOM was the most dominant ranging from 32–74% in DOC, whereas the TPI appeared to be the second most abundant fraction, constituting between 3–28% of the total NOM samples.

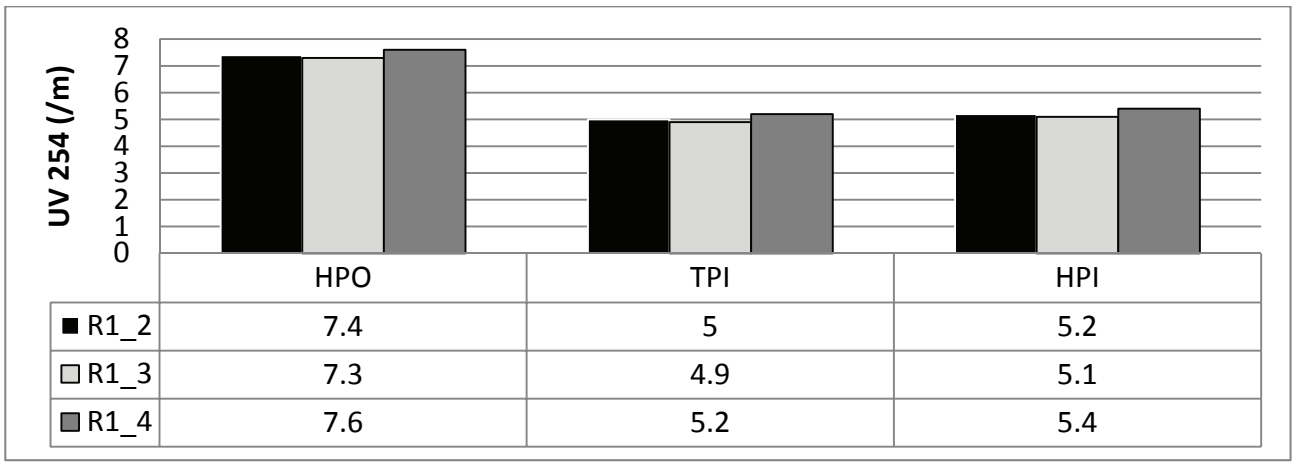

Figure 2.5 Distribution of NOM fractions of the Rietvlei 1 raw water samples from rounds 2, 3 and 4, obtained after PRAM fractionation

The rest of the samples (Loerie, Umzonyana, Vereeniging, Wiggins and Midvaal) had an almost equal distribution of the three fractions as can be seen from Table 2.7, which gives a summary of samples' NOM fractions distribution of the Loerie, Umzonyana, Vereeniging, Wiggins and Midvaal samples.

Table 2.7 A summary of the NOM fractions' distribution for the Loerie, Umzonyana, Vereeniging, Wiggins and Midvaal raw water samples

Sample and round no.	HPO	TPI	HPI
Loerie 2	8.4	7.9	6.4
Loerie 3	8.3	7.8	6.5
Loerie 4	8.6	7.4	6.1
Umzonyana 2	5.4	6.1	5.7
Umzonyana 3	5.9	6.3	5.4
Umzonyana 4	5,5	6.6	5.2
Vereeniging 2	9.1	8.2	8.1
Vereeniging 3	9.3	8.2	8.5
Vereeniging 4	9.3	8.1	8.4
Wiggins 2	3.2	3.2	3.5
Wiggins 3	3.5	3.6	3.3
Wiggins 4	3.1	3.5	3.2
Midvaal 2	7.2	6.6	7.1
Midvaal 3	7.3	6.5	7.0
Midvaal 4	7.1	6.3	7.2

2.3.6 Fluorescence emission excitation matrices (FEEMs)

The FEEM method is a technique for distinguishing between humic substances of various origins and nature (Chen *et al.*, 2003). Fluorescence EEM measurements were conducted using a Horiba AquaLog Spectrometer. The spectrometer displayed a maximum emission intensity of 1000 arbitrary units (AU). The spectrometer uses a xenon excitation source and excitation and emission slits are set to a 10 nm band pass.

To obtain FEEMs, excitation wavelengths were incrementally increased from 200 nm to 600 nm at 5 nm band pass; for each excitation wavelengths, the emission at longer wavelengths was detected at 0.3 nm steps.

To partially account for Raleigh scattering, the fluorometer's response to a blank solution was subtracted from the fluorescence spectra of the sample to be analysed. De-ionised water, with known concentrations of DOC, was used as a blank solution. Absorbance of light from the lamp by DOC molecules in the sample was accounted for by using an inner-filter correction applied to the data by using UV-Vis spectral data from the blank. The AquaLog is equipped with a reference detector to monitor and correct both the excitation source's spectrum for the emission detector and the absorbance signals. A transmission detector is attached to the sample compartment to record the sample's transmission/absorbance spectrum under the same spectral-band pass and resolution conditions as the fluorescence EEM data. The corrected EEMs were then plotted using Origins Lab, supplied with the instrument, with 20 contour lines, each contour interval representing 1/20th of the maximum fluorescence intensity.

Figure 2.6 shows the location of FEEM peaks based on literature reports at operationally defined excitation and emission wavelength boundaries of the FEEM regions (Chen *et al.*, 2003). By comparing the data obtained against standard literature Fluorescence Emission-Excitation data, important inferences of NOM characteristics can be drawn.

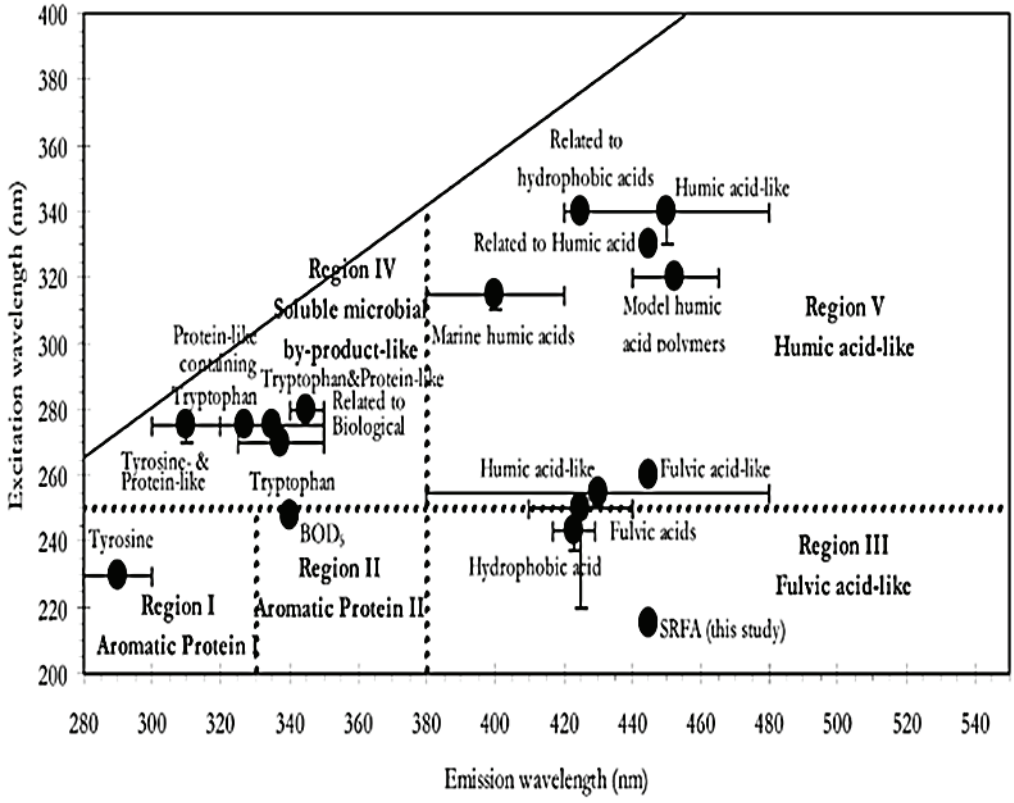

Figure 2.6 FEEM "regions" based on literature reports and operationally defined excitation and emission wavelength boundaries (Chen *et al.*, 2003)

Fluorescence emission excitation matrices attempt to give the structural information of NOM based on the UV absorption of the molecular group. Only the Loerie, George, Wiggins and Umzonyana raw water samples were analysed for their fluorescence properties (Figure 2.7).

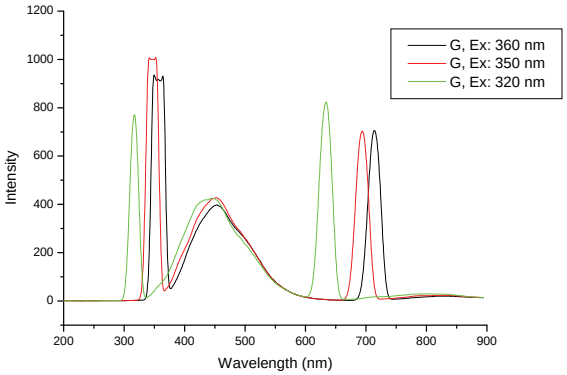

(a) George (360-320 nm)

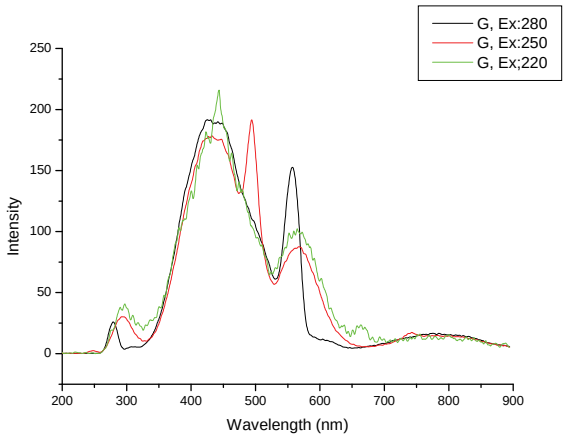

(b) George (280-220 nm)

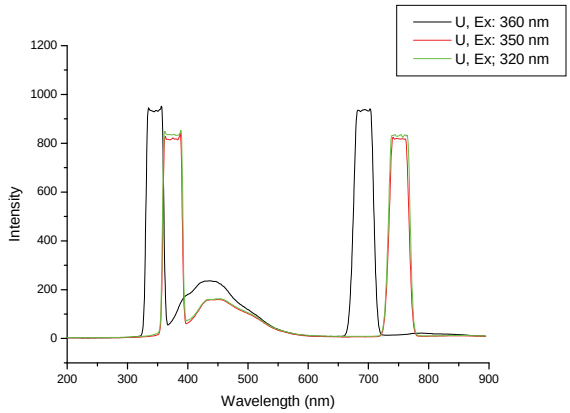

(c) Umzonyana (360-320 nm)

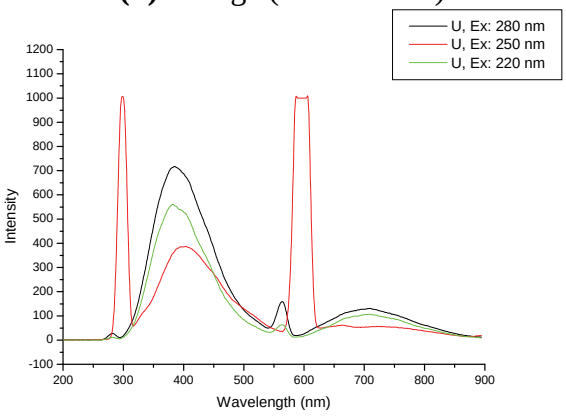

(d) Umzonyana (280-220 nm)

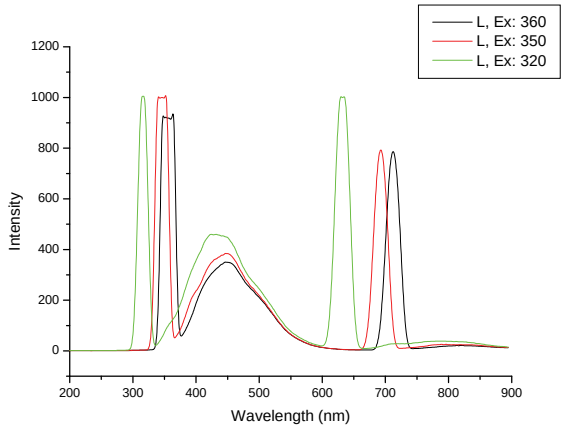

(e) Loerie (360-320 nm)

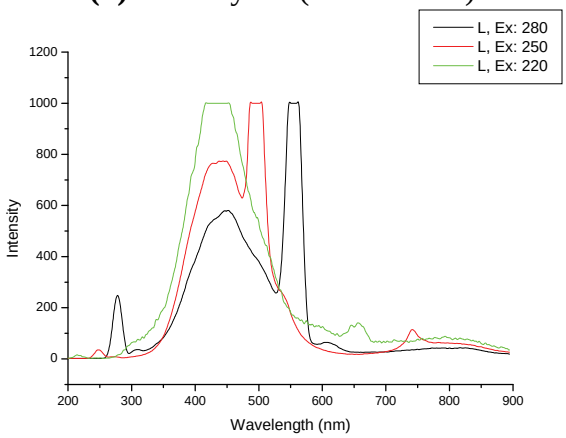

(f) Loerie (280-220 nm)

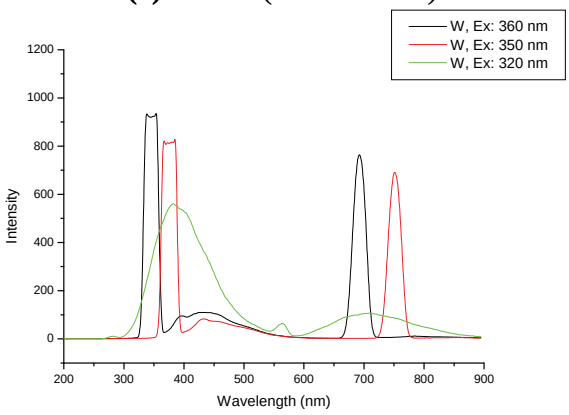

(g) Wiggins (360-320 nm)

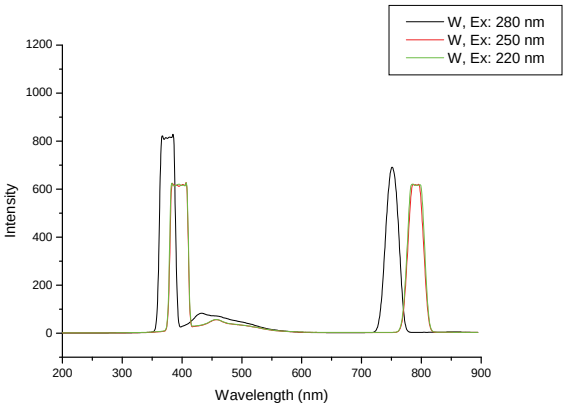

(h) Wiggins (280-220 nm)

Figure 2.7 Fluorescence excitation spectra obtained by fluorescence characterisation of samples taken during Round 1.

As can be seen from Figure 2.7a, the George samples had a very broad peak occurring at 420-500 nm with a maximum intensity occurring at 500 intensity units. This peak represents hydrophobic acids, humic and humic acid-like material. At a different excitation, again the George sample has a broad peak occurring at 280-340 nm (Figure 2.7b). This peak represents microbial by-products, e.g. tryptophan-like and fulvic acid-like material. The intensity here is approximately 200 intensity units. Figures 2.7c-h show the presence of hydrophobic acids, humic acids and humic acid-like material together with microbial by-product like tryptophan and fulvic acid like material with varying proportions as evidenced by the various peak intensities of each fraction on the samples.

The different spectrum displays the extent of the varying composition of NOM from place to place. The spectrum also displays the difference in the character of NOM as evidenced by the varying peak intensities. The Wiggins (Wiggins) sample for instance (Figures 2.7g and 2.7h), has yet another broad peak occurring at 400 nm with an intensity of 600, which is characteristic of marine humic acids. The results obtained after the second sampling indicate characteristic features of NOM (with different concentrations) similar to the ones after the first sampling. Even though FEEM analysis is not entirely conclusive, but by comparing the data against standard literature Fluorescence Emission-Excitation data, important inferences of NOM characteristics can be drawn (Chen *et al.*, 2003).

2.4 Summary

The sampling programme did provide a useful profile of the raw waters investigated, to contextualise the treatment studies that follow. The conventional parameters measured confirmed the profiles as anticipated:

- The waters that are influenced by the return flows from sewage treatment plants had higher alkalinity, pH and hardness, as well as higher levels of nutrients (Midvaal, Rietvlei and Olifantsvlei). The return effluents to stabilise these sources and there is relatively little variation.
- The water from the coastal impoundments was softer, low in alkalinity (Umzonyana, Wiggins) and, along the southern coast, progressively higher in colour (Loerie, Plettenberg Bay).
- The water from Vaal Dam (Vereeniging) was unique amongst the raw water sources, having high turbidity, medium alkalinity and low conductivity, but surprisingly high UVA.

The organic parameters provided a less clear-cut classification of the different raw waters:

- Both the UVA_{254} and the DOC ranges were remarkably similar for most of the waters, with two exceptions. The Plettenberg Bay samples were clearly higher, and the Wiggins samples clearly lower than the remaining six samples, which covered about the same range. The SUVA values, which are the ratios between UVA_{254} and DOC, were also quite similar. The Plettenberg Bay samples had higher SUVA values than the rest (predicting better removal by enhanced coagulation) and the Wiggins samples very low SUVA values (predicting poor removal by enhanced coagulation).
- The BDOC/DOC ratios of the samples covered a broad range, with a minimum of 20% up to a high of 65%. Two sites had practically constant ratios (6% range or less), while others covered ranges as high as 39%. No explanations for these large, and possibly important differences, can be offered yet. The sources with less eutrophic sources (Vereeniging and Loerie) had a high BDOC/DOC ratio, but so did the treated sewage effluent (Olifantsvlei). The Wiggins samples (lowest organic content of all the sources) had the lowest ratio, but the Plettenberg Bay samples

(highest organic content of all the sources) also had some of the lowest ratios on some occasions.

- The FEEM results show that the Plettenberg Bay samples had very broad peaks for hydrophobic acids across all rounds of sampling. The results also indicated that the Plettenberg Bay samples had high amounts of hydrophobic NOM. The results obtained for the other samples indicate that the samples had little humic substances as shown by the narrow peaks or no peaks where peaks for humic substances would be expected.
- The fractionation of NOM by PRAM varied substantially depending on the type and source of water. The Plettenberg Bay samples had a greater percentage of the HPO fraction and a lesser but equal distribution of the HPI and TPI fraction. The Rietvlei samples had an equal distribution of the HPO, TPI and HPI fraction while the other had low percentages of HPO fraction and slightly higher percentages of TPI and HPI NOM fractions.

Both the organic and inorganic parameters of the samples indicate that the eutrophic water sources (Rietvlei and Midvaal) were more similar in character than the purified sewage effluent (Olifantsvlei), providing further support to the thesis that the return of treated sewage effluents is a primary driver for these rivers and impoundments.

Ultraviolet absorbance at wavelength 254 nm was selected as the primary variable for measuring NOM. This is an analytical technique which is more readily accessible to smaller treatment plants, and is more robust with less calibration and operator skill required. Moreover, the reported results indicated that it is a stable parameter over long periods of time, provided that samples are kept refrigerated.

CHAPTER 3. UVA_{254} REMOVAL IN FULL-SCALE TREATMENT PLANTS

Ultraviolet absorbance at 254 nm was selected as the routine NOM indicator for this project, as explained in the previous chapter. To establish some typical benchmarks for treatment plant performance in terms of UVA removal, samples were taken during each site visit at a few key points along the treatment process. These results form the basis of this chapter. It should be noted that South African treatment plants, at this point, are operated for maximum turbidity removal and chlorination rather than for NOM removal. The typical NOM removal during treatment is therefore not the maximum that can be achieved. Should UVA removal become a priority, the removal efficiencies could be substantially higher.

3.1 Details of Treatment Plants

The main focus of the sampling visits was to collect adequate quantities of raw water for further characterisation and treatability studies. Additionally, some smaller samples were taken at different points in the treatment train to quantify the treatment performance in terms of UVA removal. The turbidity, temperature and conductivity of the samples were measured on site, and their UVA_{254} absorbance measured later in the laboratory.

The treatment plants had different process trains. Table 3.1 indicates which plants had which unit processes. From the perspective of NOM removal, dissolved air flotation (DAF) and settling were placed into the same category, as their NOM removal capabilities are considered to be similar. The sample numbers are provided for cross-referencing. The George sample taken during Round 1 is grouped with the Plettenberg Bay samples, as both treatment plants were treating similarly coloured water. Please refer to Appendix B for the process flowcharts of the individual treatment plants.

3.2 Effect of Maturation Ponds

The Olifantsvlei samples were taken before and after the maturation ponds following wastewater treatment with biological nitrogen and phosphorus removal. The UVA_{254}, averaged over Rounds 2 to 5, was reduced from 17.1/m to 15.3/m, for a small, but consistent removal of 5%. The maturation ponds afforded the treated water about 10 days of theoretical retention time in a series of shallow dams, exposed to sediments, the atmosphere and sunlight, not unlike water in natural systems or impoundments. This indicates that the return flows, in terms of their UVA_{254}, will not be changed much after release into natural water-courses.

3.3 Effect of Ozonation

Two treatment plants were included because they had ozonation facilities. At Midvaal, the ozonation was used during all the sampling visits. At Wiggins, the raw water quality was exceptionally good and there was no need to run the ozonation, except for Round 5. From these limited ozonation events, the effect on UVA_{254} absorbance could be estimated. For the Midvaal samples, the average UVA_{254} absorbance was reduced from 12.0/m to 7.0/m (36% removal), while the single data point at Wiggins showed removal from 2.0/m to 1.2/m (37% removal). Although ozonation appears to *remove* UVA, it must be kept in mind that ozone only *transforms* the character of NOM without necessarily removing the NOM. The following paragraphs show further downstream effects of ozonation.

Table 3.1 Sampling of full-scale treatment plants, with sample numbers

Site Round #	Raw water	After ozone	After DAF/settling	After filtration
Loerie R1	L1_1	-	L2_1	L3_1
Loerie R2	L1_2	-	L2_2	L3_2
Loerie R3	L1_3	-	L2_3	L3_3
Loerie R4	L1_4	-	L2_4	L3_4
Loerie R5	L1_5	-	L2_5	L3_5
Midvaal R1	n/m*	n/m*	n/m*	n/m*
Midvaal R2	M1_2	M2_2	M3_2	M4_2
Midvaal R3	M1_3	M2_3	M3_3	M4_3
Midvaal R4	M1_4	M2_4	M3_4	M4_4
Midvaal R5	M1_5	M2_5	M3_5	M4_5
George R1	G1_2	-	G2_1	G3_1
Plettenberg Bay R2	P1_2	-	P2_2	P3_2
Plettenberg Bay R3	P1_3	-	P2_3	P3_3
Plettenberg Bay R4	P1_4	-	P2_4	P3_4
Plettenberg Bay R5	P1_5	-	P2_5	P3_5
Umzonyana R1	R1_1	-	U2_1	U3_1
Umzonyana R2	R1_2	-	U2_2	U3_2
Umzonyana R3	R1_3	-	U2_3	U3_3
Umzonyana R4	R1_4	-	U2_4	U3_4
Umzonyana R5	R1_5	-	U2_5	U3_5
Vereeniging R1	V1_1	-	V2_1	V3_1
Vereeniging R2	V1_2	-	V2_2	V3_2
Vereeniging R3	V1_3	-	V2_3	V3_3
Vereeniging R4	V1_4	-	V2_4	V3_4
Vereeniging R5	V1_5	-	V2_5	V3_5
Wiggins R1	W1_1	-	W2_1	W3_1
Wiggins R2	W1_2	-	W2_2	W3_2
Wiggins R3	W1_3	-	W2_3	W3_3
Wiggins R4	W1_4	-	W2_4	W3_4
Wiggins R5	W1_5	W2_5	W3_5	W4_5
	Raw water	After DAF	After sand filtration	After GAC filtration
Rietvlei R1	R1_1	R2_1	R3_1	R4_1
Rietvlei R2	R1_2	R2_2	R3_2	R4_2
Rietvlei R3	R1_3	R2_3	R3_3	R4_3
Rietvlei R4	R1_4	R2_4	R3_4	R4_4
Rietvlei R5	R1_5	R2_5	R3_5	R4_5
	After wastewater treatment		After maturation ponds	
Olifantsvlei R1	O1_1		O2_1	
Olifantsvlei R2	O1_2		O2_2	
Olifantsvlei R3	O1_3		O2_3	
Olifantsvlei R4	O1_4		O2_4	
Olifantsvlei R5	O1_5		O2_5	

* n/m = not measured

3.4 Effect of Coagulation/Settling/DAF/Sand Filtration

At all the treatment plants, either settling or DAF was used as the suspended solids (SS) removal step before filtration. The removal of UVA by each treatment step is summarised in Table 3.2.

The first clearly distinguishable group is the highly coloured water from the George and Plettenberg Bay plants. The removal during coagulation, flocculation and SS removal was very high (92% and 84%), with much less removal during the subsequent filtration (3% and 5%).

The second distinguishable group contains those plants which used ozonation. Although the immediate effect of pre-ozonation was to reduce the UVA by 36%, the downstream effects are complex and not clearly understood. In both the Midvaal and Wiggins plants, the UVA increased again during coagulation, flocculation and bulk phase removal. During the final filtration step, however, the removal was quite high for the Midvaal plant (17%), but very poor for the Wiggins plant (-51%), although the latter value is derived from a single data point with very low absorbance. When the entire treatment train is considered, the use of pre-ozonation led to the lowest two UVA removals of all the treatment plants -27% (Midvaal) and -100% (Wiggins) respectively.

Table 3.2 UVA_{254} removal at full-scale water treatment steps
(Means of all available data points)

Plant	Comment	Raw	Before filtration		After filtration	
		UVA_{254}	UVA_{254}	Removal	UVA_{254}	Removal
George	Highly coloured	96.2	7.8	92%	4.5	95%
Loerie		17.3	8.0	53%	6.4	63%
Midvaal	Pre-ozonation	19.1	17.1	10%	13.9	27%
Plettenberg Bay	Highly coloured	45.1	7.1	84%	4.8	89%
Rietvlei		19.2	13.2	31%	12.9	33%
Umzonyana		15.9	12.7	20%	11.1	30%
Vereeniging		53.3	13.8	74%	12.4	77%
Wiggins	Pre-ozonation	3.3	4.9	-49%	6.6	-100%

The rest of the treatment plants are conventional plants. The UVA removal during coagulation, flocculation and bulk phase removal is quite variable, ranging from 20% for the Umzonyana plant to 74% for the Vereeniging plant. This high variability is probably due to the choice of coagulants used at the different treatment plants. It is well known that organic polymeric coagulants do not remove NOM well, while inorganic coagulants perform much better in this regard.

The filtration step in the conventional plants showed a fairly consistent UVA removal ranging from 2% for the Rietvlei plant to 10% for the Vereeniging plant.

Figures 3.1 to 3.4 show the results obtained for the Plettenberg Bay samples at different excitation-emission wavelengths (guided by the FEEM regions given in Figure 2.6). As can be seen from Figures 3.1 to 3.4, the Plettenberg Bay samples had a very broad peak occurring at 420 nm to 500 nm with a maximum intensity occurring at 600 intensity units. This peak represents hydrophobic acids, humic and humic acid-like material. At a different excitation, again the Plettenberg Bay sample had a broad peak occurring at 580 nm to 680 nm (Figure 3.4). This peak represents microbial by-products such as tryptophan-like and fulvic acid material. The intensity is approximately 200 intensity units.

The results obtained for the other samples indicate that the samples had very low aromatic content, i.e. low humic substances as evidenced by very narrow peaks or no peaks at all, where peaks for humic substances were expected. The results are also in agreement with the SUVA values, which suggest that only the Plettenberg Bay samples contain a high hydrophobic NOM. The different spectra display the extent of the varying composition of NOM from place to place and season to season. The spectra also display the difference in the character of NOM as evidenced by the varying peak intensities. The results obtained during the second and third sampling rounds indicate characteristic features of NOM (with different concentrations) similar to the ones obtained during the first sampling trip. Even though FEEM analysis is not entirely conclusive, important inferences of NOM characteristics can be drawn by comparing the data against standard literature Fluorescence Emission-Excitation data.

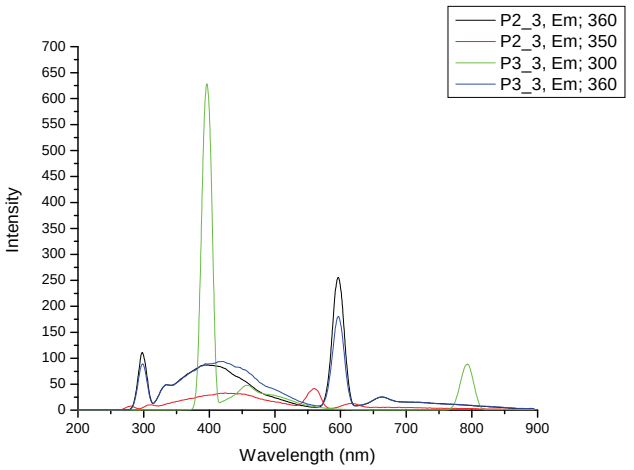

Figure 3.1 Excitation emission of the Plettenberg Bay samples before sand filtration

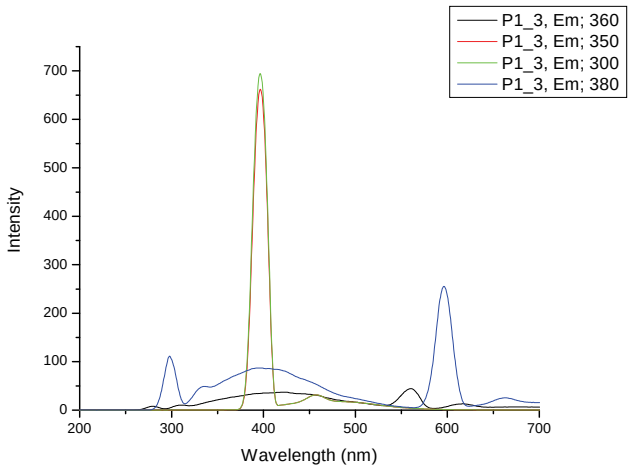

Figure 3.2 Excitation emission of a Plettenberg Bay raw water sample

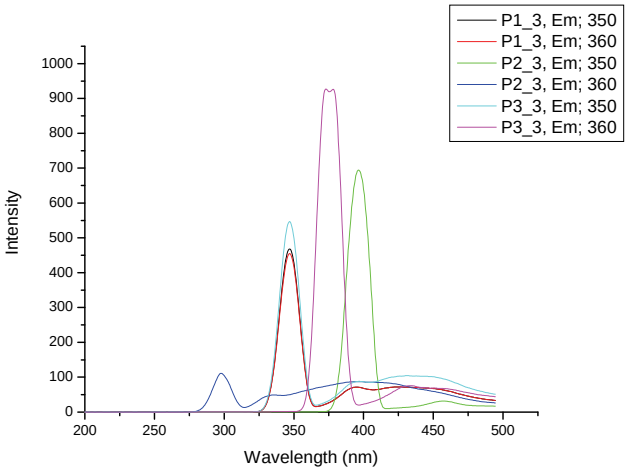

Figure 3.3 Excitation emission of Plettenberg Bay raw water sample, sample before sand filtration and after sand filtration

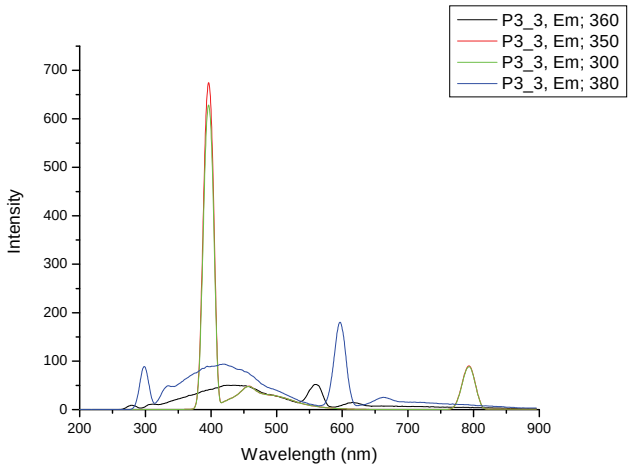

Figure 3.4 Excitation emission of the Plettenberg Bay water samples after sand filtration

3.5 Effect of GAC Filtration

There was a full-scale GAC filtration following sand filtration at Rietvlei. The three available values indicated that the removal of the raw water UVA_{254} was from 12.9/m to 10.3/m, or a removal of 15% of the raw water UVA.

3.6 Summary

In summary, the average removal of UVA_{254} was:

- 5% by maturation pond
- 36% by ozonation
- 88% by coagulation and settling (highly coloured water)
- Inconsistent removal by coagulation, flocculation, settling/DAF and filtration (non-ozonated water) from 20% to 74% of the raw water UVA, mainly due to coagulant choice
- An increase of 27% to -100% by coagulation, flocculation, settling and filtration (ozonated waters)
- 5% removal of raw water UVA by sand filtration
- 15% removal of raw water UVA by GAC filtration

CHAPTER 4. NATURAL ORGANIC MATTER REMOVAL BY ENHANCED COAGULATION

4.1 Introduction

This chapter focuses on the efficacy of enhanced coagulation (EC) for the removal of organic substances from typical source waters of South Africa. Enhanced coagulation is an extension of an existing treatment process "chemical coagulation", which has conventionally been used with metallic salts to remove only particles (turbidity and pathogens) from water. Enhanced coagulation, a process used to meet regulatory standards in the US, which strives for optimal removal of particles and NOM with the usage of coagulants such as aluminium and iron salts. The iron salt is used in this study for its common application in South Africa (SA). The removal efficiency of EC, however, depends on the physical and chemical properties of the water, as well as the operating conditions (Ghasri *et al.,* 2005). Optimum conditions for the removal of turbidity and NOM sometimes differ, with the generally higher dosage required for NOM removal as the controlling factor. However, turbidity removal at these conditions must still be achieved (Gao *et al.,* 2005).

A consistent and reproducible, yet simple jar test procedure was developed to find the optimum coagulation conditions for the removal of UVA_{254}. Batch tests on all samples were then performed to evaluate the removal efficiency of UVA_{254} and turbidity at the optimum conditions of dosage and pH. The findings reported in this study, therefore, are based on bench-scale tests performed at ambient temperature (15-23°C).

4.2 Batch Testing

These tests were done subsequent to jar testing. The same coagulation, flocculation and settling times and rates as for jar testing were used. However, the dosages used in these tests were interpolated from jar tests results. UVA_{254} curves plotted against pH specific dosage, as shown in Figure 3.2, were used to develop three criteria for choosing the dosage. Most water treatment utilities aim at UVA_{254} values of between 4 and 7 per metre (m^{-1}). The first criterion is to decrease the UVA to an absolute value of 6/m. Some water sources, not only in SA, have low initial UVA close to or below this absolute value. The second criterion would then be to reduce 65% of the initial UVA_{254} value. This removal efficiency, however, was arbitrarily chosen. The highest coagulant dosage corresponding to any of the two criteria would be chosen as optimal and it would be interpolated from the curve. The last criterion would be based on the point of diminishing return (PODR), a concept from the USEPA EC/precipitative guidance manual. The dosage corresponding to the curve's tangential slope of -0.2 would be used as the "break-even point" or the ceiling limit. Thus if it was less than one or both of the other dosages, it then became the applied dosage.

4.2.1 Criteria for Optimising Coagulation for UVA_{254} Removal

In this study, three criteria were used as guidelines for the removal of UVA_{254}. They were developed based on literature studies, general water treatment plants' targets, and findings from preliminary experiments. The criteria were used simultaneously to establish the optimum coagulant dose and also predict the UVA_{254} removal efficiency at the critical point or optimum condition. The highest coagulant dose between one to a particular removal efficiency and one to an absolute target of UVA_{254} was picked as optimal. However, if the "threshold limit" dose was lower than any of the first two criteria, it then became optimal. The three criteria are described in this section.

Removal of a Fixed Percentage of Raw Water UVA254 Absorbance

With this criterion, 35% of the raw water UV_{254} absorbance was calculated. A theoretical $FeCl_3 \cdot 6H_2O$ dose to reach this target, and the consequent pH, was mathematically interpolated from the UV_{254} and pH curves respectively. The curves were third-order polynomials.

Removal of UVA_{254} Absorbance to an Absolute Target

With this criterion, the UVA_{254} absorbance of the raw water would be reduced to a fixed 3.5/m value. Mathematical interpolations from the UVA_{254} and pH curves were done to find the $FeCl_3 \cdot 6H_2O$ dose and its consequent pH value corresponding to the absolute target.

Removal of UVA_{254} Absorbance to a Threshold Limit Value or a Point of Diminishing Return (PODR)

In this criterion, the $FeCl_3 \cdot 6H_2O$ dose and the consequent pH to correspond to a tangential slope of -0.2 (from the UV_{254} curve), which acted as both the ceiling point and "break-even point", were mathematically calculated by means of equation 4.1.

$$\frac{dy}{dx} = 3ax^2 + 2bx + c = -0.2 \tag{4.1}$$

The practical solution for "x" was equal to the $FeCl_3 \cdot 6H_2O$ dose. To find values of UVA_{254} and pH corresponding to this slope, the $FeCl_3 \cdot 6H_2O$ dose (x), was substituted in the respective UVA_{254} and pH curves.

4.2.2 Criteria for Turbidity Removal

Though the main objective of EC is the maximal removal of NOM, it also targets the removal of turbidity to levels low enough for subsequent treatment processes. In this study, therefore, algorithms to remove turbidity to practically low levels were formulated and consistently applied in all the samples. These turbidity targets were determined by considering the initial levels as illustrated in Table 4.1.

Table 4.1 Algorithms for turbidity removal

If	**Then**
2<RW<10	: NTU = 1.00
RW<2	: NTU = 0.50 × RW
10<RW	: NTU = 0.10 × RW
Where:	RW = raw water turbidity
	NTU = target turbidity

To ascertain the $FeCl_3 \cdot 6H_2O$ dosage for the set turbidity target, interpolation from the turbidity graph was done using the "straight line method". On the graph, two points of interest (one immediately higher and the other immediately lower than the target point) were used.

That is, if

- the target point was (x_3, y_3) where: x_3 is target $FeCl_3 \cdot 6H_2O$ and y_3 is the target turbidity, and

- the immediate higher point of interest on the curve would be (x_1, y_1) where x_1 is the lower $FeCl_3 \cdot 6H_2O$ and y_1 is the higher turbidity, and

- the immediate lower point of interest on the curve would be (x_2, y_2) where x_2 is the higher $FeCl_3 \cdot 6H_2O$ and y_2 is the lower turbidity, then

$$x_3 = x_2 - \left[(x_2 - x_1) \times \frac{(y_3 - y_2)}{(y_1 - y_2)} \right] \tag{4.2}$$

From the calculated dose using equation 4.2, the corresponding pH would also be interpolated from the pH/coagulant dose curve, by substituting x_3 in the polynomial.

4.3 Experimental Results

The test results for the raw water samples taken during rounds 2-5 are summarised in Table 4.2 below. The following comments are offered:

- The UVA values obtained from the jar tests followed a smooth, robust trend and the EC dosages could be predicted with good precision. The turbidity data, however, was more scattered, especially at lower dosages and turbidity values could not always be interpolated.
- Alkalinity correction was required in a substantial number of cases.
- The overall settled water quality after these tests to improve UV-absorbing compounds removal resulted in reasonable reduction of turbidity. As a consequence, meeting criteria for EC does not compromise the removal of turbidity.

Table 4.2 Jar testing results (ferric chloride dosage required to meet EC criteria)

Sample	Alk. (mg/l)	Correct for Alk.?	Na_2CO_3 (mg/l)	Criterion	$FeCl_3$ (mg/l)	pH	UVA_{254} (m^{-1}) before	UVA_{254} (m^{-1}) after	UVA_{254} removal (%)	Turbidity (NTU)
George 1	8	-	-	-	-	-	95.1	-	-	-
P. Bay 2	3.3	✓	61	Limit	17	5.2	28.3	6	78.8	4.3
P. Bay 3	12	✓	51	Limit	13.6	5.4	39.6	6	84.8	1.7
P. Bay 4	3	✓	61	Limit	16.6	5	69.2	6	91.3	1.3
P. Bay 5	3	✓	61	Limit	14.8	5.1	46.8	6	87.2	-
Loerie 1	24	-	-	-	-	-	25.8	-	-	-
Loerie 2	16	✓	47	Limit	12.3	7.1	16.3	6	63.2	0.7
Loerie 3	-	-	-	-	-	-	-	-	-	-
Loerie 4	19	✓	50	PODR	18.4	6.1	12.1	5.1	57.9	0.8
Loerie 5	18	✓	50	Limit	14	6.5	15.4	6	61.0	-
Vereeniging 1	65	-	-	-	-	-	23.4	-	-	-
Vereeniging 2	59	×	-	Limit	14.7	6.5	22.8	6	73.7	1.0
Vereeniging 3	58	×	-	Limit	14	6.2	20	6	70.0	0.9
Vereeniging 4	53	✓	8	Limit	16.3	6.1	39.1	6	84.7	1.7
Vereeniging 5	47	×	-	PODR	23	5.6	28.5	8.5	70.2	-
Wiggins 1	52	-	-	-	-	-	7.3	-	-	-
Wiggins 2	54	×	-	PODR	7.9	6.9	4.4	3.2	27.3	0.5
Wiggins 3	58	×	-	PODR	6.7	7	4	3	25.0	0.5
Wiggins 4	58	×	-	PODR	8.6	6.7	4.1	3.3	19.5	0.3
Wiggins 5	57	×	-	PODR	7.5	6.6	5.3	5	5.7	-
Olifantsvlei 1	83	-	-	-	-	-	9.8	-	-	-
Olifantsvlei 2	93.3	×	-	PODR	29.2	5.9	14.3	6.7	53.1	1.2
Olifantsvlei 3	-	×	-	PODR	29.5	6	12.9	6.2	51.9	1.1
Olifantsvlei 4	-	×	-	PODR	20.4	6.2	13	7.5	42.3	0.8
Olifantsvlei 5	-	×	-	PODR	23.9	6.1	15	8.5	43.3	-
Rietvlei 1	111	-	-	-	-	-	18.8	-	-	-
Rietvlei 2	121.1	×	-	PODR	22.9	6.6	15.8	7.5	52.5	0.8
Rietvlei 3	-	×	-	Limit	37.8	5.6	16.8	6	64.3	0.4
Rietvlei 4	-	×	-	Limit	29	5.9	21.3	6	71.8	0.7
Rietvlei 5	-	×	-	PODR	28.5	5.8	16.2	6.8	58.0	-
Umzonyana 1	138	-	-	-	-	-	15.8	-	-	-
Umzonyana 2	130.6	×	-	PODR	21.9	6.8	13.5	6.9	48.9	0.7
Umzonyana 3	-	×	-	PODR	23	6.6	14.7	6.9	53.1	0.8
Umzonyana 4	-	×	-	PODR	32.3	6.1	16.9	6	64.5	0.8
Umzonyana 5	-	×	-	Limit	18.9	5.8	22.7	6	73.6	-
Midvaal 1	103	-	-	-	-	-	16.3	-	-	-
Midvaal 2	151.7	×	-	PODR	22.9	7.2	13.1	7.8	40.5	1.1
Midvaal 3	-	×	-	PODR	28.6	6.3	15.7	7.6	51.6	1.0
Midvaal 4	-	×	-	Limit	18.5	6	33.8	6	82.2	2.3
Midvaal 5	-	×	-	%	27.7	5.7	14.6	6	58.9	-

4.4 Comparing Enhanced Coagulation with Full-Scale Plant Operation

The UVA_{254} values were recorded at the full-scale treatment plants during the site visits. It should be kept in mind that UVA removal is not a treatment goal at these plants, so the UVA removal, whatever it may be, does not reflect negatively on any treatment plant or its operation. The laboratory tests show that residual UVA_{254} values of 6/m or less are readily achievable. The absolute values of the UVA remaining after settling/DAF are shown in Table 4.3. The values that are shaded are those events when the actual UVA_{254} absorbance was below the EC goal of 6/m. In 21 of the 26 measured events, the EC goal was not reached.

Table 4.3 UVA_{254} achieved after settling/DAF at full-scale plants

Sampling round	Loerie	Midvaal	George/P. Bay	Rietvlei	Umzonyana	Vereeniging	Wiggins
R1	6.1		7.8		14.4		5.7
R2	1.8	9.3	4.6	8.2	9.6	9.2	
R3		12.1			10.6	10.7	
R4	7.7	30.4		14.4	14.1	19.7	6.4
R5	10.1	12.7	5.0	8.1	14.6	15.5	2.6

There was no reduction in UVA at the treatment plants where pure organic polyelectrolytes were used.

4.5 Modelling of results

Having established a large data base with the dosages required for EC, and the corresponding UVA removal, mathematical models were developed to predict the required dosage and anticipated UVA removal based on the analytical parameters used in this project, namely alkalinity, UVA_{254}, DOC and SUVA. Although UVA, DOC and SUVA are listed as three parameters, they represent only two degrees of freedom. If any two are known, the third parameter is predetermined. In the models that follow, all three are used, leaving it to the potential user to select the most convenient.

The importance of SUVA was discussed earlier. A few comments are warranted on the role on alkalinity. The USEPA found that TOC removal becomes more difficult as the alkalinity increases and TOC decreases. In high alkalinity waters, for instance, pH depression to a point at which TOC removal is optimal is more difficult to achieve through the addition of coagulant alone. Consequently, TOC removal efficiencies may change with season depending on the initial TOC and alkalinity level of the raw water (USEPA, 1999).

A possible explanation for the effect of alkalinity on pH is that alkalinity controls the pH of coagulant addition, consequently controlling the hydrolyzed species of metal coagulants. The higher the alkalinity of water, the more the extent of the hydrolysis process, formation of larger metallic hydroxide polymers, and increased precipitation. However, these conditions do not necessarily maximise NOM removal (Yan *et al.*, 2006; Yan *et al.*, 2009).

The USEPA also recognized that the coagulation pH is determined by the alkalinity. To guarantee good removal of organics, water utilities should aim at or below the target pH values. This could be justified by the fact that when metal coagulants are added in raw water, they act as acids, depressing the pH to an extent that depends on the dosage and the water's buffering capacity. Thus, if the buffering capacity is low, the target coagulation pH for the removal of NOM will be reached sooner (with little addition of coagulant). Moreover, the removal of UVA_{254} is affected by the alkalinity

because alkalinity controls further the hydrolyzed species of metal coagulants during flocculation. When the alkalinity is high, the extent of the hydrolysis process and the formation of larger polymers occur further, causing more precipitation.

Two model structures were explored (multiplicative and additive) with the following general forms:

$$multiplicative: Y = a.X_1^b.X_2^c \ldots$$

$$additive: Y = K.X_1 + L.X_2 + \cdots$$

The regression constants were all derived from first principles using matrix analysis and the matrix manipulation capabilities of EXCEL. The working equations for the regression constants for a three-parameter multiplicative model, for example, in matrix form, are:

$$\begin{pmatrix} N & \sum \ln x_1 & \sum \ln x_2 & \sum \ln x_3 \\ \sum \ln x_1 & \sum \ln^2 x_1 & \sum \ln x_1 \cdot \ln x_2 & \sum \ln x_1 \cdot \ln x_3 \\ \sum \ln x_2 & \sum \ln x_1 \cdot \ln x_2 & \sum \ln^2 x_2 & \sum \ln x_2 \cdot \ln x_3 \\ \sum \ln x_3 & \sum \ln x_1 \cdot \ln x_3 & \sum \ln x_2 \cdot \ln x_3 & \sum \ln^2 \cdot x_3 \end{pmatrix} \begin{pmatrix} \ln a \\ b \\ c \\ d \end{pmatrix} = \begin{pmatrix} \sum \ln y_{actual} \\ \sum \ln y_{actual} \cdot \ln x_1 \\ \sum \ln y_{actual} \cdot \ln x_2 \\ \sum \ln y_{actual} \cdot \ln x_3 \end{pmatrix}$$

The solution of this set of equations is:

$$\begin{pmatrix} \ln a \\ b \\ c \\ d \end{pmatrix} = \begin{pmatrix} N & \sum \ln x_1 & \sum \ln x_2 & \sum \ln x_3 \\ \sum \ln x_1 & \sum \ln^2 x_1 & \sum \ln x_1 \cdot \ln x_2 & \sum \ln x_1 \cdot \ln x_3 \\ \sum \ln x_2 & \sum \ln x_1 \cdot \ln x_2 & \sum \ln^2 x_2 & \sum \ln x_2 \cdot \ln x_3 \\ \sum \ln x_3 & \sum \ln x_1 \cdot \ln x_3 & \sum \ln x_2 \cdot \ln x_3 & \sum \ln^2 \cdot x_3 \end{pmatrix}^{-1} \begin{pmatrix} \sum \ln y_{actual} \\ \sum \ln y_{actual} \cdot \ln x_1 \\ \sum \ln y_{actual} \cdot \ln x_2 \\ \sum \ln y_{actual} \cdot \ln x_3 \end{pmatrix}$$

With N the number of samples.

4.5.1 Modelling UVA_{254} removal

The literature on EC is conclusive in respect of using the SUVA value as a qualitative predictor of whether the organic content of a water sample would be easily removed. Above SUVA values of about 2, there is evidence of a sizable fraction of double C-C bonds, which respond well to the normal coagulation mechanisms. Below a SUVA value of about 2, the organic material is dominated by smaller molecules which do not respond well to EC. The data set was therefore modelled in three ways – the full data set, the samples with SUVA < 2 and the samples with SUVA > 2. The best-fit models for these cases are presented in Table 4.4.

Table 4.4 Best-fit two-parameter regression models for UVA_{254} removal (%)

Selection	Model type	Equation	R^2
All samples	Additive	$32.3 + 2.87DOC_{raw} + 7.63SUVA$	0.725
	Multiplicative	$53.515 \times UV_{raw}^{0.296} \times Alk^{-0.123}$	0.770
Samples with SUVA > 2	Additive	$98.6 + 0.300UV_{raw} + 0.310Alk$	0.898
	Multiplicative	$253.571 \times UV_{raw}^{0.132} \times Alk^{-0.361}$	0.899
Samples with SUVA < 2	Additive	$31.5 + 1.59UV_{raw} + 8.86SUVA$	0.677
	Multiplicative	$33.262 \times UV_{raw}^{0.235} \times SUVA^{0.203}$	0.718

The following comments apply:

- The multiplicative models are better predictors than the additive models,
- The removal of the samples with SUVA < 2 brings a large improvement in the correlation coefficient, from 77% to 90% for the multiplicative model, and
- UVA and alkalinity are the two best predictors of UVA removal.

The next step was to try to improve the predictive ability of the models by adding a third independent parameter to the models, leading to a number of three-parameter models shown in Table 4.5.

Table 4.5 Best-fit three-parameter regression models for UVA_{254} removal (%)

Selection	Model type	Equation	R^2
All samples	Additive	$39.7 + 3.01DOC_{raw} + 6.89SUVA - 0.08Alk$	0.753
	Multiplicative	$51.969 \times UV_{raw}^{0.340} \times Alk^{-0.130} \times SUVA^{-0.080}$	0.781
Samples with SUVA > 2	Additive	$85.6 + 1.19DOC_{raw} + 3.01SUVA - 0.290Alk$	0.912
	Multiplicative	$249.486 \times DOC_{raw}^{0.146} \times Alk^{-0.361} \times SUVA^{0.120}$	0.900
Samples with SUVA < 2	Additive	$32.1 + 1.64UV_{raw} + 8.48SUVA - 0.01Alk$	0.677
	Multiplicative	$37.717 \times DOC_{raw}^{0.267} \times Alk^{-0.041} \times SUVA^{0.412}$	0.710

The following comments apply:

- Compared to the two-parameter models, there is only a marginal improvement, and
- For SUVA > 2, the additive model provided a slightly higher correlation coefficient than the multiplicative model.

4.5.2 Modelling the required dosage of ferric chloride

For the modelling of the required ferric chloride dosage, there is no rationale for splitting the data set. Although the SUVA values determine the degree to which UVA is removed, they do not influence the concentration of ferric chloride required to reach favourable coagulation conditions. Table 4.6 shows best-fit models using both two and three parameters.

Table 4.6 Best-fit models for ferric chloride dosage

Model type	Equation	R^2
Two-parameter Additive	$-9.95+1.16DOC_{raw}-0.270Alk$	0.712
Two-parameter Multiplicative	$0.041\times Alk^{1.107}\times DOC_{raw}^{0.613}$	0.766
Three-parameter Additive	$-9.72+1.22DOC_{raw}-0.250SUVA+0.270Alk$	0.712
Three-parameter Multiplicative	$0.043\times SUVA^{-0.317}\times UV_{raw}^{0.480}\times Alk^{1.132}$	0.745

The following comments apply:

- The addition of a third parameter brings no improvement. By using three parameters rather than two, SUVA is additionally incorporated, which is of no significance for the required coagulant dosage.
- The multiplicative models are better predictors than the additive models, and
- DOC and alkalinity are the two best predictors of ferric chloride dosage.

4.5.3 Application of the models

Should one use additive or multiplicative models? The multiplicative models generally have higher correlation coefficients, so they are recommended. Should one use two-parameter or three-parameter models? The models presented indicated that very little is gained by incorporating a third variable. The two-parameter model is therefore suggested for practical use. Should the models be applied to samples with SUVA values less than 2? For UVA removal, the correlation coefficients for these samples are much lower than for the samples with SUVA above 2. It is recommended that the models should only be applied for samples with SUVA > 2. For estimating the ferric chloride dosage, there is no problem using the models. The modelling, therefore, boils down to two useful equations (4.3 and 4.4 below).

For predicting the removal efficiency of UVA_{254}:

$$253.6\times UV_{raw}^{0.132}\times Alk^{-0.361} \quad (R^2 = 0.90) \tag{4.3}$$

For predicting the ferric chloride dosage in mg/ℓ:

$$0.041\times Alk^{1.107}\times DOC_{raw}^{0.613} \quad (R^2 = 0.77) \tag{4.4}$$

To illustrate, consider a sample with DOC = 4.9 mg/ℓ; alkalinity = 75 mg/ℓ; and UVA_{254} = 23/m). Calculate the SUVA value to determine whether the UVA removal model should be used (SUVA = 23/6.9 = 3.33, so model is applicable). Use the model to predict the percentage UVA removal with equation 4.3 above. (UVA removal = 253.6 × 23^0.132 × Alk^-0.361 = 80.7%.) The remaining UVA_{254} after EC should therefore be about 23 × (1 – 0.807) = 4.4/m.) Use equation 4.4 to predict the ferric chloride dosage to achieve this UVA removal. (Ferric chloride dosage = 0.041 × Alk^1.107 × DOC^0.613 = 16 mg/ℓ.)

4.6 Summary

- Turbidity was removed well at the dosages adopted for EC, hence it is not compromised by EC.
- Raw water SUVA and coagulation pH were the noticeable factors greatly affecting EC.
- A titration curve can be used with success to target specific pH values for jar testing purposes. The pH values and UVA_{254} removal efficiency interpolated from the jar tests closely matched those from independent batch tests.
- The optimum dosage for EC, for all samples irrespective of water source and season, corresponded to pH values between about 4.5 and 7.0. Samples with low alkalinity required the addition of lime to maintain the pH in this range.
- The data from this project allow a good estimate of the UVA removal that can be achieved by EC if the SUVA value is above 2, as well as the required ferric chloride dosage.

CHAPTER 5. NATURAL ORGANIC MATTER REMOVAL BY ACTIVATED CARBON

5.1 A Standard Laboratory Procedure

A standard test procedure for each sample was adopted:

- The carbon powder was obtained by grinding commercial GAC with a mortar and pestle and using the fraction that passed a 300 μm sieve.
- Six Erlenmeyer flasks were filled with 250 mℓ of raw water each, with carbon dosages between 0 and 200 mg/ℓ.
- The flasks were left on a shaker table for three days at a speed of 140 rpm, which was visually determined to be the best frequency to keep the carbon in suspension.
- A subsample was taken from each flask, and filtered through a small membrane filter before reading the UVA at wavelength 254 nm.

Concerns about changes in water temperature, adsorption time and carbon preparation were addressed with further control tests. In summary, the following was found:

- Adsorption tests performed in parallel at controlled temperatures around 5 °C and 20 °C showed small changes in the Freundlich isotherm constants which were probably statistically insignificant. The effect of the small range of test temperatures in the laboratory (18 to 22 °C) can therefore be ignored.
- Parallel tests were performed with commercial powdered activated carbon, and different size fractions obtained from crushed granular activated carbon samples. This part of the testing investigated whether the removal properties of the activated carbon are affected by its size. Three activated carbons were tested on the Rietvlei and Olifantsvlei raw waters; namely:
    - PAC: a commercial powdered activated carbon
    - GAC: a granular activated carbon tested as supplied
    - gGAC: obtained by crushing the virgin GAC and passing through a 300 μm sieve.

Only the PAC and gGAC data were compared while the GAC data could not be analysed because of poor R^2 when fitting the Freundlich isotherm equation. Two treatment criteria were used, namely 50% of UVA removal and the absolute UVA limit of 10/m. In both situations, the PAC performed better than the gGAC although the differences were small as summarized in Table 5.1. This suggests that the activated carbon size impacts on the UVA removal properties – the smaller the grain size, the better the removal, even after three days of contact time.

Table 5.1 gGAC and PAC dosages (mg/ℓ)

Plant	50% UVA removal		Absolute limit of 10/m	
	gGAC	PAC	gGAC	PAC
Olifantsvlei	99.14	91.40	89.90	83.05
Rietvlei	88.59	76.89	54.79	50.35

Problems were encountered with the filtration of the samples after adsorption, but prior to their UVA measurements. When the raw water turbidity was high, the filtration was incomplete and the UVA measurements were erratic. For this reason, the adsorption tests done on the Vereeniging samples were not taken into account. During the tests on the Round 4 samples, another type of filter paper was tried, which worked even worse and compromised some readings done on the Round 4 samples. Some Round 4 results were therefore also not taken into account.

5.2 Data Analysis

For each flask tested, the reduction in UVA_{254} was calculated and divided by the carbon dosage to obtain the solids loading. The solids loading was then plotted against the residual UVA_{254}. This is a standard procedure to determine whether the adsorption can be modelled with the Freundlich isotherm (Sontheimer *et al.*, 1988). If the data points trace a straight line on log-log plane, then the isotherm can be described by the Freundlich constants *K* and *n*. Note that a straight line on a log-log plane is equivalent to a power curve on linear axes (Summers *et al.*, 2010).

For each raw water sample, the solids loading was plotted against the residual UVA_{254} on linear scales. The power curve (corresponding to the Freundlich isotherm) was determined, as well as a second-order polynomial. If the adsorption does follow the Freundlich isotherm, then there is no difference in the regression coefficient between the two best-fit curves. If the polynomial provides a significantly better fit, then the Freundlich isotherm would not be the best isotherm. To illustrate, Table 5.2 and Figures 5.1a-e show the five raw water samples taken from the Olifantsvlei plant, with Table 5.2 showing the comparative regression coefficients. From Figures 5.1a-e, it is clear that the polynomial makes almost no difference to the quality of fit, so the Freundlich isotherm can be used with confidence. The results from the other raw water sources (not shown) support this conclusion. The Freundlich isotherm constants can be directly derived from the power curve constants.

Table 5.2 UVA_{254} results for the Olifantsvlei plant.

	UVA_{254} (m^{-1})	**R^2 Power**	**R^2 Polynomial**
1	13.1	0.96	0.97
2	16.4	0.99	0.98
3	15.8	0.97	0.97
4	15.4	0.99	0.98
5	14.3	0.99	0.99

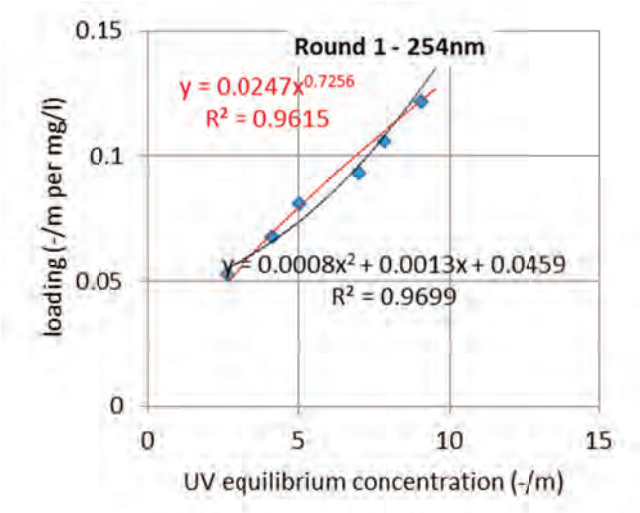

Figure 5.1(a) UVA_{254} results for the Olifantsvlei plant (Round 1)

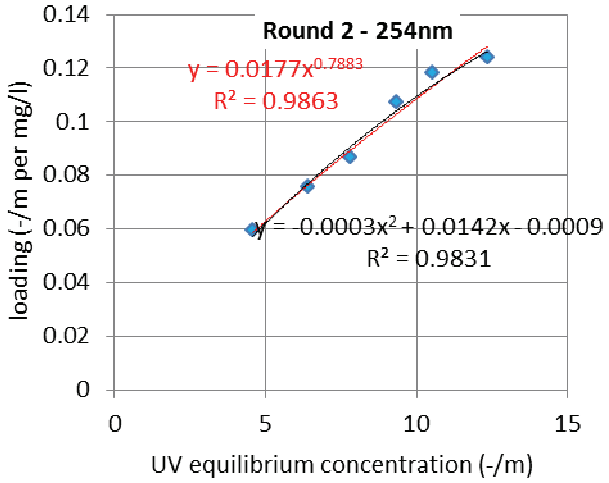

Figure 5.1(b) UVA_{254} results for the Olifantsvlei plant (Round 2)

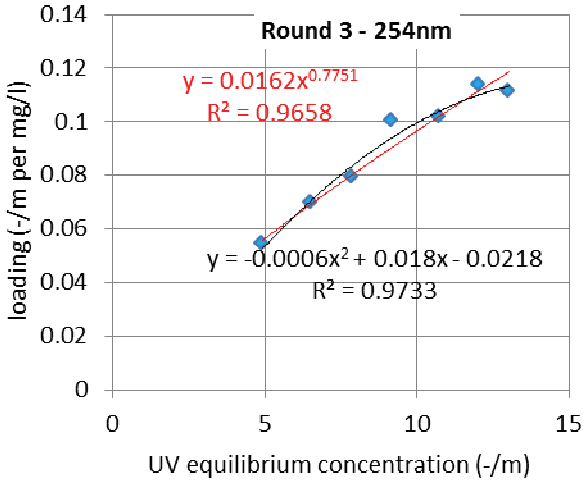

Figure 5.1(c) UVA_{254} results for the Olifantsvlei plant (Round 3)

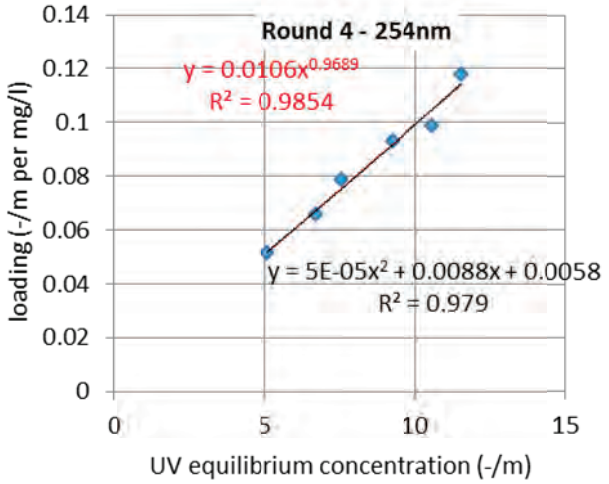

Figure 5.1(d) UVA_{254} results for the Olifantsvlei plant (Round 4)

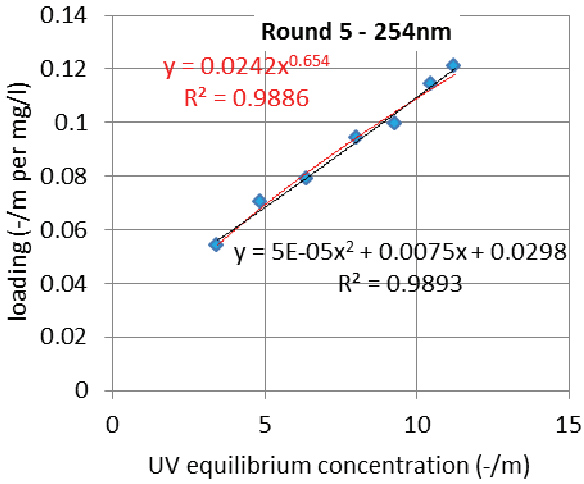

Figure 5.1(e) UVA_{254} results for the Olifantsvlei plant(Round 5)

5.3 Removal of UVA_{254}

The *K* and *n* values for all the samples that were not rejected, for experimental reasons, are shown in Table 5.3.

Table 5.3 Summary of isotherm results for UVA removal. ($D_{50\%}$ is the required dosage to remove 50% of the raw water UVA)

Plant	Round	*K*	*n*	R^2	UVA_{raw}	$D_{50\%}$
Midvaal	1	0.0277	0.5791	0.92	16.4	88
	2	0.0151	0.8018	0.98	15.3	99
	3	0.0142	0.8247	0.98	18.3	104
	5	0.0301	0.5469	0.99	14.0	80
Wiggins	1	0.0140	1.0276	0.97	7.0	69
	2	0.0219	0.9487	0.99	6.3	48
	3	0.0121	1.2177	0.99	6.1	65
	4	0.0050	1.6093	0.97	7.6	89
	5	0.0410	0.4299	0.98	4.9	41
Umzonyana	1	0.0117	0.8599	0.94	15.8	114
	2	0.0193	0.6442	1.00	14.8	106
	3	0.0145	0.7134	0.95	16.7	127
	4	0.0094	0.8761	0.96	19.0	141
Loerie	2	0.0124	0.8841	0.97	17.3	104
	3	0.0103	0.8335	0.96	6.7	119
	4	0.0152	0.7148	0.96	15.1	117
	5	0.0346	0.3182	0.94	13.3	105
Rietvlei	1	0.0277	0.5072	0.99	18.4	108
	2	0.0224	0.6325	0.97	17.2	98
	3	0.0118	0.8288	0.93	19.2	125
	5	0.0266	0.5918	0.94	16.3	89
Olifantsvlei	1	0.0247	0.7256	0.96	13.1	68
	2	0.0177	0.7883	0.99	16.4	88
	3	0.0162	0.7751	0.97	15.8	98
	4	0.0106	0.9689	0.99	15.4	101
	5	0.0242	0.6540	0.99	14.3	82
Plettenberg Bay	2	0.0072	0.7522	0.95	30.4	273

The final column in Table 5.3 is the dosage of activated carbon required to reduce the raw water UVA_{254} by 50%, as calculated using the isotherm constants. The dosages are very high compared to what can be financially tolerated by water service providers, and therefore not suggested for practical application. The results do, however, indicate that there are meaningful differences, to be discussed later.

5.4 Removal of Dissolved Organic Carbon

During this project, UVA_{254} was used as a key parameter for NOM quantification. For activated carbon adsorption, a parallel test was conducted to compare the removal of UVA_{254} and DOC. This test was performed on some of the raw samples collected during Round 4. The *K* and *n* values for all the samples that were not rejected, for experimental reasons, are shown in Table 5.4.

Table 5.4 Summary of isotherm results for DOC removal. ($D_{50\%}$ is the required dosage to remove 50% of the raw water DOC)

Plant	Round	K	n	R^2	DOC_{raw}	$D_{50\%}$
Wiggins	4	8.743E-03	1.346	0.94	4.7381	85
Umzonyana	4	1.993E-03	1.948	0.97	11.6777	94
Loerie	4	1.646E-02	0.599	0.91	10.2762	117
Olifantsvlei	4	8.022E-03	0.982	0.93	7.6750	128

The Freundlich isotherms could be determined with a high degree of precision, as evidenced by the R^2 values which were all above 0.90. The final column in Table 5.4 is the dosage of activated carbon required to reduce the raw water DOC by 50%, as calculated using the isotherm constants. Similar to the results of the previous section regarding UVA removal, the dosages are prohibitively expensive, and therefore not suggested for practical application.

How does the removal of DOC and UVA_{254} compare for activated carbon adsorption? Table 5.5 repeats the final columns of Tables 5.3 and 5.4, namely the dosage of activated carbon required for the removal of 50% of the raw water UVA_{254} and DOC.

Table 5.5 Activated carbon dosage required for 50% removal of UVA_{254} and DOC (tested on samples collected during Round 4)

Plant	for DOC	for UVA_{254}	difference
Wiggins	85	89	5%
Umzonyana	94	141	50%
Loerie	117	117	0%
Olifantsvlei	128	101	-21%

For the Wiggins and Loerie waters, there is almost no difference in the required dosage to remove either DOC or UVA_{254}. In other words, UVA_{254} could have been used as a near-to-perfect substitute parameter for DOC. In the case of the Umzonyana and Olifantsvlei plants, there were larger differences. The number of parallel tests, however, is too few to allow a definitive comparison.

5.5 Summary

- An experimental procedure was developed which tested crushed and sieved GAC in a shaker table for three days, covered a broad dosage range of 0 to 200 mg/ℓ. The procedure was applied to all the raw water samples, after excluding those samples affected by experimental hitches.
- The results could be adequately modelled with the Freundlich isotherm.
- The isotherm allows the calculation of the activated carbon dosage to remove 50% of the raw water UVA_{254}. These values do not suggest a practical treatment technology, but serve to illustrate that raw waters with similar UVA values would respond quite differently to activated carbon treatment.
- Although the emphasis of this project is on UVA_{254} as NOM parameter, control tests using DOC as response parameter showed similar removal of UVA_{254} and DOC for the same order of activated carbon dosage. UVA_{254} can therefore be used for preliminary adsorption testing, but to be confirmed during more detailed test work with parallel DOC measurement.

CHAPTER 6. NATURAL ORGANIC MATTER REMOVAL BY ION EXCHANGE

6.1 A Standard Laboratory Procedure

The equilibrium testing procedure for the IEX resins was the same as the activated carbon procedure described in Chapter 5, with the exception that the IEX resin dosage ranged from 0 to 1280 mg/ℓ. Two readily available commercial resins were used, one a strong resin and the other a weak resin, both specifically targeted to remove organic compounds from water. The resins were Lewatit MonoPlus MP 600 and the Lewatit MP 62, both having a macroporous structure with a matrix made from a cross-linked polystyrene. Other properties are listed in Table 6.1.

Table 6.1 Characteristics of ion exchange resins.

Resin	Type	Ionic form	Functional group	Capacity	Water content	Average resin size	Operating conditions	
				(eq/ℓ)	(%)	(mm)	pH	temp
LEWATIT MonoPlus MP 600	Strong base	Cl^-	Quaternary amine type II	1.1	55-60	0.6 (±0.05)	0-12	max 30°C
LEWATIT MP 62	Weak base	Free base	Tertiary amine	1.7	50-55	0.315 – 1.250	0-8	max 70°C

6.1.1 Verification of contact time

The contact time of three days, copied from the activated carbon tests, was verified for the resins selected. Water was obtained from the Westdene dam near the Auckland Park campus of the University of Johannesburg and treated by both ion exchange resins at dosages between 0 and 640 mg/ℓ. The reduction of UVA_{254} was tracked every day for five days. The results are shown in Figure 6.1, which clearly indicates that three days were adequate to reach a very near state of equilibrium, for both resins and for a wide range of resin concentrations.

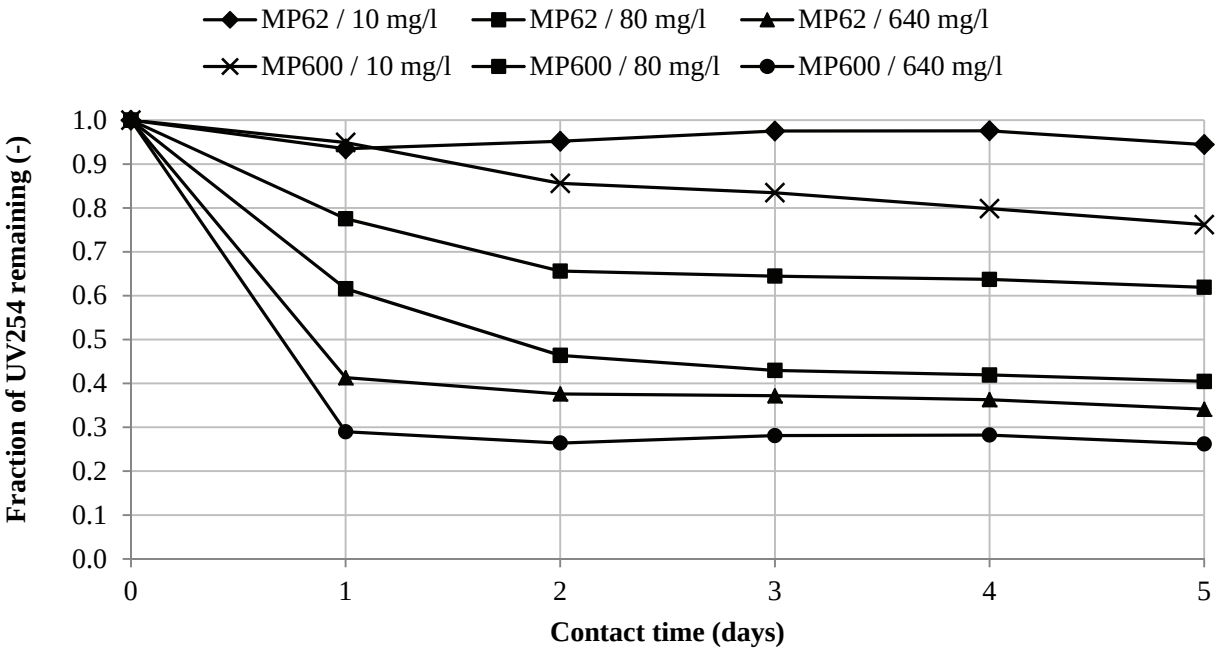

Figure 6.1 UVA_{254} remaining as a function of contact time.

6.2 Data Analysis

The first step, as with the activated carbon, was to determine whether the adsorption behaviour is adequately described by the Freundlich isotherm. Unlike activated carbon, the Freundlich isotherm did not provide a good fit to the data, shown in Table 6.2 and Figures 6.2a-d and 6.3a-d for two selected treatment plants. In many cases, the data points traced a curve which ran contrary to the power curve. The polynomial curves, also shown on the figures, provided a much better fit. This is further supported by the better correlation coefficients, although it is noted that the polynomial would inherently provide a better fit, as it requires three model parameters as opposed to the two parameters of the power curve.

Table 6.2 Weak IEX resin UVA_{254} results

Round	Loerie plant			Olifantsvlei plant		
	UVA_{254} (/m)	**R^2 Power**	**R^2 Polynomial**	**UVA_{254} (/m)**	**R^2 Power**	**R^2 Polynomial**
2	17.7	0.98	1.00	15.2	0.93	0.99
3	7.5	0.88	1.00	16.6	0.98	1.00
4	15.0	0.79	0.95	14.9	0.89	1.00
5	17.3	0.85	0.98	17.8	0.84	0.99

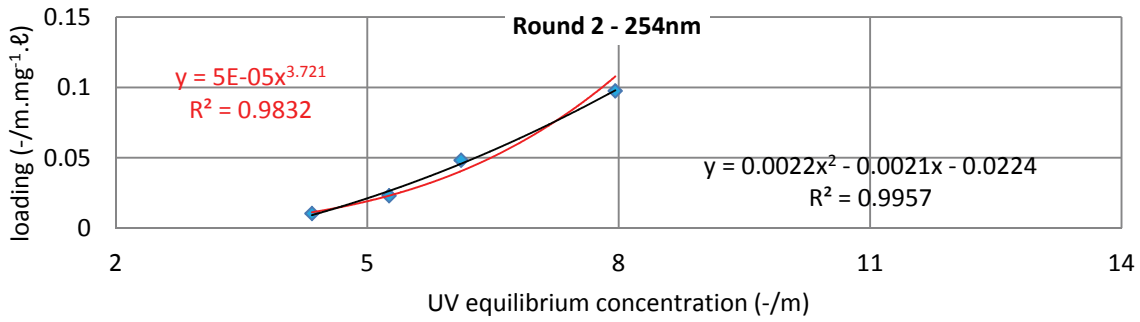

Figure 6.2(a) Weak IEX resin UVA_{254} results for the Loerie plant (Round 2)

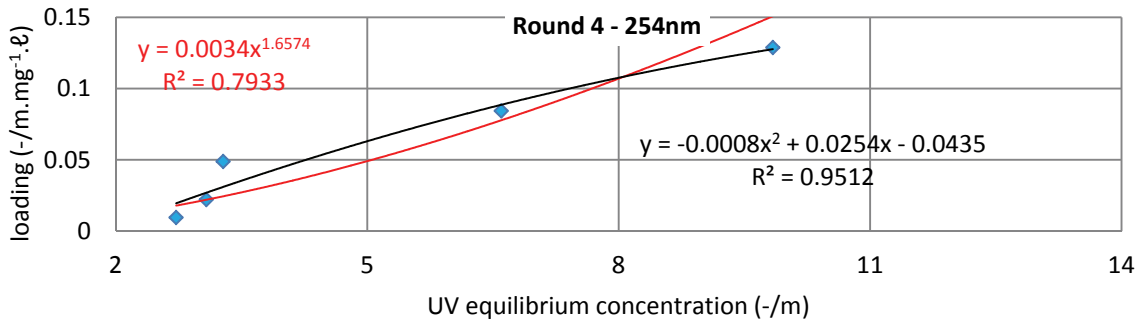

Figure 6.2 (b) Weak IEX resin UVA_{254} results for the Loerie plant (Round 4)

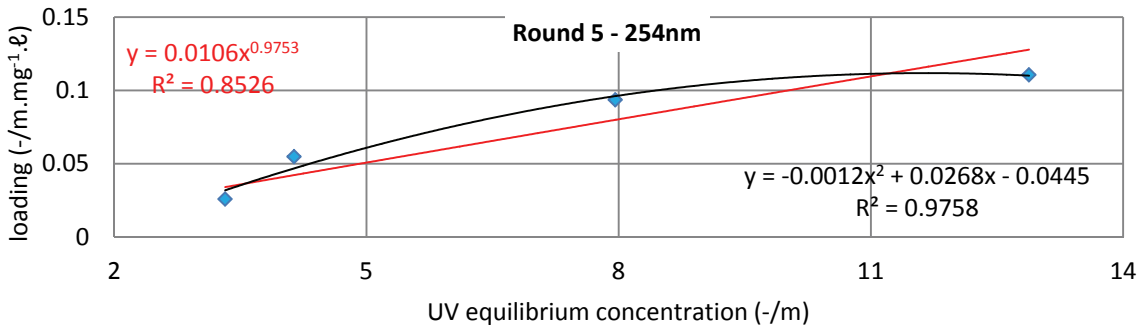

Figure 6.2 (c) Weak IEX resin UVA_{254} results for the Loerie plant (Round 5)

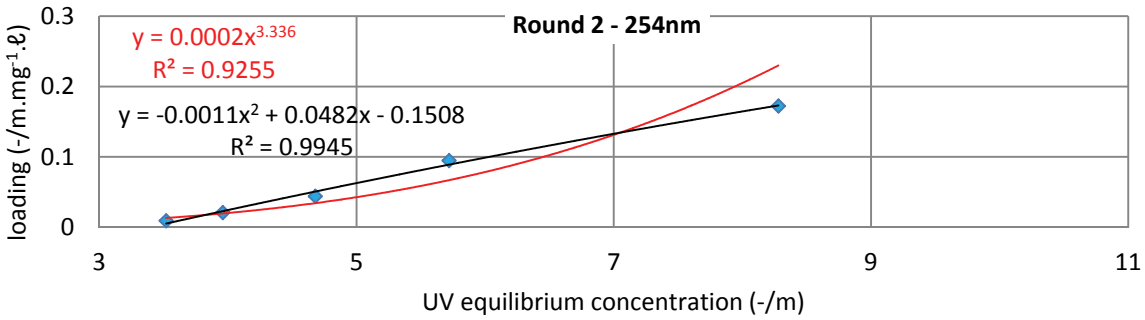

Figure 6.3 (a) Strong IEX resin UVA_{254} results for the Olifantsvlei plant (Round 2)

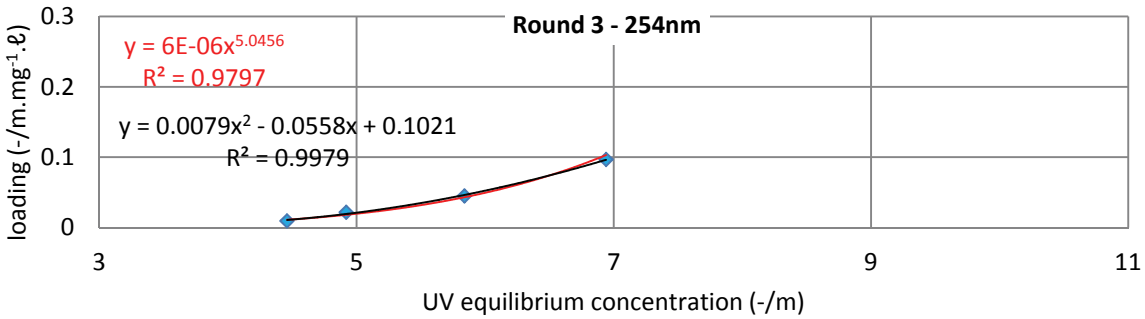

Figure 6.3 (b) Strong IEX resin UVA_{254} results for the Olifantsvlei plant (Round 3)

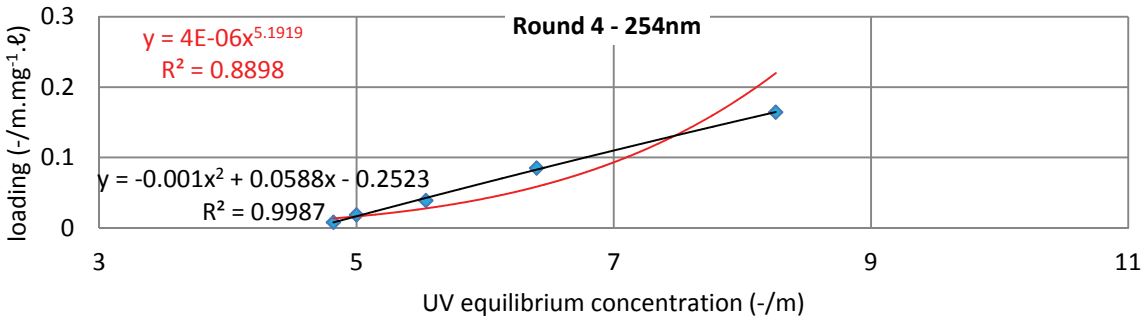

Figure 6.3 (c) Strong IEX resin UVA_{254} results for the Olifantsvlei plant (Round 4)

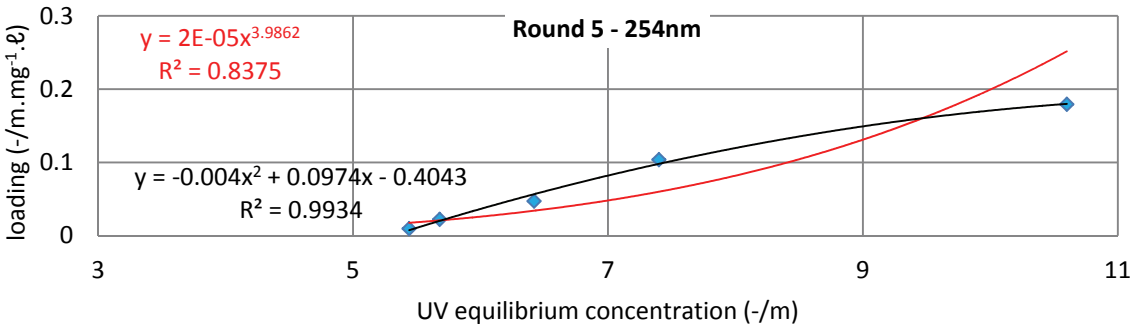

Figure 6.3 (d) Strong IEX resin UVA_{254} results for the Olifantsvlei plant (Round 5)

6.3 Adsorption Results

Tables 6.3 and 6.4 summarise all the test results for the two IEX resins tested. The final column in both tables presents the IEX dosage required for 50% removal of the raw water UVA. This dosage was calculated using the polynomial fit.

Table 6.3 Summary of isotherm results (weak resin). ($D_{50\%}$ is the required dosage to remove 50% of the raw water UVA)

Plant	Round	Polynomial model			R^2	UVA_{raw}	$D_{50\%}$
		a	b	c			
Midvaal	2	0.0025	-0.0097	0.0037	1.00	15.5	98
	3	-0.0001	0.0139	-0.0568	0.98	18.0	150
	5	-0.0006	0.0190	-0.0470	1.00	13.8	124
Wiggins	2	0.0187	-0.0686	0.0556	1.00	6.4	116
	3	0.0095	-0.0396	0.0412	0.99	6.6	236
	4	0.0050	-0.0081	-0.0103	0.98	7.3	136
	5	-0.0083	0.0601	-0.0470	0.99	4.5	49
Umzonyana	2	0.0017	-0.0082	0.0112	1.00	15.3	160
	3	-0.0005	0.0199	-0.0668	0.99	17.1	128
	4	-0.0009	0.0265	-0.0803	1.00	18.9	105
	5	0.0002	-0.0024	0.0332	1.00	31.5	350
Loerie	2	0.0022	-0.0021	-0.0224	1.00	17.7	67
	4	-0.0008	0.0254	-0.0435	0.95	15.0	74
	5	-0.0012	0.0268	-0.0445	0.98	17.3	89
Rietvlei	2	-0.0004	0.0227	-0.0745	1.00	16.9	95
	3	3.0E-05	0.0101	-0.0392	0.99	18.9	160
	5	-0.0006	0.0200	-0.0585	1.00	19.7	123
Vereeniging	2	-0.0018	0.0531	-0.2977	1.00	21.7	163
	3	-8.0E-05	0.0061	-0.0066	0.94	22.0	216
	5	-0.0004	0.0180	-0.0908	0.98	27.5	170
Olifantsvlei	2	0.0008	0.0079	-0.0487	1.00	15.4	129
	3	5.0E-05	0.0098	-0.0381	0.98	16.4	180
	5	-0.0009	0.0250	-0.0669	1.00	14.9	107
Plettenberg Bay	2	-0.0002	0.0075	-0.0072	1.00	30.8	253
	3	-0.0001	0.0059	0.0085	0.99	40.6	233
	5	-0.0001	0.0102	-0.1030	1.00	51.6	276

Table 6.4 Summary of isotherm results (strong resin). ($D_{50\%}$ is the required dosage to remove 50% of the raw water UVA)

Plant	Round	Polynomial model			R^2	UVA_{raw}	$D_{50\%}$
		a	b	c			
Midvaal	2	-0.0019	0.0588	-0.1740	0.98	14.9	47
	3	0.0079	-0.0511	0.0884	1.00	18.4	32
	5	-0.0040	0.0920	-0.3489	0.99	17.2	59
Wiggins	2	-0.0321	0.2580	-0.4330	0.98	6.6	48
	3	0.0449	-0.1508	0.0998	1.00	6.3	45
	4	0.1054	-0.6786	1.1052	0.99	7.7	70
	5	-0.0773	0.6618	-1.3325	0.99	7.2	75
Umzonyana	2	-0.0037	0.0992	-0.2877	1.00	15.7	30
	3	0.0047	0.0269	-0.1516	1.00	17.3	20
	4	-0.0090	0.1670	-0.5389	1.00	19.3	41
	5	-0.0028	0.0917	-0.4939	0.97	28.6	58
Loerie	2	0.0024	-0.0022	-0.0182	0.95	17.7	59
	5	-0.0044	0.0975	-0.3137	0.98	19.0	44
Rietvlei	2	3.0E-06	0.0381	-0.1224	0.95	17.1	42
	3	0.0073	-0.0472	0.0744	0.99	19.4	32
	5	-0.0057	0.1199	-0.4128	1.00	19.7	46
Vereeniging	3	0.0012	-0.0026	0.0015	0.97	23.6	86
	4	-0.0014	0.0449	-0.1682	1.00	25.7	72
	5	-0.0020	0.0662	-0.3476	1.00	27.6	75
Olifantsvlei	2	-0.0011	0.0482	-0.1508	0.99	15.2	50
	3	0.0079	-0.0558	0.1021	1.00	16.6	45
	4	-0.0010	0.0588	-0.2523	1.00	14.9	57
	5	-0.0040	0.0974	-0.4043	0.99	17.8	61
Plettenberg Bay	2	-0.0003	0.0139	-0.0119	1.00	30.8	118
	3	-9.0E-05	0.0073	-0.0010	0.99	44.8	191
	5	-0.0001	0.0101	-0.0305	0.99	52.2	158

6.4 Comparison between Weak and Strong IEX Resins

As in the case of activated carbon, the response of the different samples to both the IEX resins was quite different, even if the UVA_{254} values are similar. The dosages calculated for 50% UVA_{254} removal are high, but they serve a useful purpose in demonstrating the differences in NOM character, and provide a basis for comparison amongst different treatment processes. Table 6.5 summarises the D50% results for the weak and strong resins, averaged for each different raw water source.

In all cases, strong IEX resin performed better on a mass basis. For some sources (Loerie and Plettenberg Bay), the advantages of strong IEX resins were less pronounced, while for others (notable Umzonyana), the difference was large. On average, about 2.4 times more weak IEX resin is required. It is noted that weak and strong IEX resins had roughly the same unit cost, but that the regeneration of strong IEX resins requires a strong acid with concomitantly larger disposal problems.

Table 6.5 Required IEX dosages for 50% removal of UVA_{254} from different raw water sources, averaged over the different sampling rounds.

Source	MP62	MP600	MP62/MP600
Midvaal	124	46	2.7
Wiggins	134	60	2.3
Umzonyana	186	37	5.0
Loerie	78	52	1.5
Rietvlei	126	40	3.2
Vereeniging	193	81	2.4
Olifantsvlei	139	52	2.7
Plettenberg Bay	254	56	1.6
Average	**154**	**65**	**2.4**

6.5 Summary

- A test procedure, first developed for isotherm testing of activated carbon, worked well for the adsorption of UVA_{254} on both strong and weak IEX resins.
- A contact time of three days was adequate to reach equilibrium.
- Over the wide range of dosages used (up to 1280 mg/ℓ), the Freundlich isotherm did not provide a good fit and a polynomial had to be used to get a satisfactory fit.
- The calculated dosage to remove 50% of the UVA_{254} differs amongst the different raw waters, and is very high in comparison to typical usage rates in practice.
- In terms of UVA only, the weak IEX resin did not perform as well as the strong IEX resin – on average, about 2.4 times more weak resin has to be used to obtain the same UVA removal.

CHAPTER 7. NATURAL ORGANIC MATTER REMOVAL BY NANOMATERIALS

7.1 Background

The photocatalytic degradation of pollutants in water has attracted much attention in the past several decades as more and new emerging pollutants are detected in the environment (Bolong *et al.*, 2009). Water availability problems are expected to grow in the coming decades even in regions currently considered water-rich. These challenges call for intensive research to identify effective, robust new methods of purifying water at lower cost using less energy, while at the same time minimising usage of chemicals and impact on the environment. Among many semiconductor photocatalysts, TiO_2 has received the most attention due to its high photocatalytic activity, chemical and biological stability, insolubility in water, acidic and basic media, non-toxicity, availability and low cost (Sojic *et al.*, 2010). When TiO_2 is irradiated with a photon of energy equal to or greater than its band-gap width, electrons are promoted from the valence band to the conduction band. This leads to the formation of electron/hole (e^-/h^+) pairs. Free electrons are produced in the empty conduction band (e^- CB) leaving behind electron vacancies or holes in the valence band (h^+ VB). In aqueous systems, holes react with surface OH groups and water molecules to produce HO• radicals, which are known to be strongly oxidising. The radicals can oxidise organic pollutants to the mineralised final products, i.e. CO_2, H_2O and corresponding inorganic ions, if the compound contains hetero-atoms (Martins *et al.*, 2009).

An important drawback of TiO_2 photocatalysis is its wide band gap of 3.0 eV to 3.2 eV. Only a small fraction of the solar spectrum ($\lambda < 380$ nm, corresponding to the UV region) is utilised in sensitising the TiO_2. The artificial generation of photons required for photocatalyst activation is the most important source of costs in photocatalytic wastewater treatment plants. This suggests using the sun as an economically and ecologically sensible light source (Malato *et al.*, 2009). Another problem of using TiO_2 as a photocatalyst is electron/hole recombination, which, in the absence of proper electron acceptors, is extremely fast and thus represents a major energy-wasting step as well as limiting the achievement of a high quantum yield. Efforts are currently underway to optimise the TiO_2 structure and properties for enhanced photocatalytic efficiency. Modification of TiO_2 nanoparticles through noble metal doping is increasingly being considered for maximising its photocatalytic efficiency. These metals may facilitate electron-hole separation and promote interfacial electron transfer or they may decrease the TiO_2 band gap, which benefits electron transfer from the valence band to the conduction band, facilitating the formation of oxidative species such as hydroxyl radicals (Mills and Hunte, 1997; Obare and Meyer, 2004; Han *et al.*, 2009). Anionic species such as nitrogen, carbon and sulphur have also been shown to form new impurity levels close to the valence or conduction band of TiO_2 thereby lowering the band gap and shifting the absorption edge to the visible-light region (Asahi *et al.*, 2001). More recently, the simultaneous doping of two kinds of atoms into TiO_2 has attracted considerable interest, since it could result in a higher photocatalytic activity and peculiar characteristics compared with single-element doping. It is widely believed that a second element confers a synergistic sensitising effect to non-metal-doped TiO_2, thereby enhancing visible light-induced photoactivity. Non-metal/platinum group metal co-doping of TiO_2 may result in a material with excellent photocatalytic performance compared to singly-doped TiO_2.

In this work, nitrogen, palladium co-doped TiO_2 nanoparticle photocatalysts were synthesised by a modified sol-gel method and investigated for their visible light-induced photocatalytic degradation of NOM fractions using simulated solar radiation.

7.2 Results

7.2.1 Fourier Transform Infrared Characterisation

Fourier Transform Infrared (FT-IR) studies were performed in order to determine the presence of functional groups as well as to study the surface changes on the nanoparticles (Figure 7.1). OH groups and water on the surface of the particles were confirmed by appearance of a broad band at about 3300 cm^{-1} and at 1644 cm^{-1}, respectively. The OH peak at 1644 cm^{-1} is associated with O-H bending of the adsorbed water. A highly intense peak centred around 520 cm^{-1} was attributed to the Ti-O bond. This peak could not be clearly observed because of the reduced capability of the instrument at wavenumbers of below 450 cm^{-1}. A CH peak, probably due to impurities or residual organic compounds, was also observed at about 2934 cm^{-1}.

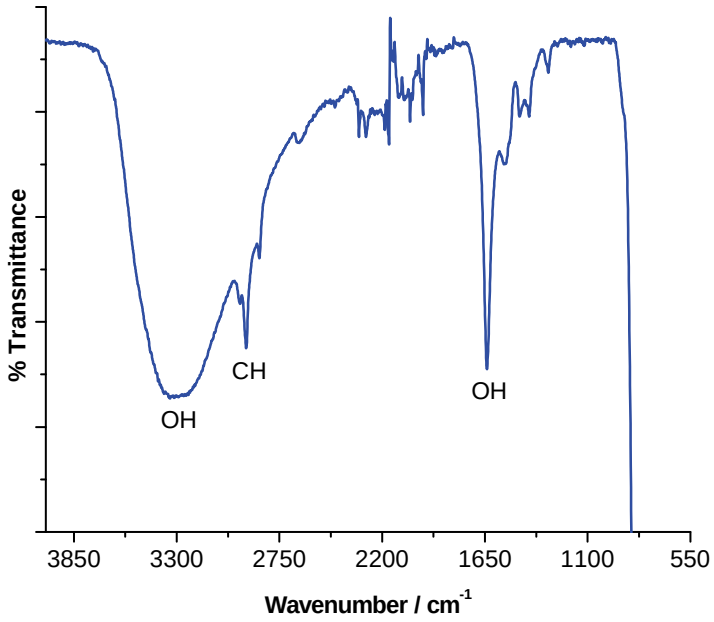

Figure 7.1 Fourier Transform Infrared spectrum of N, Pd co-doped TiO_2 (0.5% Pd)

7.2.2 Raman characterisation

Raman analysis was carried out on a Perkin Elmer Raman microscope in the 50 $cm^{-1}$to 800 cm^{-1} frequency range using the 785 nm exciting line (Figure 7.2). Anatase TiO_2 shows six Raman active fundamental modes at 144cm^{-1} (E_g), 197cm^{-1} (E_g), 397cm^{-1} (B_{1g}), 518cm^{-1} (A_{1g} + B_{1g}) and 640cm^{-1} (E_g) (Morikawa *et al.*, 2008). Well-resolved Raman peaks were observed at 141 cm^{-1} (E_g), 397cm^{-1} (B_{1g}), 517 cm^{-1} (A_{1g} + B_{1g}) and 639 cm^{-1} (E_g), indicating that anatase was the predominant phase. No Raman lines due to palladium appeared in the N, Pd co-doped sample, confirming the presence of the dopant in low concentrations on the crystal lattice (Kuvarega *et al.*, 2011). Sharp, narrow intense peaks at low wavenumbers confirmed the presence of the particles in the crystalline state. The TiO_2 crystalline structure was not altered by the doping procedure.

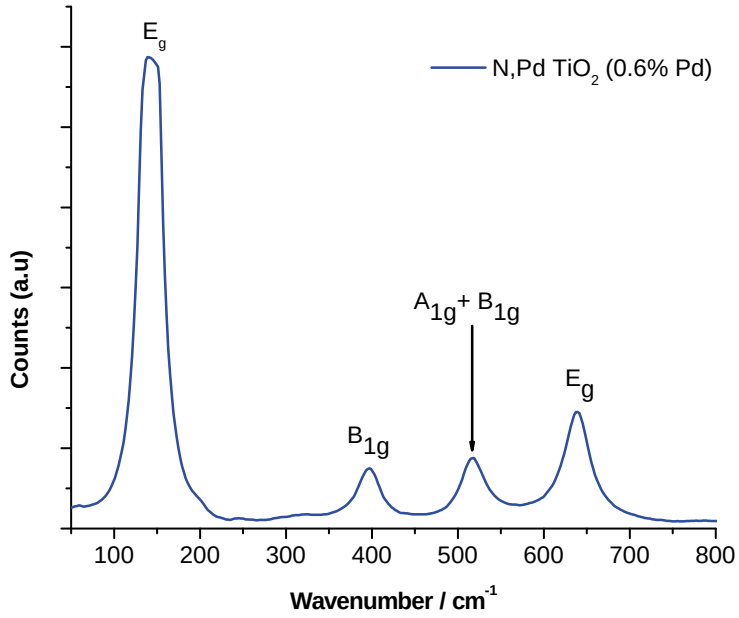

Figure 7.2 Raman spectrum of N, Pd co-doped TiO_2

7.2.3 X-ray diffraction characterisation

X-ray diffraction (XRD) patterns of the N, Pd co-doped TiO_2 subjected to heat treatment at 500ºC for 2 h are shown in Figure 7.3. Post-synthesis treatment by thermal annealing resulted in increased crystallinity with anatase as the principal phase in agreement with Raman spectra. Resolved peaks at 2θ values of 25.3, 37.6, 48.2, 53.9, 54.8, 62.7 and 75.2 corresponding to the (101), (004), (200), (105), (211), (204) and (215) planes, respectively, are attributed to the anatase phase of TiO_2 (Kuvarega *et al.*, 2011). Calcination resulted in intense and sharp anatase peaks. This is clearly indicative of an improvement in the degree of crystallinity corresponding to the formation of larger particles with fewer defects. A PdO peak (101) at 2θ value of 33.8 confirmed the presence of Pd in the oxide form. Pd will most likely occupy interstitial positions on the lattice because of its relatively large size compared to Ti (0.86 Å for Pd^{2+} and 0.68 Å for Ti^{4+}) (Shah *et al.*, 2002). The crystallite size was calculated using the Scherer equation (7.1 below):

$$D = \frac{k\lambda}{\beta \cos\theta} \tag{7.1}$$

Where:

D is crystallite particle size
k is a constant of 0.9
λ is the wavelength (nm) of characteristic X-ray applied
β is the full width at half maximum (FWHM) of the anatase (101) peak obtained by XRD
θ is Bragg angle (Yan *et al.*, 2005)

Results of the particle size determination gave an average value of 15.79 nm.

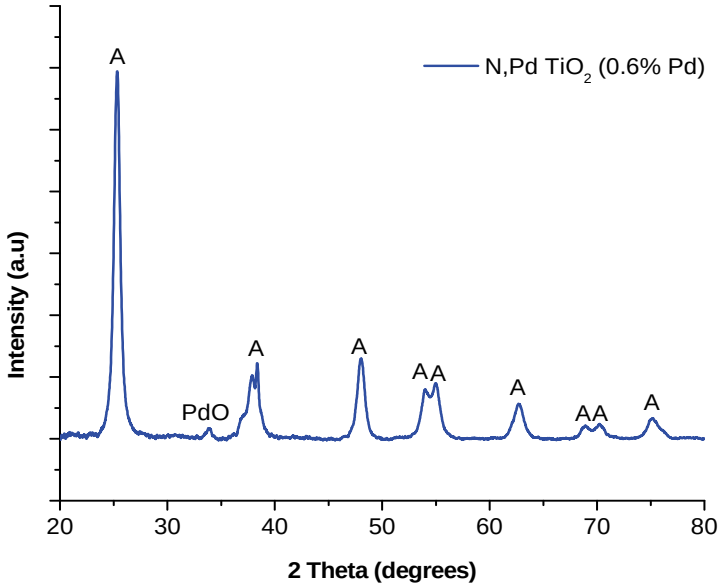

Figure 7.3 XRD pattern of N, Pd co-doped TiO_2. (A – anatase)

7.2.4 Optical properties

The optical properties of the material are shown in Figure 7.4. The spectra are characterised by an intense fundamental absorption due to anatase TiO_2 in the region between 300 nm and 400 nm (Figures 7.4a and b). There is a red shift in the absorption edge for N, Pd co-doped TiO_2 that can be attributed to the presence of Pd and N in the TiO_2. Commercial TiO_2 gave a well-defined absorption with an edge of about 380 nm whilst the co-doped TiO_2 showed tailing of the fundamental TiO_2 band into the high wavelength region with an edge at about 750 nm. Increased absorption in the visible-light region could be due to d–d transitions of PdO particles, (Choi *et al.*, 2010), corresponding to the brown colour of the powders. The presence of N could also have led to a red shift in the absorption edge due to the excitation of electrons from localised nitrogen 2p levels in the band gap to the vacant conduction band of the TiO_2.The absorption around 400 nm is due to a charge transfer transition between the lattice oxygen ligands (O^{2-}) and a central titanium ion (Ti^{4+}) (Han *et al.*, 2009). A plot of the absorption coefficient versus wavelength (Kubelka-Munkplot) showed increased absorption by the co-doped TiO_2 in the high energy UV region (Figure 7.4c). The reflectance spectral data were converted to the Kubelka-Munk function, $F(R)$ by applying equation 7.2:

$$F(R) = \frac{(1 - R)^2}{2R} \qquad (7.2)$$

Where reflectance, $R = R_{sample}/R_{reference}$

The Kubelka-Munk function can be transformed to a Tauc plot –- a plot of $[F(R).hv]^n$vs.hv (Figure 7.4d). A direct band-gap semiconductor gives a linear Tauc region just above the optical absorption edge with $n = 2$, whilst an indirect semiconductor gives a linear region with $n = 0.5$ (Kuvarega *et al.*, 2011). The semiconductor band gap is a key indicator of its light harvesting efficiency under solar illumination. A direct band-gap semiconductor was assumed for the N, Pd TiO_2 since a linear region just above the gap edges was observed with $n = 0.5$. A band gap of about 2.48 eV for the N, Pd co-doped TiO_2 was realised from the Tauc plot. Commercial TiO_2 gave a band gap of about 3.15

eV. The red-shift in the absorption edge is typically attributed to the *sp* - *d* exchange interaction between the TiO_2 band electrons and localised *d*-electrons associated with the doped Pd ions. Band tailing is evidence of the presence of impurities and disorder in the band structure of the material leading to inter-band gap states. Therefore, the low-energy absorption onset is likely an electron transition from the valence band to the nitrogen- or palladium-derived impurity states (Kuvarega *et al.*, 2011).

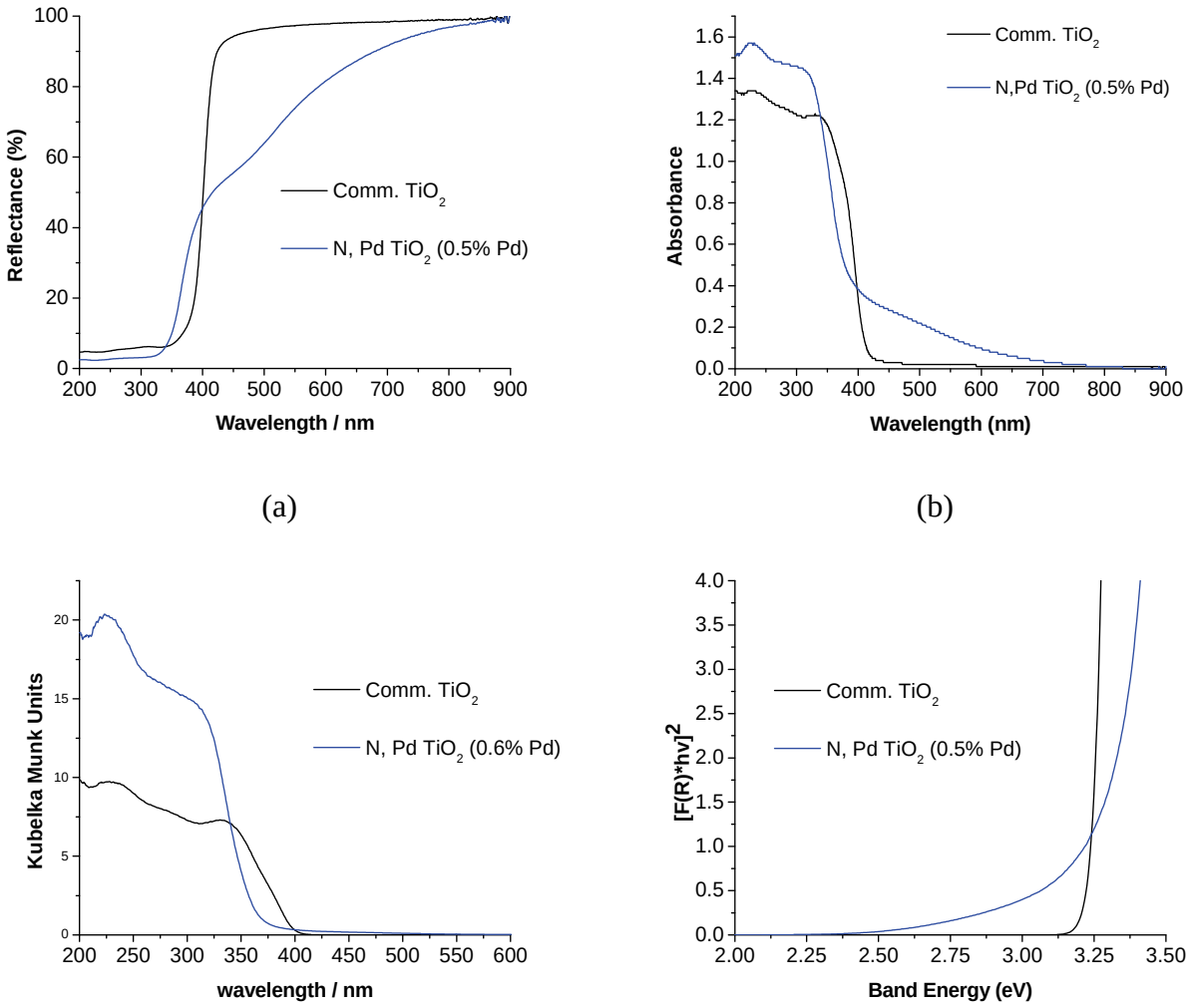

Figure 7.4 (a) Diffuse reflectance spectra; (b) absorption spectra; (c) Kubelka-Munk plots; and (d) Tauc plots of N, Pd co-doped TiO_2 and commercial TiO_2 (Degussa P25)

Scanning electron micrographs of N, Pd co-doped TiO_2 show the material consisted of small, nearly spherical particles (Figure 7.5a). Particles were not of uniform size and showed high degree of agglomeration. The size of the particles was in the nanometre range. Transmission electron micrographs confirmed the presence of Pd deposits on the surface of the N-doped TiO_2 (Figure 7.5b) with particles that were nearly spherical and some showing elongated morphologies. Pd deposits were well dispersed on many of the TiO_2 particles and showed diameters predominantly ranging from 1 nm to 2 nm. The size of the TiO_2 particles was approximately in the range of 15 nm to 20 nm consistent with XRD measurements. This is in agreement with reported results (Weishaar *et al.*, 2009).

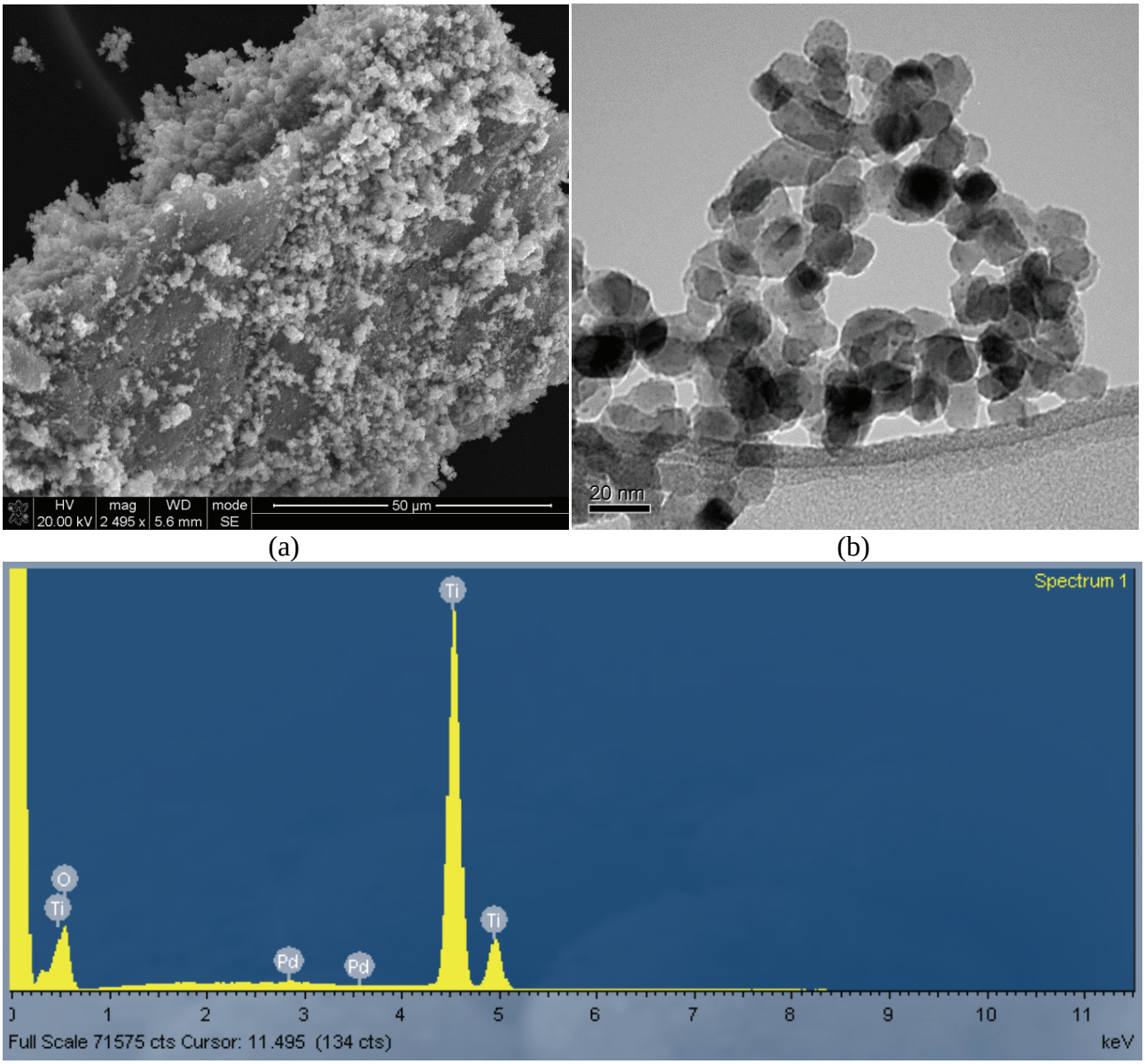

Figure 7.5 (a) SEM image; (b) TEM image; and (c) EDX spectrum of N, Pd co-doped TiO_2 (0.5% Pd)

The elemental composition of the various samples was estimated by EDX analysis. The EDX spectra of the co-doped TiO_2 showed signals directly related to the dopants (Figure 7.5c). Ti and O appeared as the main components with low levels of Pd. This confirmed the formation of N, Pd co-doped TiO_2.

The thermogram of N, Pd co-doped TiO_2 heated at 500ºC showed a small mass loss around 100ºC, attributed to the loss of water adsorbed onto the particle surfaces (Figure 7.6). A continuous small weight loss from 100ºC up to about 900ºC could be due to the loss of nitrogen or carbon-related materials entrapped within the nanoparticles. The total mass loss of about 4.5% shows the exceptionally high thermal stability of the material. It also confirms that much of the nitrogen and carbon material was lost through calcination at 500ºC (Kuvarega *et al.*, 2011).

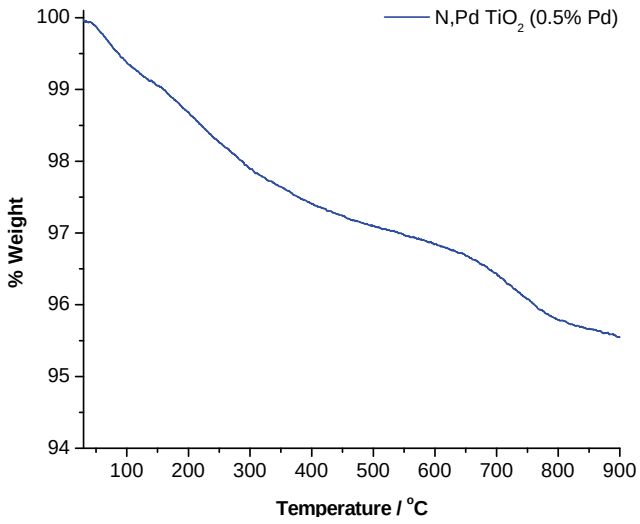

Figure 7.6 TGA curve of N, Pd co-doped TiO_2

7.2.5 Bulk water characterisation of samples

Table 7.1 gives the characterisation of the bulk NOM sample from Plettenberg Bay, the determinants being DOC, SUVA, turbidity, conductivity and pH.

Table 7.1 Characterisation of the bulk NOM sample

Sample	DOC (mg/ℓ)	SUVA (ℓ·mg^{-1}·m^{-1})	Turbidity (NTU)	Conductivity (mS/m)	pH
P1	21.44	5.20	14.6	0.12	6.73
P2	9.98	4.67	1.87	0.12	6.73
P3	11.37	4.62	0.27	0.12	6.39

The Plettenberg Bay water is characteristic of the organically coloured surface water found on the south-west coast in South Africa; its brownish colour is usually due to humic and fulvic substances. This is evidenced by high DOC values of the raw water (P1) samples (21.44 mg/ℓ, 9.98 mg/ℓ and 11.37 mg/ℓ for the first, second and third sampling, respectively). The turbidity of the raw water samples is also high (ranging from 14.64 NTU to 0.27 NTU), indicative of a high content of colloids and clay particles in these samples.

It is interesting to note that DOC removal efficiencies of all the water-treatment plants are relatively high, as can be seen with an 85% DOC removal efficiency.

As a general rule, SUVA < 2 ℓ·mg^{-1}·m^{-1} implies that the sample is mainly composed of non-humic substances while, SUVA > 4 ℓ·mg^{-1}·m^{-1} implies that the sample is mainly composed of humic substances (Kiwa, 2006). The SUVA values of all the samples (Table 7.2) exceeded 4 ℓ·mg^{-1}·m^{-1}, implying that the NOM consists mostly of hydrophobic NOM, thus a greater percentage of the samples comprises humic substances.

7.2.6 Ultraviolet-visible (UV-Vis) spectrophotometric analysis

Ultraviolet absorbance is usually measured at a wavelength of 254 nm (and reported in cm^{-1}), which is the wavelength used as an industrial standard for the maximum UVA absorption of NOM samples. The absorption at this wavelength has been reported to represent the aromatic character of the organic species. An increase in UVA at 254 nm indicates that NOM is increasing in aromaticity and unsaturated carbon bonds (Kiwa, 2006). Ultraviolet absorbance was also measured at 214 nm,

272 nm and 300 nm for a more in-depth analysis of the NOM character in this study. As has already been discussed in Section 2.6, UV absorbance at 214 nm is indicative of nitrites and nitrates, and UVA_{272} nm has been reported in the literature to be the best predictor for trihalomethane (THM) formation (Liu *et al.*, 2006), while UVA_{300} nm is used locally (South Africa) by Rand Water and other water-purification plants as a measure of DOC. Figure 7.7 shows a UVA scan obtained for the bulk characterisation of the samples.

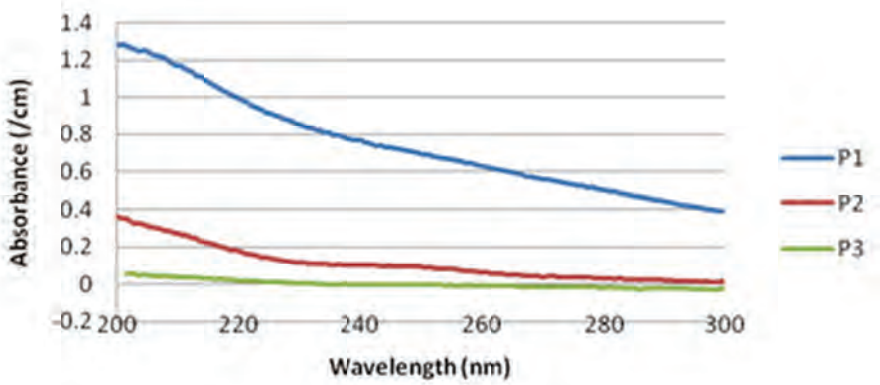

Figure 7.7 UVA scan of samples

There is a great decrease in the UVA of the samples after each treatment process, implying that there is an effective NOM removal by the different water treatment process. The samples generally have a high UVA_{254} absorbance implying that the samples are highly aromatic in nature and therefore constitutes mostly of hydrophobic NOM.

7.2.7 Natural organic matter photodegradation studies

Under UV radiation, photons excite electrons (e^-) from the valance band (VB) of TiO_2 to the conduction band (CB), creating holes (h^+) in the VB. The created charge carriers quickly recombine and only a fraction of the electrons and holes participate in the photocatalytic reaction, resulting in low reactivity. Introduction of nitrogen and palladium in the TiO_2 will result in the formation of impurity states close to the valence band. This enhances the visible-light activity of the nanoparticles as electrons can be excited from the nitrogen 2p orbitals to the TiO_2 conduction band (Kuvarega *et al.*, 2011).

In the presence of Pd, the photo-generated electrons are trapped, leading to electron-hole separation. The holes can scavenge surface-adsorbed water or hydroxyl groups, generating highly reactive hydroxyl radicals. The electrons on the other hand scavenge the oxygen molecules to form very reactive superoxide radicals (Kuvarega *et al.*, 2011). Both radicals are highly reactive towards the degradation of the organic compounds such as NOM. The NOM is degraded to harmless products, namely carbon dioxide and water. Figure 7.8 shows the proposed mechanism for the photodegradation of NOM by the N, Pd co-doped TiO_2.

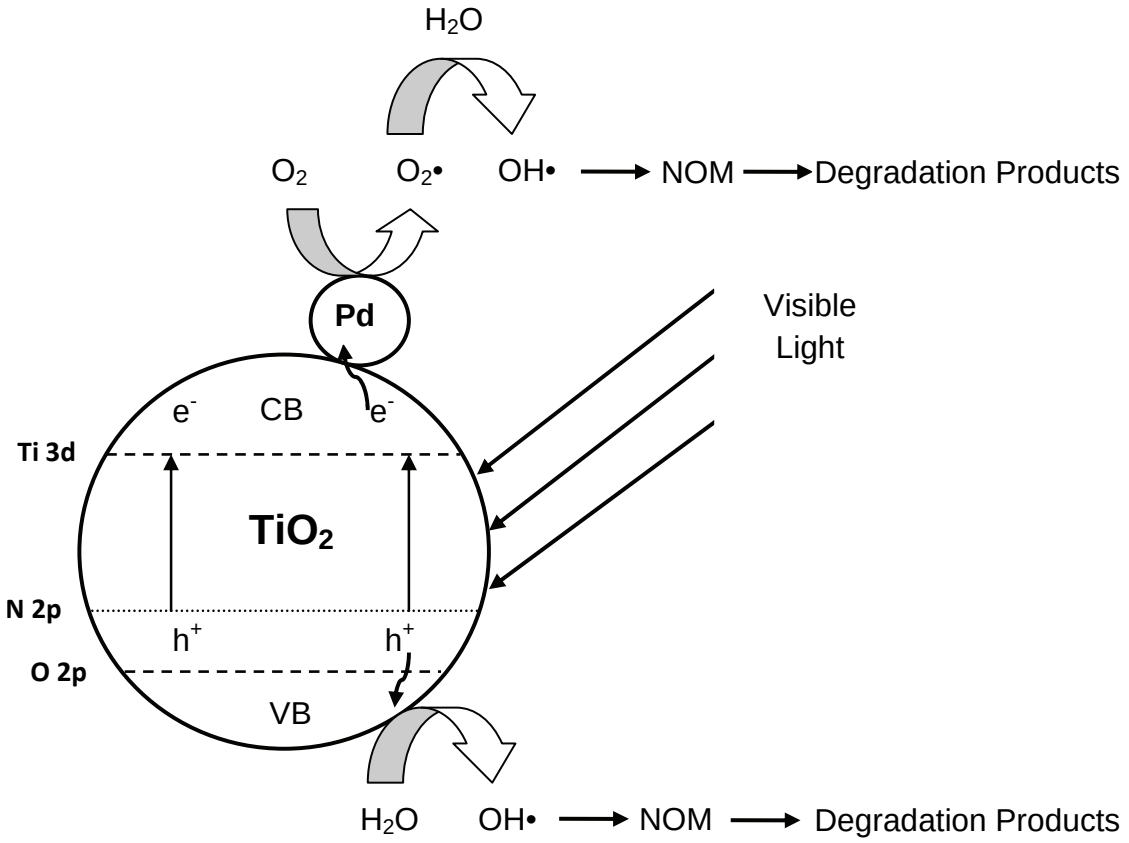

Figure 7.8 Proposed photocatalytic degradation mechanism of NOM by N, Pd co-doped TiO_2

The NOM fractions of dissolved organic materials are usually defined by the physical or chemical isolation procedure. The chemical description of the HPO, HPI and TPI NOM fractions is given as follows:

Hydrophobic (HPO): carboxylic acids of five to nine carbons, one- and two-ring aromatic carboxylic acids, aromatic acids, one- and two-ring phenols and tannins, proteins with one- and two-ring aromatic amines except for pyridine and high-molecular-weight alkyl (Marhaba and Van, 2000).

Hydrophilic (HPI): aliphatic acids of less than five carbons, hydroxyl acids, sugars, low molecular weight alkyl monocarboxylic acids and dicarboxylic acids, amphoteric proteinaceous materials containing amino acids, amino sugars, peptides and proteins (Marhaba and Van, 2000).

Transphilic (TPI): a mixture of hydrocarbon and carboxyl compounds, aliphatic amides, alcohols, aldehydes, esters, polysaccharides and ketones with less than five carbons (Marhaba and Van, 2000).

Natural organic matter removal by different water-treatment processes is primarily decided by both the chemical and physical properties of certain fractions of NOM i.e. hydrophobic and higher-molecular-weight NOM fractions are more effectively removed by coagulation than the other fractions, i.e. hydrophilic and lower-molecular-weight NOM (Hammes and Egli, 2005). The correlation between the NOM fractions and their ability to undergo photocatalytic degradation by N, Pd co-doped TiO_2 is thus investigated herein. Figure 7.9, 7.10 and 7.11 show the behaviour of the three NOM fractions over a period of 120 min of simulated solar irradiation in the presence of N, Pd co-doped TiO_2.

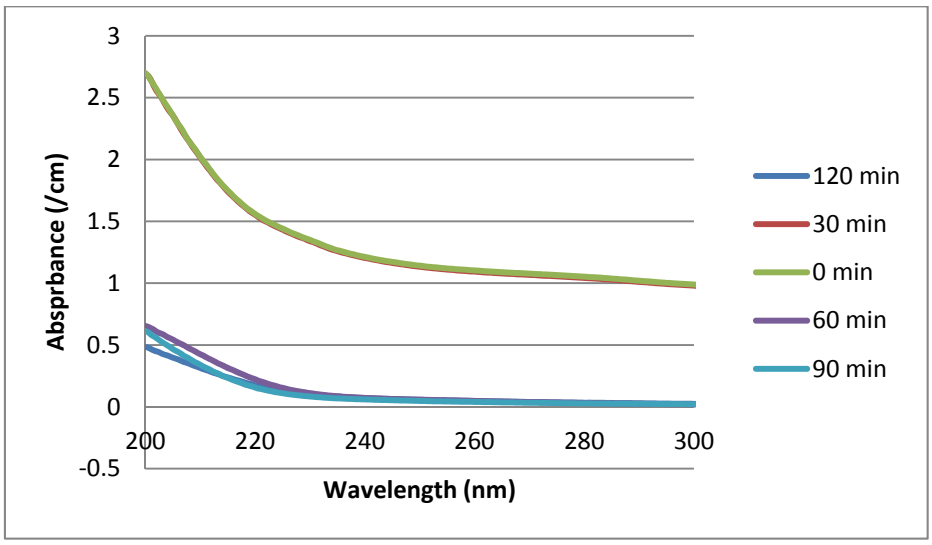

Figure 7.9 Ultraviolet scan over time of hydrophobic (HPO) NOM fraction

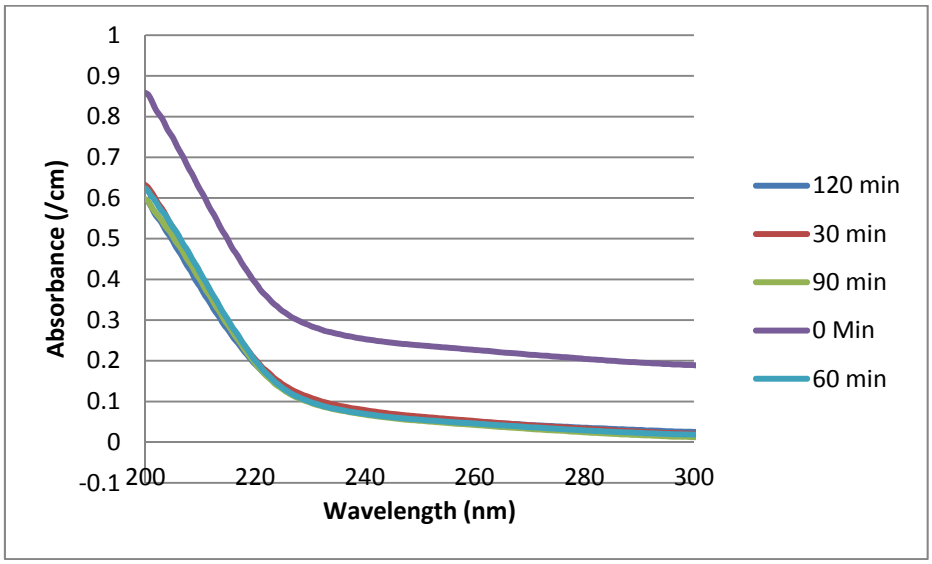

Figure 7.10 Ultraviolet scan over time for the hydrophilic (HPI) NOM fraction

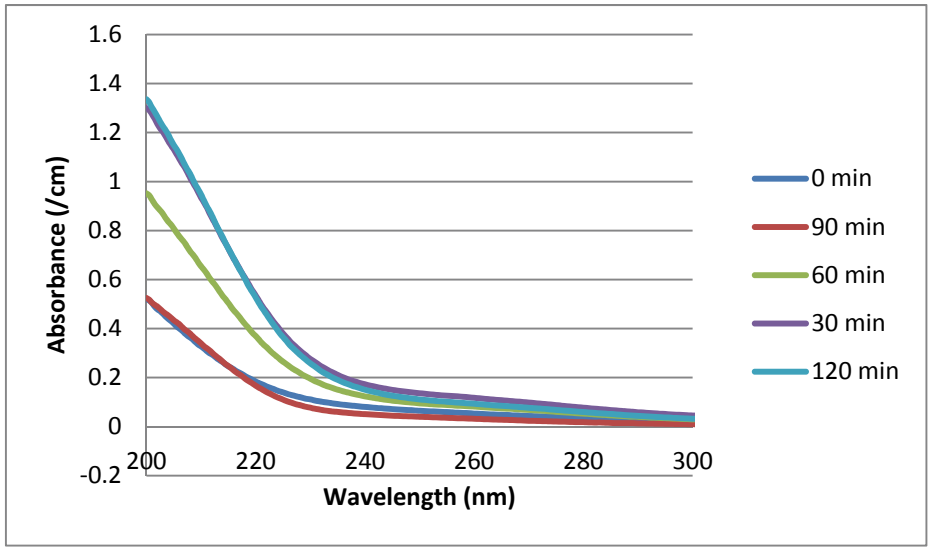

Figure 7.11 Ultraviolet scan over time for the transphilic (TPI) NOM fraction

The hydrophobic fraction (Figure 7.9) underwent the highest photodegradation, with a 96% UVA_{254} reduction (from 1.124 to 0.042 absorbance units) and the transphilic NOM fraction (Figure 7.11) was the least photo-degraded with a 14% UVA_{254} reduction. The hydrophilic NOM fraction had a 19% UVA_{254} reduction of the NOM content by photodegradation (Figure 7.10). Table 7.2 gives a summary of UVA results of the photodegradation experiments.

Table 7.2 UVA over time for the different samples

		UVA_{254} (/m)		
	Time (min)	**P1**	**P2**	**P3**
C18 (hydrophobic)	0	112.4	23.3	12.7
	30	111.8	5.9	10.3
	60	4.5	5.6	5.9
	90	4.5	5.1	6.1
	120	4.2	4.9	3.7
CN (hydrophilic)	0	3.7	3.2	3.7
	30	3.2	3.0	3.3
	60	3.2	2.9	3.2
	90	3.2	2.9	2.9
	120	3.0	2.0	2.4
NH_2 (transphilic)	0	8.6	5.9	5.3
	30	7.9	5.5	5.2
	60	7.9	5.4	4.9
	90	7.6	5.3	4.5
	120	7.4	5.0	4.5

Table 7.3 summarises the UVA_{254} reduction of the three NOM samples by photodegradation. The highest photodegradation of the NOM fractions was achieved in the hydrophobic fraction (71% to 96%) supporting literature observations that the hydrophobic NOM fraction is the more easily removed by NOM treatment protocols. The least NOM reduction occurred in the transphilic fraction (14% to 15%). However, these results are still far better than those achieved by most NOM removal methods such as coagulation, whose NOM removal efficiencies are in the range of about 75% compared to the 96% reduction achieved in the hydrophobic (HPO) NOM fraction (as evidenced by the 96% UVA_{254} reduction). The high NOM photodegradation efficiency for the hydrophobic fraction can be explained by the stronger interaction with the N, Pd co-doped TiO_2 nanoparticles leading to preferential attack by the HO• radicals.

Table 7.3 UVA_{254} reduction (%) of the three NOM samples by photocatalytic degradation

NOM fraction	**P1 (%)**	**P2 (%)**	**P3 (%)**
HPO	96	78	71
HPI	19	38	35
TPI	14	15	15

7.3 Summary

Visible-light active N, Pd co-doped TiO_2 was successfully synthesised by a modified sol-gel method. Co-doping reduced the band gap of TiO_2 and shifted the absorption edge to the visible-light region. This resulted in successful application of visible light for activating the co-doped TiO_2 for NOM photodegradation. The nanocatalyst was found to be efficient in NOM degradation compared to conventional NOM treatment methods. Improved photoactivity was attributed to the synergistic effects of N and Pd co-doping of TiO_2. The hydrophobic fraction (HPO) showed the highest

degradation efficiency of 96% because of the increased interaction with the nanoparticles. Results from this study showed that N, Pd co-doped TiO_2 is a promising photocatalytic material for NOM removal in water-treatment systems and can be considered a good candidate for future photocatalytic applications.

CHAPTER 8. DISCUSSION, CONCLUSIONS AND RESEARCH NEEDS

8.1 Routine Measurement of NOM at Drinking Water Treatment Plants

One of the reasons why full-scale drinking water plants pay little regard to the removal of NOM, is the difficulty of measuring it. The usual measure of NOM is DOC, a parameter which requires an expensive instrument normally reserved for large off-site laboratories where trained technicians, gas supplies, calibration standards, etc. are readily available. The legislated standard of SANS 241 for NOM is also framed in terms of DOC.

The measurement of UVA_{254} is an immediate, more robust parameter that is more accessible to water treatment plants, both in terms of cost and operational skills. It was adopted as the principal indicator of NOM in this project, with good results. It provided a useful profile of the different raw water sources (closely in agreement with DOC), and served well to measure the removal of NOM through the typical treatment plant processes. In the laboratory, it provided a smooth response to increasing coagulant dosages (much less erratic than DOC) which enabled the accurate pinpointing of the coagulant dosages required for enhanced coagulation. For adsorption studies, it provided isotherms of good fit for activated carbon and IEX resins. In the case of activated carbon, the isotherms were also determined in terms of DOC removal and, once again, there were reasonable parallels between UVA_{254} and DOC.

For those researchers and water providers interested to further investigate NOM during water treatment, this project suggests that the measurement of UVA_{254}, or full-spectrum UV scans should be seriously considered, and always included as a routine parameter for quality control.

8.2 Advanced Measurements of NOM

This project identified and applied three advanced NOM characterisation methods, namely BDOC, PRAM and FEEM. All three methods were, to our knowledge, were never used before on South African water sources.

The BDOC results were difficult to explain and the values did not follow any of the groupings suggested by the other parameters. The values obtained from the PRAM and FEEM analyses partly confirmed which had earlier been inferred by other methods (e.g. measuring humic acids directly whereas they could earlier only be inferred from relatively high SUVA values). These advanced methods did, however, introduce new compounds and insights which cannot be fully evaluated yet. A broader database and better understanding are required.

8.3 The Nature and Variability of NOM in Raw Water Sources

The different characteristics of NOM in different parts of South Africa have been recognised by water treatment professionals for many years. This project confirmed these differences by sampling eight different sources on five different occasions, spread over two years. Broadly speaking, the NOM from the eutrophic inland waters near the Gauteng area resembled the NOM from purified sewage effluent. The Vaal Dam, which does not capture much purified effluent, had a unique character amongst the waters samples. The coastal waters showed much greater NOM variability. Starting in the Southern Cape (George and Plettenberg Bay) the water was highly coloured with humic acid, but progressively had less organic material as one moves up the East Coast, with some

colour near Port Elizabeth (Loerie), even less at East London (Umzonyana) with the lowest NOM concentration in Durban (Wiggins).

The good news for process designers is that the character of the NOM at the different locations stayed relatively constant over the study period. This implies that, once the NOM is properly characterised and the appropriate process design is done, the treatment plant should be able to deal with the NOM during the normal seasonal variability. Rare, anomalous events could, of course, alter the character and treatability of NOM more drastically than was observed during this study.

8.4 Comparison of Established Treatment Technologies

The treatment performance of enhanced coagulation, activated carbon, and two ion exchange resins was described earlier. A measure is required to compare the relative performance of the processes in an intuitive way.

For the purposes of this report, it is proposed that an equivalent of the *solids loading* concept is used. For analytical parameters that are expressed in units of *mass per volume,* it is conventional to calculate the solids loading as the *mass of contaminant removed divided by the dosage of the chemical*. For example, if the concentration of say DOC is reduced from 10 to 3 mg/ℓ by the addition of 20 mg/ℓ of activated carbon, then the solids loading would be (10 – 3)/20 = 0.35 g DOC/g carbon. When UVA is used as the response parameter, then the solids loading concept can only be used if we arbitrarily treat absorbance as a mass concentration. For example, if UVA would be reduced from 10 to 3/m by the addition of 20 mg/ℓ of activated carbon, then the solids loading would be (10 – 3)/20 = 0.35 $\ell.g^{-1}.m^{-1}$. This approach was in fact taken in the chapters dealing with adsorption by activated carbon and IEX resins.

This version of “solids loading” in terms of UVA is used here, but standardising the solids loading for fixed endpoints of UVA removal. For enhanced coagulation, the endpoints were well defined and it is a simple matter to calculate the solids loading in terms of the UVA removed, expressed per mass of $FeCl_3$ coagulant. For activated carbon and the IEX resins, there were no endpoints defined and 50% UVA removal was used as an arbitrary endpoint to demonstrate how the required dosages of adsorbent differed (refer to Tables 5.4; 5.5; 5.6; 6.4; and 6.5). For these adsorbents, the solids loading is calculated using 50% UVA removal.

The inverse of the solids loadings is a direct indication of the required concentration of each chemical to remove one unit of UVA, should readers find this a more intuitive interpretation.

8.4.1 Enhanced Coagulation

The solids loading for enhanced coagulation is shown in Figure 8.1. It is clear that some waters are much more amenable to enhanced coagulation than others. For example, the amount of UVA that can be loaded onto 1 mg of $FeCl_3$ is about ten times more for the Plettenberg Bay samples that for the Rietvlei samples.

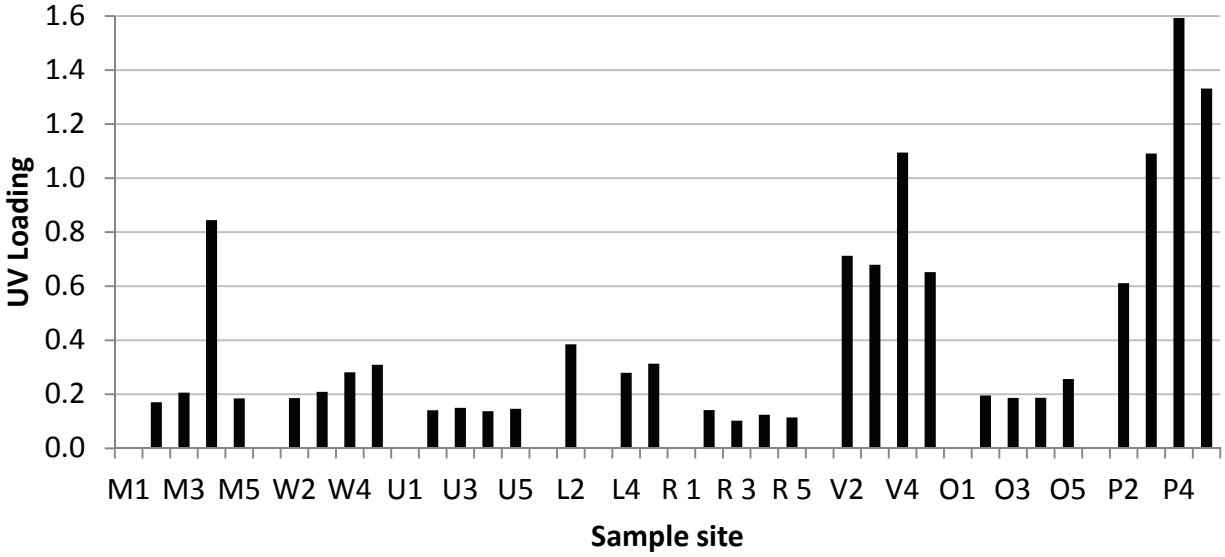

L = Loerie, M = Midvaal, O = Olifantsvlei, P = Plettenberg Bay, R = Rietvlei, U = Umzonyana, V = Vereeniging, W = Wiggins. Number indicates sampling round.

Figure 8.1 UVA loading on $FeCl_3$ for 65% removal at different sampling sites

8.4.2 Activated Carbon

The solids loading for activated carbon is shown in Figure 8.2. The UVA loading on activated carbon is more consistent than for enhanced coagulation.

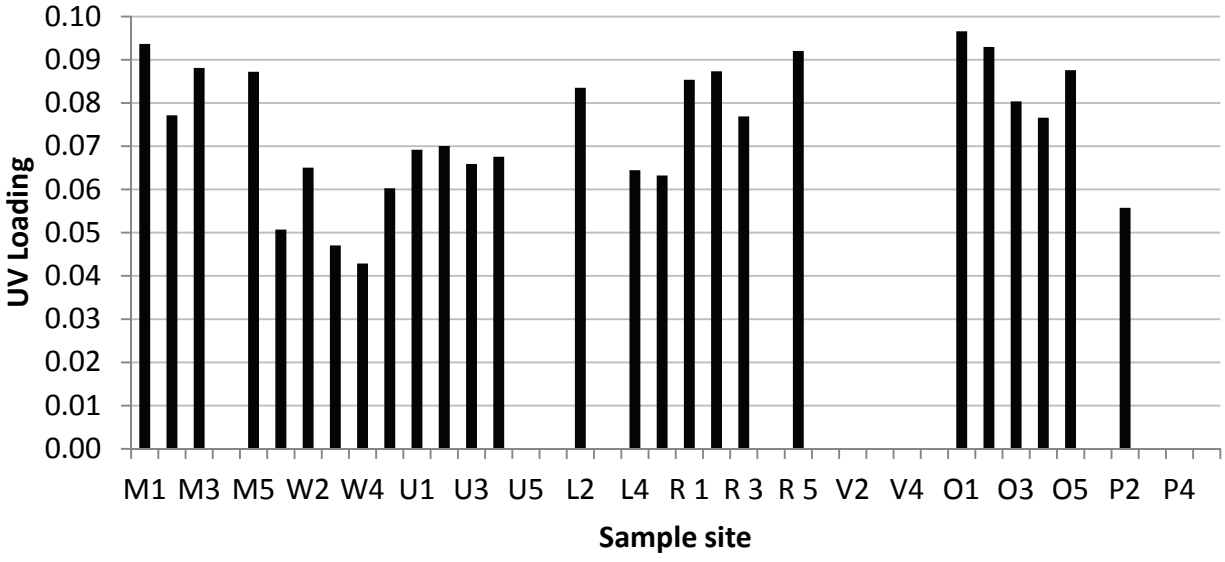

L = Loerie, M = Midvaal, O = Olifantsvlei, P = Plettenberg Bay, R = Rietvlei, U = Umzonyana, V = Vereeniging, W = Wiggins. Number indicates sampling round.

Figure 8.2 UVA loading on GAC for 50% removal at different sampling sites

8.4.3 Ion Exchange

The solids loadings for the ion exchange resins are shown in Figures 8.3 and 8.4. The strong resin allows for much more UVA loading than the weak resin. The weak resin loading is about the same as for activated carbon, but the strong resins can adsorb about three times more UVA.

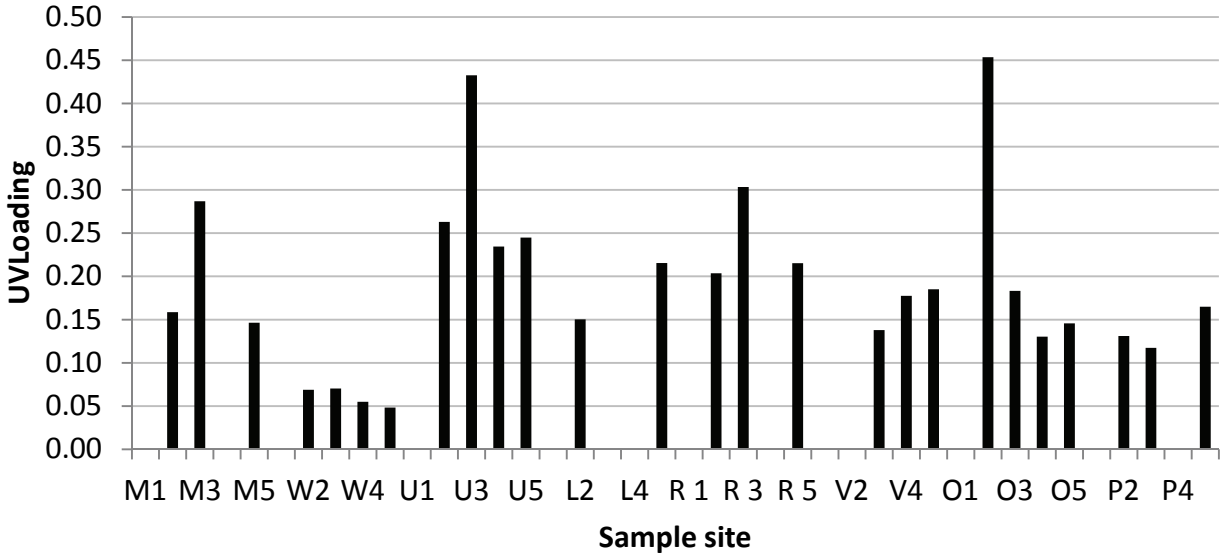

L = Loerie, M = Midvaal, O = Olifantsvlei, P = Plettenberg Bay, R = Rietvlei, U = Umzonyana, V = Vereeniging, W = Wiggins. Number indicates sampling round.

Figure 8.3 UVA loading on strong resin (MP600) for 50% removal at different sampling sites

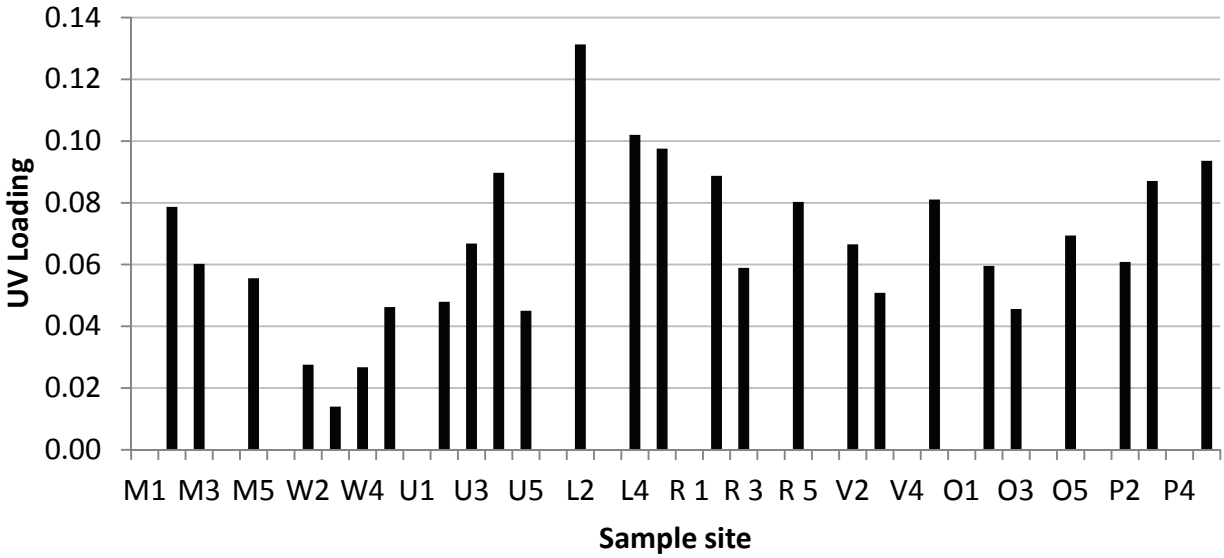

L = Loerie, M = Midvaal, O = Olifantsvlei, P = Plettenberg Bay, R = Rietvlei, U = Umzonyana, V = Vereeniging, W = Wiggins. Number indicates sampling round.

Figure 8.4 UVA loading on weak resin (MP62) for 50% removal at different sampling sites

8.4.4 Comparison of Treatment Processes

How do the treatment processes stack up, when looking at one specific sampling site at a time? Figures 8.5a-c show such comparisons. From what was presented before, the Plettenberg Bay (P) source water, high in humic acid and SUVA, is a good candidate for enhanced coagulation, as indeed practised at that plant. Figure 8.5(a) shows the solids loading for the different processes at this plant. The loading of NOM onto $FeCl_3$ is about ten times higher than on either activated carbon or IEX resins. The other source waters are not so easy to predict. Although the Vereeniging (V) source water did not have a high SUVA (median of 2.4), its NOM can be loaded much more effectively onto $FeCl_3$ than on the IEX resins, as shown in Figure 8.5(b). On the other hand, the Umzonyana (U) source water with about the same SUVA (median 2.1), showed a reverse response. Here the allowable NOM loading onto the strong resin was about twice as high as on $FeCl_3$, and about four times as high as on the weak resin and activated carbon. This is shown in Figure 8.5(c).

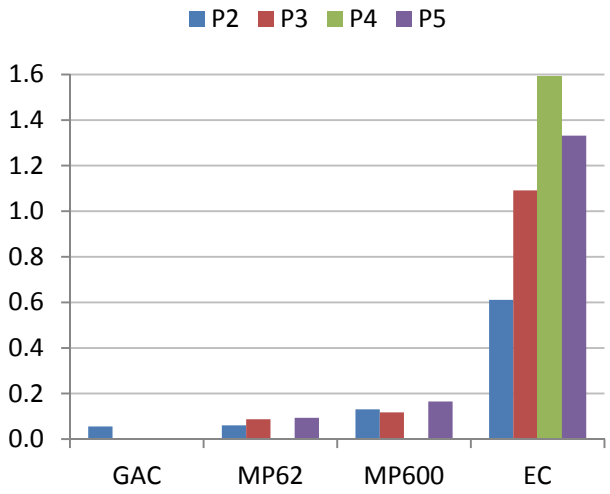

Figure 8.5 (a) UVA loading for Plettenberg Bay

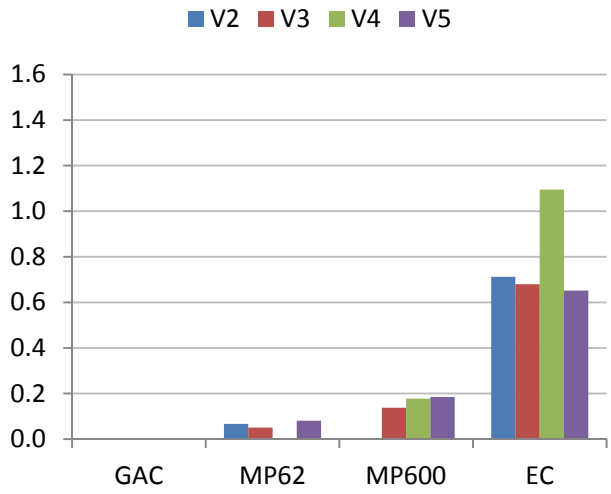

Figure 8.5 (b) UVA loading for Vereeniging

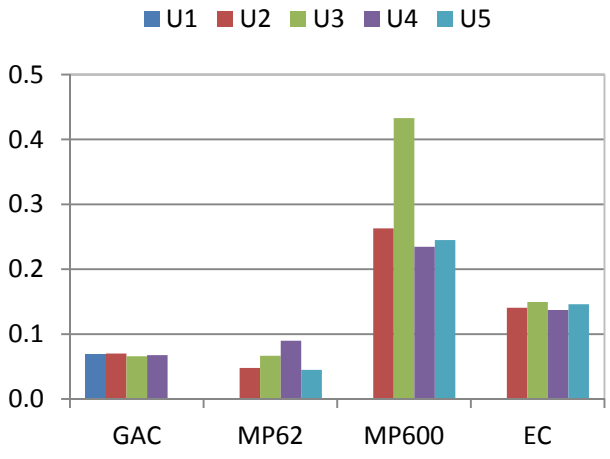

Figure 8.5 (c) UVA loading for Umzonyana

It is emphasised yet again that the direct adsorption on raw water NOM by either activated carbon or IEX resins is not suggested as a practical treatment option, but used to demonstrate how different the adsorbability of different types of NOM could be. The results conclusively show that the relative merit of each process has to be tested first. From the limited data available, it is not yet possible to predict the process performance of activated carbon and IEX resins.

The results do show a way forward in terms of practical process design. In most cases, enhanced coagulation allows the highest solids loading and can be implemented at very little costs, other than slightly higher coagulant demand. Enhance coagulation should therefore be considered as the first barrier for NOM reduction, and the more expensive adsorption options should be reserved to add an extra step of NOM removal, if required.

8.5 Research Needs and Opportunities

This project suggests four important and interesting avenues for future research:

1. Better matching of the results of the advanced NOM characterisation methods with the treatment performance of different processes
2. Revision of the activated carbon and IEX test procedures for better application to secondary treatment after enhanced coagulation, covering narrower dosage ranges and therefore getting better isotherm descriptions
3. Broadening the treatment performance studies to include TOC and some of the advanced NOM characterisation techniques
4. Including the use of membranes as a treatment process to be investigated for NOM removal

REFERENCES

APHA, AWWA and WPCF (American Public Health Association/American Water Works Association/Water Pollution Control Federation). 311 C EDTA Titrimetric Method. In: Standard methods for the examination of water and waste water (1985) 16th edn., *Washington DC, USA.* 507-508.

APHA, AWWA and WPCF (American Public Health Association/American Water Works Association/Water Pollution Control Federation). 403 Alkalinity. In Standard methods for the examination of water and waste water (1985) 16th edn., *Washington DC, USA.* 507-508.

ASAHI R., MORIKAWA T., OHWAKI T., AOKI K. and TAGA Y. (2001). Visible-light photocatalysis in nitrogen-doped titanium oxides. *Science* **293**, 269.

BELL-AJY K., ABBASZADEGAN M., IBRAHIM E., VERGES D. and LECHEVALLIER M. (2000). Conventional and optimized coagulation for NOM removal. *Journal AWWA.* **92** (10), 44-58.

BOLONG N., ISMAIL A.F., SALIM M.R. and MATSUURA T. (2009). A review of the effects of emerging contaminants in wastewater and options for their removal. *Desalination* **239**, 229-246.

CHEN J., LE BOEUF E.J., DAI S., and GU B. (2003). Fluorescence spectroscopic studies of natural organic matter fractions. *Chemosphere* **50**, 639-647.

CHENG W.P. (2002). Comparison of hydrolysis/coagulation behaviour of polymeric and monomeric iron coagulants in humic acid solution. *Chemosphere,* **47**, 963-969.

CHOI J., PARK H. and HOFFMANN M.R. (2010). Effects of single metal-ion doping on the visible-light photoreactivity of TiO_2. *J. Phys. Chem. C* **114**, 783-792.

EDZWALD J. and HAARHOFF J. (2012). Pre-treatment Coagulation and Flocculation. In: Dissolved air flotation for water clarification. *McGraw Hill Education*. Chapter 6, 6.1-6.50.

EDZWALD J.K., and TOBIASON J.E. (2011). Chemical principles, source water composition, and watershed protection. In: *Water quality and treatment. A hand book on drinking water,* Edzwald J.K. (ed.), 6th edn, American Water Works Association, *McGraw-Hill, Inc*, 3.1–3.76.

GAO B.Y. and YUE Q.Y. (2005). Natural organic matter (NOM) removal from surface water by coagulation. *J. Environmental Science*, **17** (1), 124-127.

GHASRI A., MAHVI A., MESDAGHINIA A., RAFIEE M.T., TORABIAN A. and VAEZI F. (2005). Control of disinfection by products formation potential by enhanced coagulation. *Int. J. Environ. Sci. Tech.*, **2** (4), 335-342.

HAMMES F.A. and EGLI T. (2005). New method for assumable organic carbon determination using flow-cytometric enumeration and a natural microbial consortium as inoculums. *Environ. Sci. Technol.* **39**, 3289-3294.

HAN F., KAMBALA V.S.R., SRINIVASAN M., RAJARATHNAM D. and NAIDU R. (2009). Tailored titanium dioxide photocatalysts for the degradation of organic dyes in wastewater treatment: A review. *Applied Catalysis A: General* **359**, 25-4.

KIM D., CHA J., HONG S., KIM D. and KIM C. (2009). Control of corrosive water in advanced water treatment plant by manipulating calcium carbonate precipitation potential. *Korean J. Chem. Eng.*, **26** (1), 90-101.

KIM H.C., HONG J.H. and LEE S. (2006). Fouling of microfiltration membrane by natural organic matter after coagulation treatment: A comparison of different initial mixing conditions. *Journal of Membrane Science* **283**, 288-272.

KIWA N.V. (2006). Selection of anionic resins for NOM removal. Proc. 2011 IWA Specialty Conference on Natural Organic Matter. Costa Mesa, CA, USA, July 27-29. BTO 042, 9-16.

KUVAREGA A.T., KRAUSE R.W.M. and MAMBA B.B. (2011). Nitrogen/palladium-codoped TiO_2 for efficient visible light photocatalytic dye degradation. *J. Phys. Chem. C* **115**, 22110-22120.

MALATO S., IBANEZ P.F., MALDONADO M.I., BLANCO J. and GERNJAK W. (2009). Decontamination and disinfection of water by solar photocatalysis: Recent overview and trends. *Catalysis Today* 147, 1-59.

MARTINS A.F., MAYER F., CONFORTIN E.C. and FRANK C.S. (2009). A study of photocatalytic processes involving the degradation of the organic load and amoxicillin in hospital wastewater. *Clean* **37** (4-5), 365-371.

MERRILL D.T., LANE R.W., PISIGAN R.A., RICHARDS G.G., ROSSUM J.R., SCANLAN L.P., SINGLEY J.E. and WHITNEY G.R. (1990). Joint Task Group on Calcium Carbonate Saturation: Suggested Methods for Calculating and Interpreting Calcium Carbonate Saturation Indexes. *Journal AWWA,* **82** (7), 71-77.

MILLS A. and HUNTE S.L. (1997). An overview of semiconductor photocatalysis. *Journal of Photochemistry and Photobiology A: Chemistry* **108**, 1-35.

MORIKAWA T., OHWAKI T., SUZUKI K., MORIBE S. and KUBOTA S.T. (2008). Visible-light-induced photocatalytic oxidation of carboxylic acids and aldehydes over N-doped TiO_2 loaded with Fe, Cu or Pt. *Applied Catalysis B: Environmental* **83**, 56-62.

OBARE S.O. and MEYER G.J. (2004). Nanostructured materials for environmental remediation of organic contaminants in water. *Journal of Environmental Science and Health A* **39** (10), 2549-2582.

PINTER E.R. (2005). *Corrosive Water: Impact and solutions for rural growth centres, water supply systems in developing countries, case study: Uganda.* PhD thesis, University of Natural Resources and Applied Life Sciences, Vienna, Austria.

ROSARIO-ORTIZ F.L., SNYDER S. and SUFFET I.H. (MEL). (2007). Characterisation of the polarity of natural organic matter under ambient conditions by the polarity rapid assessment method (PRAM). *Environ. Sci. Technol.* **41** (14), 4895-4900.

SAWYER C.N. and MCCARTY (1967) 2nd edn. McGraw-Hill series in sanitary science and water resources engineering. *McGraw-Hill, Inc* 327-340.

SHAH S.I., LI W., HUANG C.P. and JUNG O.C. (2002). Study of Nd^{3+}, Pd^{2+}, Pt^{4+}, and Fe^{3+} dopant effect on photoreactivity of TiO_2 nanoparticles. Proceedings of the National Academy of Sciences of the United States of America 99 (9), 6482-6486.

SHARP E.L., PARSONS S.A. and JEFFERSON B. (2006). Seasonal variations in natural organic matter and its impact on coagulation in water treatment. *Science of the Total Environment*, **363** (1-3), 183-194.

SOJIC D., DESPOTOVIC V., ABRAMOVIC B., TODOROVA N., GIANNAKOPOULOU T. and TRAPALIS C. (2010). Photocatalytic degradation of mecoprop and clopyralid in aqueous suspensions of nanostructured N-doped TiO_2. *Molecules* **15**, 2994-3009.

SONTHEIMER H., CRITTENDEN J.C. and SUMMERS R.S. (1988). *Activated Carbon for Water Treatment,* 2nd ed. DVGW – Forschungsstelle, Federal Republic of Germany.

Standard Methods (1985). Standard methods for the examination of water and waste water. 16th edn, *American Public Health Association/American Water Works Association/Water Pollution Control Federation,* Washington DC, USA.

SUMMERS R.S., KNAPPE D.R.U. and SNOEYINK V.L. (2010). Adsorption of Organic Compounds by Activated Carbon. In *Water Quality & Treatment – A Handbook on Drinking Water,* 6th ed. Edited by Edzwald J.K.E. Denver: *American Water Works Association*.

USEPA (1999). Enhanced coagulation and enhanced precipitative softening guide manual. *EPA.* 815-R-99-012.

WEISHAAR J.L., AIKEN R G., BERGAMASCHI B.A., FRAM M S., FUJII R. and MOPPERS K. (2003). Evaluation of specific ultraviolet absorbance as an indicator of the chemical composition and reactivity of dissolved organic carbon. *Environ. Sci. Technol.* **37**, 4702-4708.

WEISHAAR J.L., AIKEN R.G., BERGAMASCHI B.A., FRAM M.S., FUJII R., WU Z., SHENG Z., LIU Y., WANG H., TANG N. and WANG J. (2009). Characterisation and activity of Pd-modified TiO_2 catalysts for photocatalytic oxidation of NO in gas phase. *Journal of Hazardous Materials* **164**, 542-548.

YAN M., WANG D., NI J., QU J., NI W. and LEEUWEN V. (2009). Natural organic matter (NOM) removal in typical North-China water plant by enhanced coagulation: Targets and techniques. *Separation and Purification Technology,* **68**, 320-327.

YAN M., WANG D., YOU S., QU J. and TANG H. (2006). Enhanced coagulation in a typical North-China water treatment plant. *Water Research,* **40**, 3621-3627.

YAN M.C., CHEN F., ZHANG J.L. and ANPO M. (2005). Preparation of controllable crystalline titania and study on the photocatalytic properties. *J. Phys. Chem. B* **109**, 8673-8678.

YU J., WANG D., YAN M., YE C., YANG M. and GE X. (2007). Optimized coagulation of high alkalinity, low temperature and particle water: pH adjustment and polyelectrolytes as coagulant aids. *Environ. Monit. Assess.*, **131**, 377-386.

APPENDIX A: METHODOLOGIES

A.1 Natural organic matter removal by enhanced coagulation

A.1.1 Sample volumes and preparation

- Collect raw water, before any pre-treatment, into 2 × 25 ℓ containers and store in the dark at approx. 4ºC.
- Remove a sub-sample from the containers one day before the start of testing, and leave in the laboratory to attain room temperature (in this study, between 15 and 23°C).

A.1.2 Instruments and reagents

- Alkalinity (mg $CaCO_3$/ℓ) was determined using protocol 403 outlined in Standard Methods (16^{th} edition, 1985). Use the required instruments and reagents.
- Calcium hardness (mg Ca/ℓ) was determined using protocol 311 C, outlined in Standard Methods (16^{th} edition, 1985). Use the required instruments and reagents.
- Measure pH, electrical conductivity, and temperature with standard laboratory procedures (for this project a HANNA HI 98130 combination waterproof pH, EC/TDS and temperature meter was used).
- Measure turbidity with a standard nephelometric procedure (for this project a HACH 2100 portable turbidity meter with appropriate sample cells with lids was used).
- Measure absorbance with a standard spectrophotometric procedure (for this project an ULTROSPEC II: UV/Vis spectrophotometer, Model 80-2091-73, Biochrom, England, was used).
- Teledyne Tekmar, TOC fusion total organic carbon analyser.
- A six-place standard jar test apparatus (for this project, a FC6S jar test apparatus from VELP SCIENTIFICA was used).
- 1000 mℓ beakers.
- 900 mℓ samples.
- 25 mℓ beakers.
- 25 mℓ graduated pipettes.
- 50 mℓ bulb pipettes with 90º bend at the tip.
- Pipette dispenser/pipette bulb.
- 50 mℓ beakers.
- 2 × 1 cm and 2× 5 cm quartz cuvette cells.
- Non-sterile 33 mm MILLEX – HV MILLIPORE 0.45 µm filter units.
- 20 mℓ ONCE® disposable syringes.
- HANNA magnetic stirrer and stirrer bar.
- 1 × microburret.
- Ferric chloride hexahydrate ($FeCl_3 \cdot 6H_2O$), prepared from reagent grade granular ferric chloride.
- Standardized sodium carbonate (Na_2CO_3) (to increase alkalinity).

A.1.3 Procedure

Ferric Chloride Dosage Range Determination

- Perform an alkalinity titration with 0.1 N HCl and record the acid volume to drop the pH to 7.0; 6.0; 5.5; 5.0; and 4.5 respectively. If the alkalinity is 60 mg/ℓ or more, skip the next step.
- If the alkalinity is less than 60 mg/ℓ, use the STASOFT software to predict how much Na_2CO_3 should be added to raise the alkalinity to 60 mg/ℓ. The use of STASOFT requires the determination of calcium, which has to done first. Add the calculated Na_2CO_3 quantity to a new sample and perform an alkalinity titration as in the step above.
- Make a ferric chloride solution of 1 mg/ℓ as Fe. Find the equivalence between the 0.1 N HCl and the ferric chloride solution. (If this step causes problems, it may be easier to redo the alkalinity titration by using the ferric chloride solution directly as titrant.)
- The ferric chloride dosages for the jar test are selected as
    - Jar 1 – no ferric chloride
    - Jar 2 – pH 7.0 after dosage
    - Jar 3 – pH 6.0 after dosage
    - Jar 4 – pH 5.5 after dosage
    - Jar 5 – pH 5.0 after dosage
    - Jar 6 – pH 4.5 after dosage

Jar Testing

- 6 × 900 mℓ samples are placed in 6 × 1000 mℓ beakers.
- Using a 25 mℓ graduated pipette and pipette dispenser transfer five different $FeCl_3$ volumes to 25 mℓ beakers.
- The samples are mixed with the paddles were completely submersed in each sample at the following settings:
    - 2 min rapid mix at 200 rpm.
    - 10 min slow mix (flocculation) at 30 rpm.
    - 30 min settling time at 0 rpm (measure pH, conductivity and temperature during this period).
- Collect samples collected from the centre of each beaker using the 50 mℓ bulb pipettes and a pipette dispenser, transfer the samples into 6 × 50 mℓ beakers, with 20 mℓ of each sample used to measure turbidity.
- The remaining sample is then filtered using the specified filter units and disposable syringes and used to determine UVA at wavelengths 214, 254, 272 and 300 nm.

A.2 NOM Removal by Granular Activated Carbon

A.2.1 Sample volumes and preparation

- Collect raw water, before any pre-treatment, into 2 × 25 ℓ containers and store in the dark at approximately 4°C.

A.2.2 Instruments and reagents

- Measure pH, electrical conductivity, and temperature with standard laboratory procedures (for this project a HANNA HI 98130 combination waterproof pH, EC/TDS and temperature meter was used).
- Measure the ultraviolet absorbance with a standard spectrophotometric procedure (for this project an ULTROSPECT II: UV/Vis spectrophotometer, Model 80-2091-73, was used).
- Measure DOC with TELEDYNE TEKMAR, TOC fusion total organic carbon analyser.
- Measure the mass with an analytical balance (Analytical Balance SARTORIUS, AG GOTTINGEN CP225D).
- 250 mℓ graduated cylinder.
- 500 mℓ glass Erlenmeyer flasks.
- 600 mℓ beaker.
- 100 mℓ beaker.
- Paired UV spectrophotometry quartz cuvette cells (1 cm and 5 cm).
- HANNA magnetic stirrer and stirrer bars.
- Orbital shaker table (ROTABIT, J.P SELECTA, CD. 3000618).
- Orbital shaker table (Orbital platform shaker, SELECTECH Model 262).
- Overhead stirrer (HEIDOLPH, Type RZR 50)
- Non-sterile 33 mm MILLEX – HV MILLIPORE 0.45 µm filter units.
- Square weighing dish units in polystyrene (20 mℓ, 41 × 41 × 8 mm H).
- Stainless steel spatula units.
- 10 mℓ ONCE® disposable syringes.
- 20 mℓ ONCE® and 20 mℓ Omnifix® disposable syringes.
- Mortar and pestle in porcelain.
- Vibratory sieve shaker (ANALYSETTE 3 SPARTAN, FRITSCH)
- 30 µm mesh sieve, receiving pan and lid.

A.2.3 Procedure

Granular Activated Carbon Pre-treatment

- Granular activated carbon (GAC) used: CARBSORB® 30 and 40
- Grind about 100 g of GAC using a mortar and pestle.
- Using a vibratory sieve shaker, collect and store in a glass bottle the sample that passes through a 300 µm mesh sieve after vibration at an amplitude of 2.00 mm for 5 minutes.
- Repeat the steps 2 and 3 of the procedure until the quantity is enough. This will constitute the activated carbon sample.

Batch Test

- Using an analytical balance, weigh out and record seven masses of the pre-treated activated carbon in weighing dishes using spatula. The following masses are weighed: 6.25, 8.25, 12.50, 16.50, 25.00, 33.25 and 50.00 mg.
- Using an overhead stirrer at a speed of 300 rpm, stir at least 3 litres of raw water samples for a minimum of 30 minutes.
- Using a 600 mℓ beaker, transfer 250 mℓ of raw water sample into a 250 mℓ graduated cylinder.

- Pour the 250 mℓ water sample from the graduated cylinder as well as one mass of the pre-treated weighed carbon in a 500 mℓ Erlenmeyer flask. (Repeat this step for all the activated carbon masses).
- Place the seven Erlenmeyer flasks on the shaker table. An eighth flask containing only raw water with no GAC, which acts as a control sample, is also placed on the shaker table.
- Switch on the shaker table and shake for 72 hours (3 days) at a speed of 140 rpm.
- After 3 days filter the eight water samples using a 10 or 20 mℓ syringe and 33 mm Millipore 0.45 µm filter.
- Using a 1 or 5 cm cell, measure the ultraviolet absorbance at wavelengths 214, 254, 272 and 300 nm.
- Keep and store about 100 mℓ of the eight filtered waters for DOC analysis.
- Pour the unfiltered samples in a 100 mℓ beaker and measure pH, conductivity and temperature while they are mixed with a magnetic stirrer.

A.3 NOM Removal by Ion Exchange Resins

A.3.1 Sample volumes and preparation

- Collect raw water, before any pre-treatment, into 2 × 25 ℓ containers and store in the dark at approximately 4°C.

A.3.2 Instruments and reagents

- Measure pH, electrical conductivity, and temperature with standard laboratory procedures (for this project a HANNA HI 98130 combination waterproof pH, EC/TDS and temperature meter was used).
- Measure ultraviolet absorbance with a standard spectrophotometric procedure (for this project an ULTROSPECT II: UV/Vis spectrophotometer, Model 80-2091-73, was used).
- Measure DOC with TELEDYNE TEKMAR, TOC fusion total organic carbon analyser.
- Measure the mass with an analytical balance (Analytical Balance SARTORIUS, AG GOTTINGEN CP225D).
- 250 mℓ graduated cylinder.
- 500 mℓ glass Erlenmeyer flasks.
- 600 mℓ beaker.
- 100 mℓ beaker.
- Paired UV spectrophotometry quartz cuvette cells (1 cm and 5 cm).
- HANNA magnetic stirrer and stirrer bars.
- Orbital shaker table (ROTABIT, J.P SELECTA, CD. 3000618).
- Orbital shaker table (Orbital platform shaker, SELECTECH Model 262).
- Vacuum/Pressure pump (MILLIPORE XX5522050).
- Overhead stirrer (HEIDOLPH, Type RZR 50)
- Glass fibre prefilter units (47 mm diameter).
- Non-sterile 33 mm MILLEX – HV MILLIPORE 0.45 µm filter units.
- Square weighing dish units in polystyrene (20 mℓ, 41 × 41 × 8 mm H).
- Stainless steel spatula units.
- 10 mℓ ONCE® disposable syringes.
- 20 mℓ ONCE® and 20 mℓ Omnifix® disposable syringes.

- Jar test mixer (FC 6 S, Jar Test, VELP SCIENTIFICA).
- 2% NaOH solution.
- 3.7% NaCl solution.
- Demineralised water.

A.3.3 Procedure

Pre-treatment of the Weak Ion Exchange Resin – LEWATIT® MP 62

- Neutralisation: mix the ion exchange resin MP 62 with an excess of 2% NaOH solution for 24 hours. The mixer used is the jar test mixer.
- Rinse the resin MP62 with demineralized water for 2 hours.
- Conditioning: mix the rinsed resin with an excess of 3.7% HCl solution for 24 hours. The mixer used is the jar test mixer.
- Rinse several times with an excess of demineralized water for 24 hours.
- Use a laboratory vacuum/pressure pump (with a glass fibre prefilter) to filter and dry the ion exchange resin.
- Air-dry overnight the wet resin prior to use.

Pre-treatment of the Strong Ion Exchange Resin – LEWATIT® MonoPlus MP 600

- Air-dry the resin MP 600 overnight prior to use.

Batch Test

- Using an analytical balance, weigh out and record seven masses of the pre-treated activated carbon in weighing dishes using spatula. The following masses are weighed: 10.00, 25.00, 60.00, 135.00 and 320.00 mg.
- Using an overhead stirrer at a speed of 300 rpm, stir at least 3 litres of raw water samples for a minimum of 30 minutes.
- Using a 600 mℓ beaker, transfer 250 mℓ of raw water sample into a 250 mℓ graduated cylinder.
- Pour the 250 mℓ water sample from the graduated cylinder as well as one mass of the pre-treated ion exchange resin in a 500 mℓ Erlenmeyer flask. (Repeat this step with all the resin masses).
- Place the five Erlenmeyer flasks in the shaker table. Add in the shaker table a sixth flask containing only raw water with no resin added; this sample acts as a control sample.
- Switch on the shaker table and shake for 72 hours (3 days) at a speed of 140 rpm at room temperature.
- After 3 days filter all the water samples using a 10 or 20 mℓ syringe and 33 mm Millipore 0.45 µm filter.
- Using a 1 or 5 cm cell, measure the ultraviolet absorbance at wavelengths 214, 254, 272 and 300 nm.
- Keep and store about 100 mℓ of the six filtered waters for DOC analysis.
- Pour the unfiltered samples in a 100 mℓ beaker and measure pH, conductivity and temperature while they are mixed with a magnetic stirrer.

A.4 Biodegradable Dissolved Organic Carbon (BDOC) Analysis

Biodegradable dissolved organic carbon in drinking water is an indicator of bacterial re-growth potential in the distribution network. The method of analysis chosen entailed measuring the reduction of DOC over six days by bacteria fixed on biologically active sand (BAS). An inoculum of BAS, obtained from the Rietvlei (the sand filtration bed), was washed until there was no further release of DOC. This was achieved by washing the BAS ten times or more with a 500 mℓ rinsing solution (10 mℓ sodium thiosulphate solution, 0.1M: 490 mℓ deionised water). The DOC and UVA content of the final washing were then measured to determine the background DOC and UVA due to the sand. The inoculums were then rinsed with 100 mℓ of the raw water sample to be analysed, and the solution was allowed to stand for twenty minutes to facilitate an acclimation of biomass to the water before gently pouring it out.

A volume of water sample (~350 mℓ) and inoculated sand (~100 g) were then placed in clean Erlenmeyer flasks, aerated and kept at room temperature for six days. Each flask was covered with an aluminium foil paper to prevent any atmospheric interference in the conditioning of the bacteria and samples in the flask. The heterotrophic bacterium in the sand digests part of the carbon in the sample to obtain energy, at the same time consuming the carbon of the sample. Meanwhile, daily measurements of the DOC concentration were taken until no further change in DOC is observed.

Biodegradable dissolved organic carbon was then calculated as the difference between the initial DOC and the minimum DOC value reached.

Three different solutions (5 mg/ℓ, 8 mg/ℓ and 10 mg/ℓ) of sodium acetate were prepared and used as controls and were analysed at the same time with the samples (under similar conditions as those of the samples) in order to monitor the activity of the bacteria in known concentrations of substrate. Sodium acetate was chosen because it is organic and has been widely used in many bacterial decay studies (Tukundwa and Mvula, 2007). The fraction that does not undergo biodegradation is referred to as the non-biodegradable dissolved organic carbon (NBDOC). Figure A.1 shows the experimental setup for BDOC analysis.

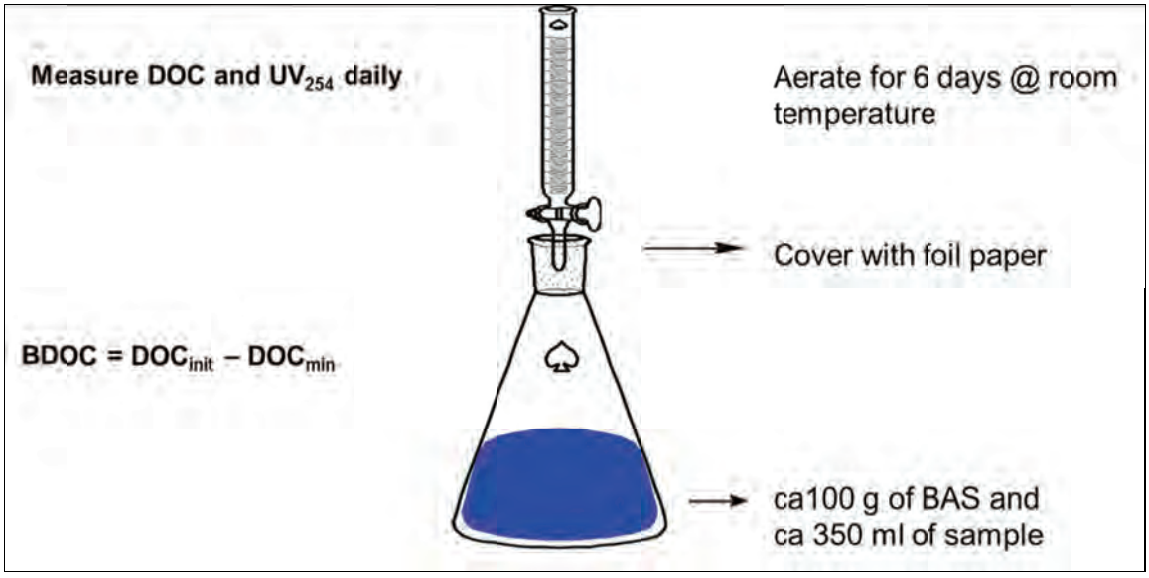

Figure A.1 Experimental setup for BDOC analysis

A.5 Fluorescence Excitation Emission Matrices (FEEM) Characterisation

Fluorescence EEM measurements were conducted using a Horiba AquaLog Spectrometer. The spectrometer displayed a maximum emission intensity of 1000 arbitrary units (AU). The spectrometer uses a xenon excitation source and excitation and emission slits are set to a 10 nm band pass. To obtain FEEMs, excitation wavelengths were incrementally increased from 200 nm to 600 nm at 5 nm band pass; for each excitation wavelengths, the emission at longer wavelengths was detected at 0.3 nm steps.

To partially account for Raleigh scattering, the fluorometer's response to a blank solution was subtracted from the fluorescence spectra of the sample to be analysed. De-ionised water, with known concentrations of DOC, was used as a blank solution. Absorbance of light from the lamp by DOC molecules in the sample was accounted for by using an inner-filter correction applied to the data by using UV-Vis spectral data from the blank. The AquaLog is equipped with a reference detector to monitor and ratiometrically correct both the excitation source's spectrum for the emission detector and the absorbance signals. A transmission detector is attached to the AquaLog's sample compartment to record the sample's transmission/absorbance spectrum under the same spectral-band pass and resolution conditions as the fluorescence EEM data. The corrected EEM's were then plotted using Origins Lab, supplied with the instrument, with 20 contour lines, each contour interval representing 1/20th of the maximum fluorescence intensity.

A.6 Polarity Rapid Assessment Method (PRAM)

The experimental conditions of this method have been reported and were discussed in detail by Rosario-Ortiz *et al.* (2007). The characterisation of NOM with PRAM is based on preferential adsorption of dissolved organic matter (DOM) fractions onto solid-phase extraction (SPE) sorbents. Three different types of sorbents were used, namely; polar sorbents, non-polar sorbents and anion exchange resins.

Table A.1 shows the different cartridges with the various types of sorbents used. The use of different SPE cartridges sequentially allows for a multidimensional characterisation of the polarity of NOM. Figure A.2 shows the experimental setup, including the SPE cartridges used for PRAM analysis while Figure A.3 shows an example of the PRAM experimental setup in the laboratory.

Table A.1 The different SPE cartridges and various types of sorbents used

SPE cartridge	Type of sorbent
C18, C8, C2	Non-polar
CN, Silica, Diol	Polar
NH_2	Weak anion exchange
SAX	Strong ion exchange

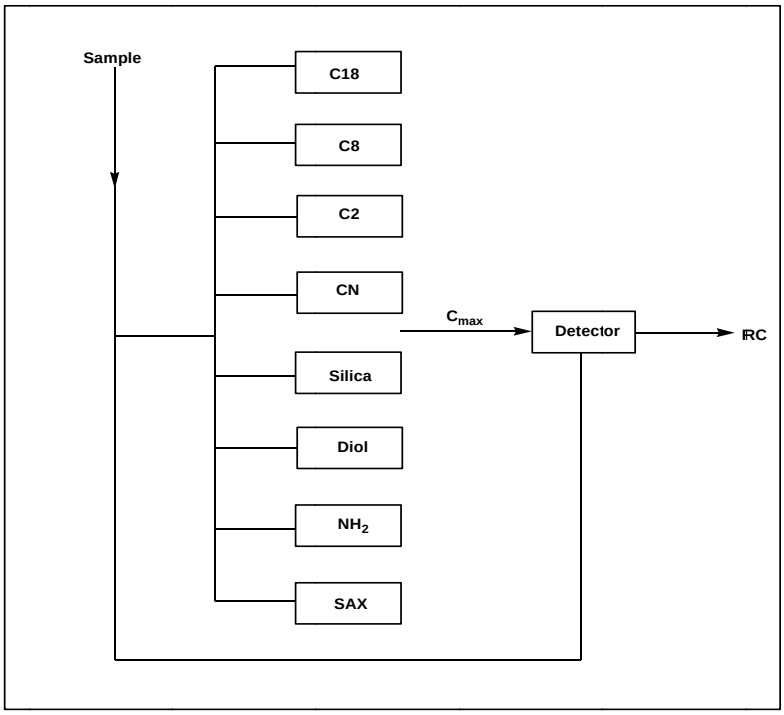

Figure A.2 Experimental setup for PRAM

Figure A.3 The PRAM setup in the laboratory

The SPE cartridges were rinsed by flushing with deionised water until a steady UVA_{254} signal is obtained (approximately 15 min) in order to remove any UV-absorbing organic residue on the SPE sorbent. The breakthrough is then measured by UVA_{254} and DOC. The retention coefficient (RC) (Equation A.1) is defined as one minus the maximum breakthrough level achieved and describes the capacity of each SPE sorbent for specific NOM components (Rosario-Ortiz *et al.*, 2007).

$$RC = 1 - \frac{C_{\max}}{C_0} \qquad \text{A.1}$$

Where: C_0 and C_{max} refer to the initial sample concentration and maximum breakthrough concentrations, respectively.

The C18 cartridge was used to generate the hydrophobic (HPO) NOM fraction, the CN SPE cartridge eluted the hydrophilic (HPI) NOM fraction while the NH_2 SPE cartridge was used for the generation of the transphilic (TPI) NOM fraction. Sufficient amounts of 0.1 M NaOH (approximately 10 mℓ) were used to elute the HPO and HPI fractions retained by the C18 and CN SPE cartridges, respectively; the TPI fraction was thus collected as the fraction that passes through the NH_2 SPE cartridge as shown in Figure A.3.

A.7 The Modified PRAM

The Modified PRAM, instead of producing all six NOM fractions, only gives three fractions and thus is a very rapid method of NOM characterisation. This method only results in the hydrophobic NOM fraction (HPO), the hydrophilic NOM fraction (HPI) and the transphilic NOM fraction (TPI). All three fractions provide good information for the characterisation of the NOM in based on its composition as these three fractions best represent the composition of the NOM with respect to its aromaticity.

In this modified method, the PRAM methodology should be followed as discussed earlier, the exception being the use of only three SPE cartridges to collect the three fractions. The C18 cartridge is used to generate the hydrophobic (HPO) NOM fraction, the CN SPE cartridge elutes the hydrophilic (HPI) NOM fraction while the NH_2 SPE cartridge generates the transphilic (TPI) NOM fraction. Sufficient amounts of 0.1 M NaOH (approximately 10 mℓ) are used to elute the HPO and HPI fractions retained by the C18 and CN SPE cartridges, respectively; the TPI fraction is thus collected as the fraction that passes through the NH_2 SPE cartridge as shown in Figure A.4.

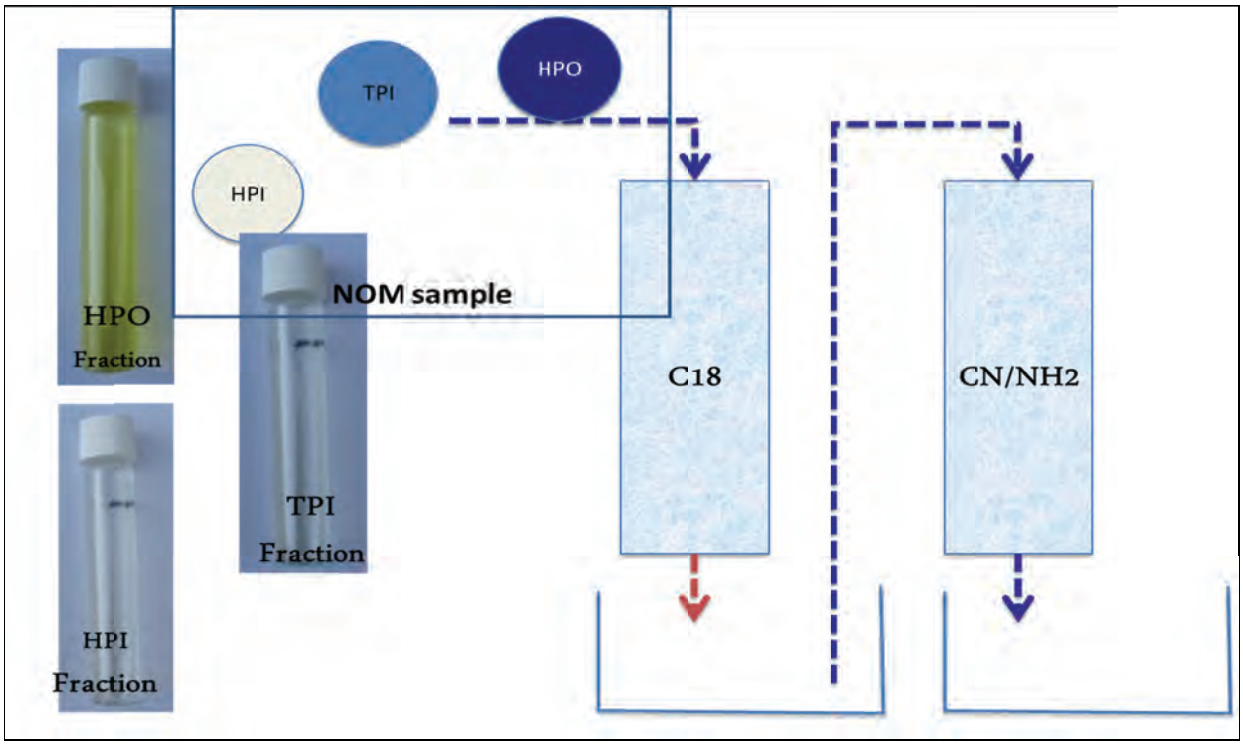

Figure A.4 Experimental setup for the modified PRAM

A.8 A Standard Laboratory Procedure for NOM Photodegradation by Nanomaterials (N-Pd co-doped TiO_2)

A.8.1 Preparation of materials

N, Pd co-doped TiO_2 was prepared by a modified sol-gel method using ammonium hydroxide as a source of nitrogen, solvent for the Pd precursor and a hydrolysing reagent. Titanium isopropoxide, $Ti(OC_3H_7)_4$, (10 mℓ), (97%, Sigma Aldrich, Germany), was added to 2-propanol, C_3H_8O, (50 mℓ), (99.8%, Sigma Aldrich, Germany) and stirred for about 10 min. An appropriate amount of palladium diamine dichloride, $Pd(NH_3)_2Cl_2$, (45% Pd, PGM Chemicals, RSA) to give a Pd:Ti proportion of 0.5% was dissolved in ammonia, NH_3, (3 mℓ), (25%, Merck, Germany). The ammonia solution was then slowly added to the isopropoxide/propanol solution under vigorous stirring for about 90 min. The resulting sol was dried in air at 80ºC for 12 h to obtain a white powder. The powder was calcined for 2 h at 500ºC in air in an electric furnace and characterised by various methods.

A.8.2 Further characterisations

Fourier Transform Infrared spectra were obtained on a Perkin Elmer (FT-IR Spectrum 100) spectrophotometer equipped with a diamond/ZnSe universal attenuated total reflectance sample accessory (ATR) using 4 cm^{-1} resolution and averaging 30 scans. Samples were analysed in their powder form.

Raman spectra were recorded on a Czerny-Turner micro-Raman spectrometer (Perkin Elmer Raman microscope) equipped with a cooled charged coupled device (CCD) detector set at -50ºC and an Olympus microscope. Signals were obtained on excitation of the samples by a red diode laser (785 nm). Measurements were done with the beam path set at 50X at an exposure time of 15 s.

X-ray diffraction (XRD) measurements were performed using an X-ray diffractometer (Philips PANanalytical X'pert) operated with a Cu *K*α radiation source using a wavelength (λ) of 0.15406 nm generated at 40 kV and 40 mA. The Cu Kα radiation (λ = 0.15406 nm), Ni filtered (0.02 mm) and masked (11.6 mm), was collimated with Soller slits (0.04 rad). Measurements were performed over the range of 2θ degree angles from 0° to 80°. Samples in their powder form were mounted on a Si sample holder using a bracket sample stage. Data analysis was performed using X'pert data collector software. The crystallite sizes were estimated by applying the Scherer equation to the FWHM of the (101) peak of the anatase phase. Optical properties were investigated using diffuse reflectance UV-VIS absorption spectrophotometry on a Shimadzu UV - 2540 (Japan) equipped with an IRS 240 integrating sphere attachment. $BaSO_4$ was used as the reflectance standard.

Scanning electron microscopy (SEM) studies were performed on an FEI/FIB NOVA microscope to observe the surface morphology of the powders after calcination. Surface elemental composition was probed using an energy dispersive X-ray spectrometer (EDX) attached to the SEM.

Transmission electron microscopy (TEM) analysis was performed under bright field on a Tecnai G2 Spirit microscope to observe surface morphology, structure and grain size of the nanoparticles.

Thermogravimetric analysis (TGA) was performed on a Perkin Elmer Pyris™ thermal analyser at a heating rate of 10ºC/min under nitrogen flow over a range of 30ºC to 900ºC in order to obtain thermal stability data.

A.8.3 Evaluation of photocatalytic activity

The photocatalytic performance of the materials was quantified by measuring the rate of degradation of NOM fractions under simulated solar radiation. An aliquot of 0.1 g of the catalyst was suspended in 20 mℓ of NOM solution. A solar simulator (Oriel, Newport), with an Oriel 500W Xenon lamp was employed as a source of radiation. The power output was set at 375 W in order to give an irradiance of 1 000 Wm^{-2} at 25ºC, using an Air Mass 1.5 Global Spectral Filter. An Oriel PV reference cell system equipped with a 2 cm × 2 cm monocrystalline silicon photovoltaic cell and a Type K thermocouple was used to set the simulator irradiance to 1 sun. Prior to photocatalytic reactions, the suspensions were ultra sonicated for 20 min and then magnetically stirred in the dark for an hour to allow for adsorption equilibrium before illumination.

Aliquots (2 mℓ) of the suspension were withdrawn using a 6 mℓ Neomedic disposable syringe and filtered through an 0.2 µm Pall® Acrodisc® Syringe Filter with PSF membrane at 30 min intervals for at least 120 min. Variations in the concentration of NOM fractions under simulated solar illumination were monitored using a Shimadzu UV-2450 spectrophotometer (Japan). Figure A.5 shows the experimental setup for the photocatalytic degradation experiments.

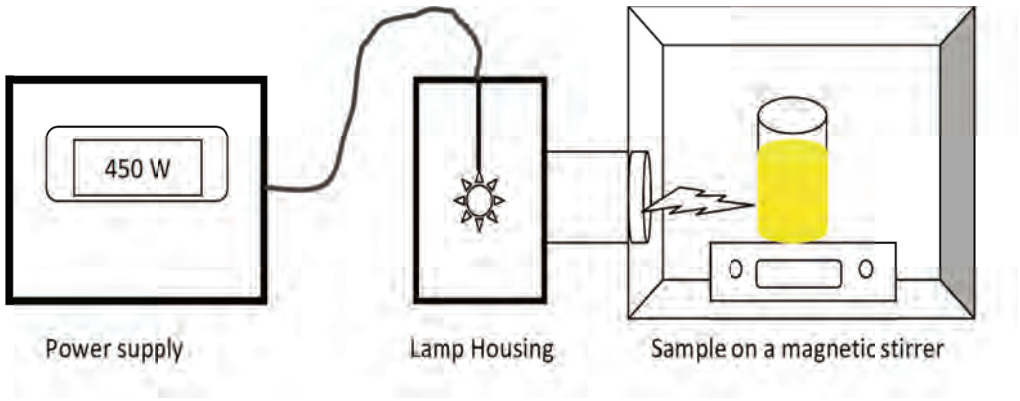

Figure A.5 Photocatalytic degradation experimental setup

APPENDIX B: PROCESS TRAINS AND SAMPLE POINT LOCATIONS

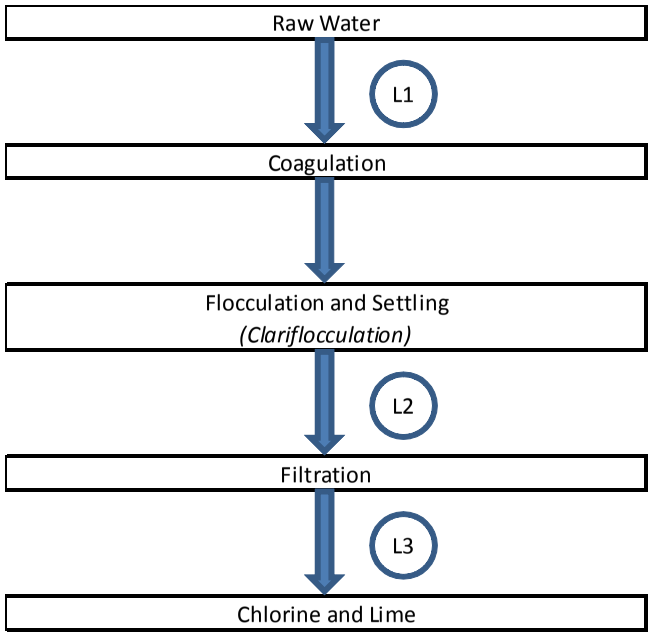

Figure B.1 Process treatment train at Loerie Water Treatment Works

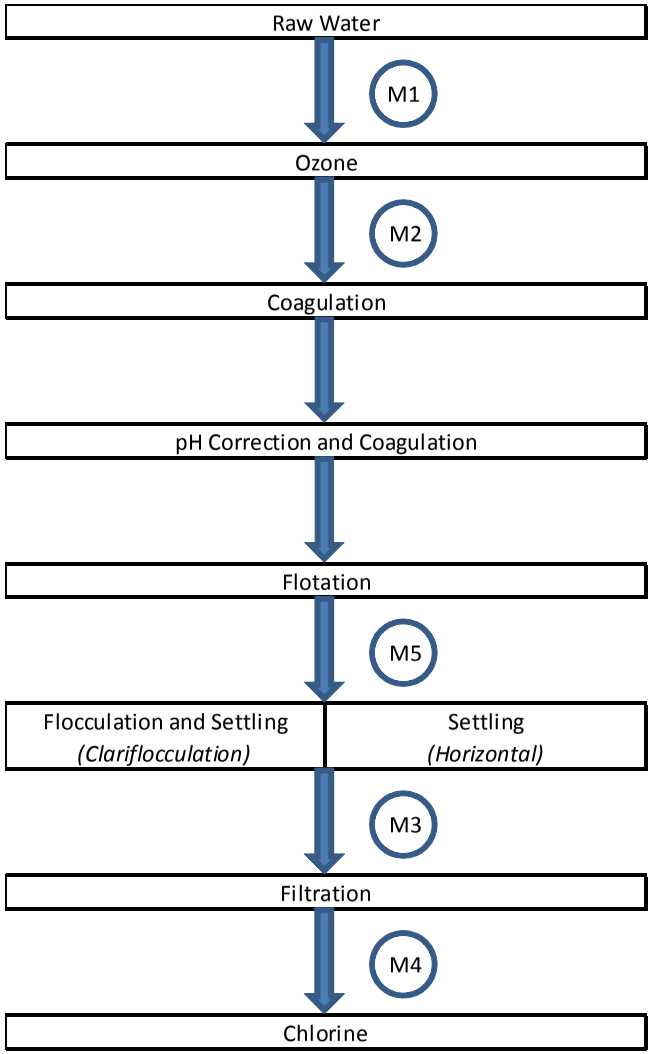

Figure B.2 Process treatment train at Midvaal Water Treatment Works

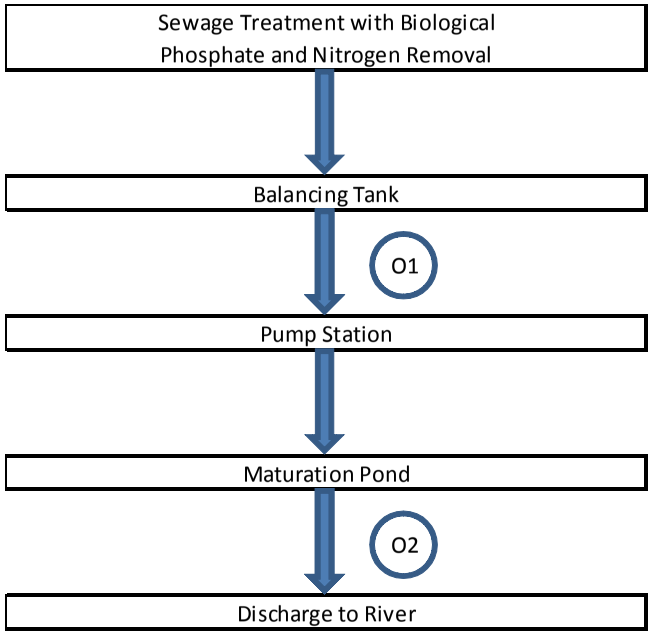

Figure B.3 Process treatment train at Olifantsvlei Waste Water Treatment Works

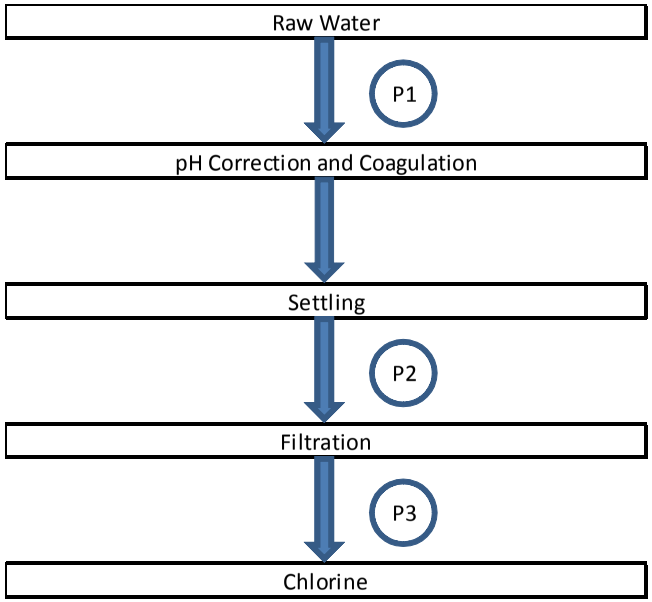

Figure B.4 Process treatment train at Plettenberg Bay Water Treatment Works

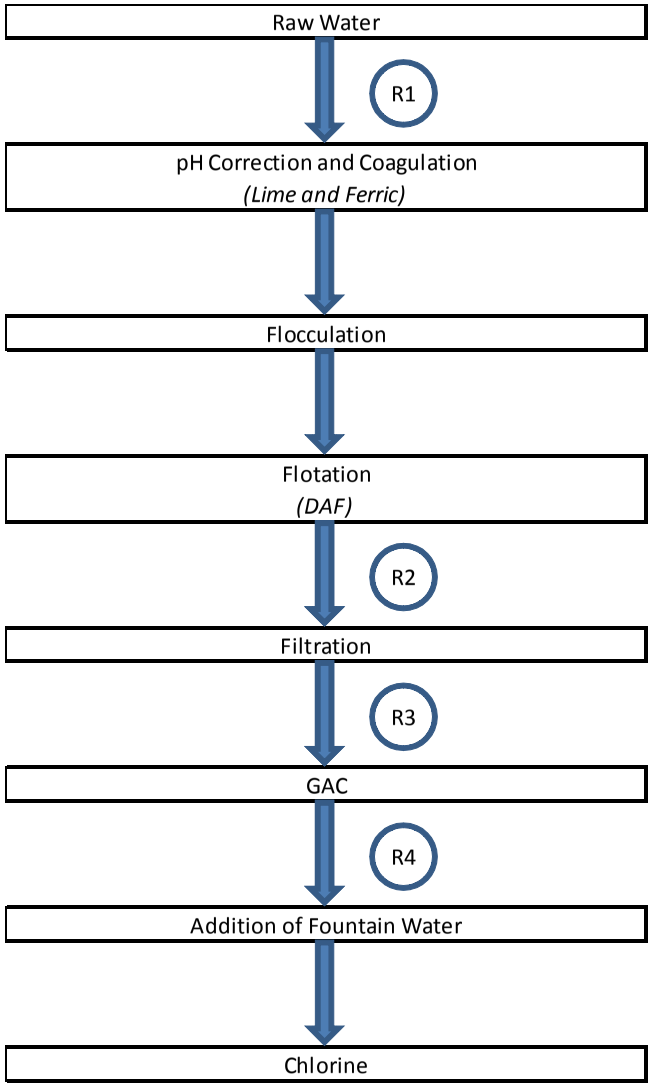

Figure B.5 Process treatment train at Rietvlei Water Treatment Plant

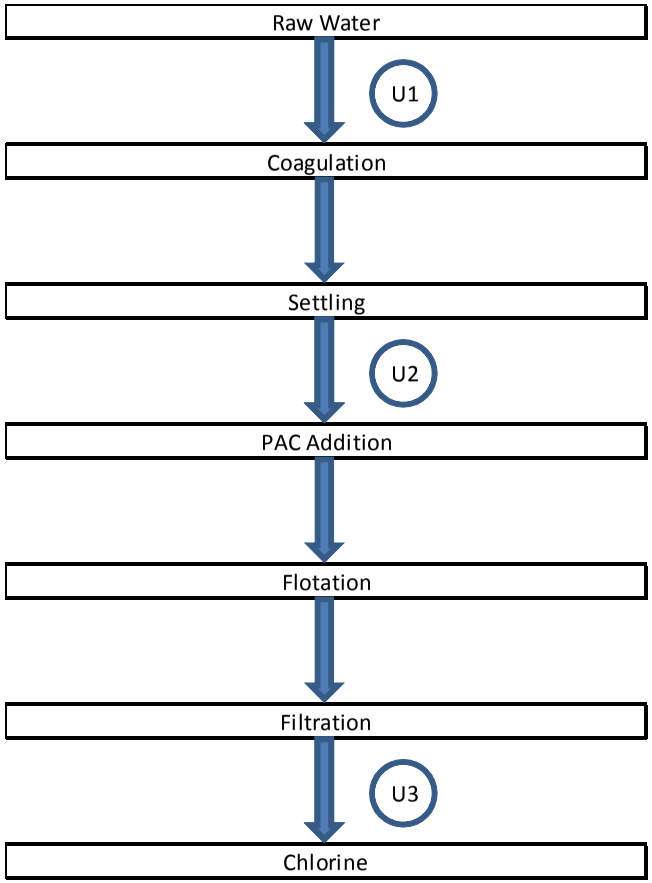

Figure B.6 Process treatment train at Umzonyana Water Treatment Works

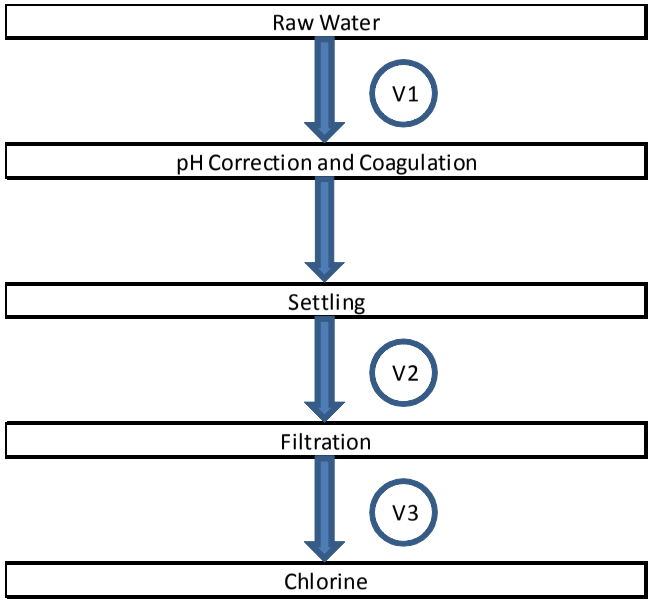

Figure B.7 Process treatment train at Vereeniging Water Treatment Plant

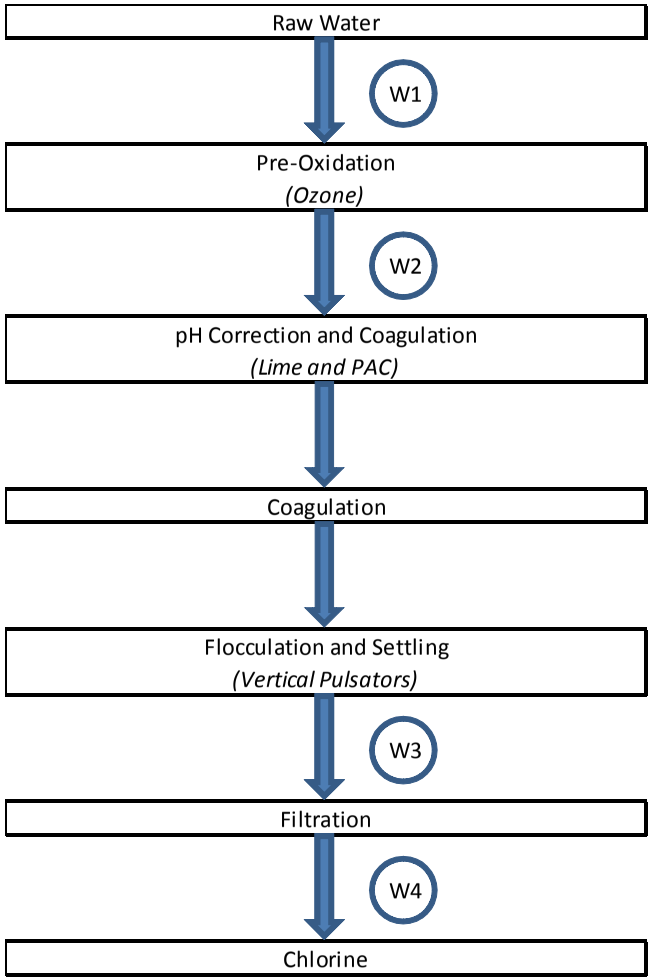

Figure B.8 Process treatment train at Wiggins Water Works

APPENDIX C: SUMMARY OF ADSORPTION DATA

C.1 Activated Carbon Adsorption Tests

Data that did not meet the statistical screening criteria (see Chapter 5) are not shown.

The dosage in the first column of tables C.1 to C.5 represents the target dosage. The loadings in subsequent columns are calculated from the actual dosages. UVA is expressed in/m; loading expressed in ℓ/mg·m.

C.2 Weak Resin MP 62 Adsorption Tests

Data are shown in Tables C.6 to C.9 and omit datum points did not meet the statistical screening criteria (see Chapter 6) are not shown. The dosage in the first column represents the target dosage. The loadings in subsequent columns are calculated from the actual dosages.

C.3 Strong Resin MP 600 Adsorption Tests

Data that did not meet the statistical screening criteria (see Chapter 6) are not shown in Tables C.10 to C.13. The dosage in the first column represents the target dosage. The loadings in subsequent columns are calculated from the actual dosages. UVA expressed in/m; loading expressed in ℓ/mg·m.

Table C.1 Carbon testing (Round 1)

GAC dosage (mg/ℓ)	Midvaal		Wiggins		Umzonyana		Loerie		Rietvlei		Vereeniging		Olifantsvlei		P. Bay	
	UVA	loading	UVA	loading	UVA	loading	UVA	loading	UVA	loading	UVA	loading	UVA	loading	UVA	loading
0	16.4	-	7.0	-	15.8	-			18.4	-			13.1	-		
25	13.0	0.134	5.0	0.080	12.9	0.118										
33			4.9	0.063	12.5	0.101			14.8	0.110			9.1	0.122		
50	10.9	0.108	4.0	0.059	11.4	0.088			13.4	0.100			7.9	0.106		
66	9.5	0.105	3.6	0.051	10.2	0.084			11.8	0.100			7.0	0.093		
100	8.2	0.082	2.8	0.041	8.7	0.071			9.6	0.087			5.1	0.081		
133	6.1	0.077	2.4	0.035	7.0	0.066			7.9	0.079			4.2	0.067		
200	3.7	0.063	1.9	0.026	5.6	0.051			5.4	0.065			2.7	0.052		

Table C.2 Carbon testing (Round 2)

GAC dosage (mg/ℓ)	Midvaal		Wiggins		Umzonyana		Loerie		Rietvlei		Vereeniging		Olifantsvlei		P. Bay	
	UVA	loading	UVA	loading	UVA	loading	UVA	loading	UVA	loading	UVA	loading	UVA	loading	UVA	loading
0	15.3	-	6.3	-	14.8	-	17.3	-	17.2	-			16.4	-	30.4	-
25	12.5	0.112														
33	11.5	0.115	3.8	0.076	11.7	0.095	13.1	0.128	13.2	0.120			12.3	0.124	27.4	0.091
50	10.4	0.098	3.0	0.066	10.5	0.087	11.8	0.110	12.1	0.102			10.5	0.118	26.3	0.083
66	9.5	0.088	2.7	0.055	9.4	0.082	10.9	0.097	10.5	0.102			9.4	0.107	25.1	0.081
100	7.6	0.077	2.0	0.043	7.6	0.072	8.9	0.084	8.6	0.086			7.8	0.086	22.8	0.076
133	6.4	0.067	1.6	0.036			7.7	0.072	6.9	0.077			6.4	0.075	21.2	0.070
200	4.7	0.053	1.2	0.025			5.5	0.059	4.9	0.061			4.6	0.059	17.6	0.064

Table C.3 Carbon testing (Round 3)

GAC dosage (mg/ℓ)	Midvaal		Wiggins		Umzonyana		Loerie		Rietvlei		Vereeniging		Olifantsvlei		P. Bay	
	UVA	loading	UVA	loading	UVA	loading	UVA	loading	UVA	loading	UVA	loading	UVA	loading	UVA	loading
0	18.5	-	6.1	-	16.7	-	6.7	-	19.2	-			15.8	-		
25	15.2	0.133	4.4	0.070	14.3	0.095	5.6	0.042	16.4	0.111			13.0	0.111		
33	14.4	0.126	4.0	0.064	13.7	0.089	5.3	0.040	15.1	0.125			12.1	0.113		
50	12.5	0.122	3.4	0.055	12.3	0.088	4.7	0.039	14.1	0.101			10.7	0.102		
66	11.6	0.105	3.0	0.048	11.1	0.085	4.4	0.035	12.6	0.100			9.2	0.100		
100	9.6	0.089	2.5	0.036	9.1	0.076	3.5	0.031	11.1	0.081			7.9	0.079		
133	8.1	0.079	2.1	0.031	8.2	0.064	3.0	0.027	6.9	0.077			6.4	0.075	21.2	0.070
200	6.0	0.063	1.7	0.022	6.3	0.052	2.5	0.021	4.9	0.061			4.6	0.059	17.6	0.064

Table C.4 Carbon testing (Round 4)

GAC dosage (mg/ℓ)	Midvaal		Wiggins		Umzonyana		Loerie		Rietvlei		Vereeniging		Olifantsvlei		P. Bay	
	UVA	loading	UVA	loading	UVA	loading	UVA	loading	UVA	loading	UVA	loading	UVA	loading	UVA	loading
0			7.6		19.0	-	15.1	-					15.4			
25					16.2	0.111	12.8	0.094								
33			5.2	0.071	15.4	0.109	12.0	0.096					11.5	0.118		
50			4.7	0.059	14.4	0.093	10.9	0.084					10.6	0.099		
66			4.2	0.050	13.1	0.090	10.3	0.074					9.3	0.093		
100			3.6	0.040	11.5	0.075	8.3	0.068					7.6	0.078		
133			3.1	0.034	9.8	0.069	7.1	0.061					6.7	0.066		
200			2.8	0.024	7.5	0.057	5.1	0.050					5.1	0.052		

Table C.5 Carbon testing (Round 5)

GAC dosage (mg/ℓ)	Midvaal		Wiggins		Umzonyana		Loerie		Rietvlei		Vereeniging		Olifantsvlei		P. Bay	
	UVA	loading	UVA	loading	UVA	loading	UVA	loading	UVA	loading	UVA	loading	UVA	loading	UVA	loading
0	14.0		4.9				13.3		16.3				14.3			
25	11.1	0.115	3.1	0.072			11.5	0.072	13.1	0.130			11.3	0.121		
33	10.5	0.106	2.7	0.066			11.0	0.072	12.3	0.122			10.5	0.115		
50	9.0	0.101	2.2	0.056			9.7	0.075	11.0	0.108			9.3	0.100		
66	8.0	0.091	1.7	0.048			8.8	0.069	9.7	0.100			8.1	0.095		
100	5.8	0.081	1.0	0.039			6.7	0.066	8.2	0.082			6.4	0.079		
133	4.7	0.070	0.6	0.032			5.4	0.060	6.1	0.077			4.9	0.071		
200	3.0	0.055	0.2	0.023			3.4	0.050	3.9	0.062			3.5	0.054		

Table C.6 Weak Resin testing (Round 2)

Resin dosage (mg/ℓ)	Midvaal		Wiggins		Umzonyana		Loerie		Rietvlei		Vereeniging		Olifantsvlei		P. Bay	
	UVA	loading	UVA	loading	UVA	loading	UVA	loading	UVA	loading	UVA	loading	UVA	loading	UVA	loading
0	15.5		6.4		15.3		17.7		16.9		21.7		15.4		30.8	
40																
100	7.8	0.077	3.3	0.031	8.5	0.067	8.0	0.098	8.3	0.087	12.5	0.091	8.2	0.071	22.5	0.083
240	6.2	0.039	2.9	0.014	6.8	0.035	6.1	0.048	5.9	0.046	9.6	0.050	6.5	0.037	14.3	0.069
540	5.2	0.019	2.7	0.007	5.5	0.018	5.3	0.023	4.7	0.023	8.4	0.024	5.5	0.018	8.0	0.042
1280	4.4	0.009	2.6	0.003	4.4	0.009	4.3	0.010	4.0	0.010	7.8	0.011	4.8	0.008	4.1	0.021

Table C.7 Weak Resin testing (Round 3)

Resin dosage (mg/ℓ)	Midvaal		Wiggins		Umzonyana		Loerie		Rietvlei		Vereeniging		Olifantsvlei		P. Bay	
	UVA	loading	UVA	loading	UVA	loading	UVA	loading	UVA	loading	UVA	loading	UVA	loading	UVA	loading
0	18.0		6.6		17.1				18.9		22.0		16.4		40.6	
40	13.6	0.109	4.5	0.054	12.8	0.107			14.5	0.111	18.6	0.085	12.7	0.093		
100	10.1	0.079	3.7	0.029	9.1	0.080			10.9	0.080	15.9	0.061	9.6	0.068	31.3	0.090
240	7.8	0.042	3.4	0.014	6.9	0.042			8.3	0.044	9.5	0.052	7.8	0.036	20.6	0.083
540	6.5	0.021	2.9	0.007	5.3	0.022			6.5	0.023	6.7	0.028	5.9	0.019	9.5	0.058
1280	4.7	0.010	2.6	0.003	4.1	0.010			4.6	0.011	3.7	0.014	4.5	0.009	3.9	0.029

Table C.8 Weak Resin testing (Round 4)

Resin dosage (mg/ℓ)	Midvaal		Wiggins		Umzonyana		Loerie		Rietvlei		Vereeniging		Olifantsvlei		P. Bay	
	UVA	loading	UVA	loading	UVA	loading	UVA	loading	UVA	loading	UVA	loading	UVA	loading	UVA	loading
0			7.3		18.9		15.0									
40			4.8	0.064	14.3	0.116	9.8	0.129								
100			3.8	0.035	9.7	0.093	6.6	0.084								
240			3.5	0.016	6.4	0.052	3.3	0.049								
540			2.8	0.008	4.8	0.026	3.1	0.022								
1280			2.7	0.004	4.0	0.012	2.7	0.010								

Table C.9 Weak Resin testing (Round 5)

Resin dosage (mg/ℓ)	Midvaal		Wiggins		Umzonyana		Loerie		Rietvlei		Vereeniging		Olifantsvlei		P. Bay	
	UVA	loading	UVA	loading	UVA	loading	UVA	loading	UVA	loading	UVA	loading	UVA	loading	UVA	loading
0	13.8		4.5		31.5		17.3		19.7		27.5		14.9		51.6	
40	10.3	0.087	2.5	0.050	26.9	0.115	12.9	0.111	15.1	0.115	22.6	0.121	10.9	0.099	47.9	0.092
100	7.5	0.063	1.6	0.029	23.1	0.084	8.0	0.094	10.6	0.091	17.6	0.099	7.6	0.073	41.5	0.101
240	5.2	0.036	1.3	0.013	18.0	0.056	4.1	0.055	6.9	0.053	11.0	0.069	5.3	0.040	30.4	0.088
540	4.0	0.018	1.1	0.006	12.7	0.035	3.3	0.026	5.1	0.027	8.5	0.035	4.2	0.020	21.3	0.056
1280	3.2	0.008	0.9	0.003												

Table C.10 Strong Resin testing (Round 2)

Resin dosage (mg/ℓ)	Midvaal		Wiggins		Umzonyana		Loerie		Rietvlei		Vereeniging		Olifantsvlei		P. Bay	
	UVA	loading	UVA	loading	UVA	loading	UVA	loading	UVA	loading	UVA	loading	UVA	loading	UVA	loading
0	14.9	-	6.6	-	15.7	-	17.7	-	17.1	-			15.2	-	30.8	-
40	8.0	0.172	3.5	0.077	6.9	0.220	9.9	0.195	8.7	0.208			8.3	0.172	24.6	0.152
100	5.3	0.095	2.8	0.039	4.9	0.109	6.9	0.108	5.6	0.114			5.7	0.095	17.1	0.135
240	4.5	0.043	2.6	0.017	4.0	0.049	6.2	0.048	5.2	0.049			4.7	0.044	8.8	0.092
540	3.9	0.020	2.4	0.008	3.5	0.023	5.3	0.023	3.7	0.025			4.0	0.021	4.6	0.048
1280	3.4	0.009			3.5	0.010	3.5	0.011	3.6	0.011			3.5	0.009	2.9	0.022

Table C.11 Strong Resin testing (Round 3)

Resin dosage (mg/ℓ)	Midvaal		Wiggins		Umzonyana		Loerie		Rietvlei		Vereeniging		Olifantsvlei		P. Bay	
	UVA	loading	UVA	loading	UVA	loading	UVA	loading	UVA	loading	UVA	loading	UVA	loading	UVA	loading
0	18.4		6.3		17.3		6.7		19.4		23.6		16.6		44.8	
40							3.7	0.073			14.7	0.223				
100	6.9	0.115	2.8	0.034	5.3	0.120	3.0	0.037	7.3	0.121	11.7	0.119	6.9	0.097	31.1	0.137
240	5.6	0.053	2.6	0.015	4.3	0.054	2.6	0.017	5.9	0.056	7.3	0.068	5.8	0.045	19.8	0.104
540	4.8	0.025	2.5	0.007	4.0	0.025	2.5	0.008	5.4	0.026	6.5	0.032	4.9	0.022	9.5	0.065
1280	4.0	0.011			3.6	0.011	2.6	0.003	4.5	0.012	5.7	0.014	4.5	0.010	5.2	0.031

Table C.12 Strong Resin testing (Round 4)

Resin dosage (mg/ℓ)	Midvaal		Wiggins		Umzonyana		Loerie		Rietvlei		Vereeniging		Olifantsvlei		P. Bay	
	UVA	loading	UVA	loading	UVA	loading	UVA	loading	UVA	loading	UVA	loading	UVA	loading	UVA	loading
0			7.7		19.3						25.7		14.9			
40			4.1	0.091	10.0	0.232					17.7	0.200	8.3	0.164		
100			3.7	0.040	5.9	0.134					10.6	0.152	6.4	0.085		
240			3.3	0.018	4.8	0.060					6.7	0.079	5.5	0.039		
540			3.2	0.008	4.5	0.027					5.7	0.037	5.0	0.018		
1280					4.3	0.012					4.8	0.016	4.8	0.008		

Table C.13 Strong Resin testing (Round 5)

Resin dosage (mg/ℓ)	Midvaal		Wiggins		Umzonyana		Loerie		Rietvlei		Vereeniging		Olifantsvlei		P. Bay	
	UVA	loading	UVA	loading	UVA	loading	UVA	loading	UVA	loading	UVA	loading	UVA	loading	UVA	loading
0	17.2		7.2		28.6		19.0		19.7		27.6		17.8		52.2	
40	10.4	0.170	4.0	0.079	19.5	0.228	10.3	0.219	10.8	0.222	20.2	0.184	10.6	0.179	45.7	0.163
100	7.0	0.102	3.5	0.037	10.7	0.179	6.1	0.129	6.6	0.131	11.8	0.158	7.4	0.104	34.8	0.174
240	5.9	0.047	3.3	0.016	9.0	0.082	5.2	0.058	5.2	0.060	8.7	0.079	6.4	0.047	22.3	0.125
540	5.4	0.022	3.3	0.007	7.3	0.039	4.4	0.027	4.8	0.028			5.7	0.022	12.2	0.074
1280	4.8	0.010			7.2	0.017	4.0	0.012			6.9	0.016	5.4	0.010	7.1	0.035